

# TECHNISCHE UNIVERSITÄT MÜNCHEN

Lehrstuhl für Mikrobiologie

## **Chromosome and megaplasmid partitioning in**

### ***Thermus thermophilus* HB27**

Haijuan Li

Vollständiger Abdruck der von der Fakultät Wissenschaftszentrum Weihenstephan für Ernährung, Landnutzung und Umwelt der Technischen Universität München zur Erlangung des akademischen Grades eines

Doktors der Naturwissenschaften

genehmigten Dissertation.

Vorsitzender: Univ.-Prof. Dr. Rudi F. Vogel

Prüfer der Dissertation:

1. Univ.-Prof. Dr. Wolfgang Liebl
2. Univ.-Prof. Dr. Siegfried Scherer

Die Dissertation wurde am 02. 06. 2014 bei der Technischen Universität München eingereicht und durch die Fakultät Wissenschaftszentrum Weihenstephan für Ernährung, Landnutzung und Umwelt am 17. 07. 2014 angenommen.



---

## Contents

<b>Contents.....</b>	<b>1</b>
<b>Abbreviations .....</b>	<b>4</b>
<b>1. Introduction.....</b>	<b>6</b>
<b>2. Materials and methods.....</b>	<b>20</b>
2.1 Bacteria strains and growth media.....	20
2.1.1 Strains and plasmids .....	20
2.1.2 Growth media.....	26
2.1.3 Growth conditions.....	29
2.1.4 Storage of strains and control of purity.....	30
2.2 DNA manipulations .....	31
2.2.1 General techniques.....	31
2.2.2 DNA isolation, purification and quality evaluation .....	31
2.2.2.1 Plasmid DNA isolation from <i>E. coli</i> .....	31
2.2.2.2 Genomic DNA isolation .....	32
2.2.2.3 DNA isolation from agarose gels .....	32
2.2.2.4 Direct PCR product purification .....	32
2.2.2.5 DNA analysis using agarose gel electrophoresis .....	33
2.2.2.6 DNA quantification .....	33
2.2.2.7 DNA sequencing .....	34
2.2.3 Enzymatic modification of DNA.....	34
2.2.3.1 Restriction.....	34
2.2.3.2 Dephosphorylation of linearized DNA .....	35
2.2.3.3 Ligation .....	35
2.2.3.4 Gibson Assembly of DNA fragments .....	35
2.2.4 <i>In vitro</i> DNA amplification.....	36
2.2.4.1 Analytical PCR .....	36
2.2.4.2 Preparative PCR.....	37
2.2.4.3 Quantitative PCR .....	38
2.2.5 Southern hybridization.....	39
2.2.6 Pulsed field gel electrophoresis .....	42
2.2.7 Transformation .....	44
2.2.7.1 Transformation of <i>E. coli</i> .....	44
2.2.7.2 Transformation of <i>T. thermophilus</i> .....	44

2.3 RNA manipulations .....	44
2.3.1 RNA isolation.....	45
2.3.2 Reverse transcription-polymerase chain reaction (RT-PCR).....	45
2.4 Protein manipulations and biochemical methods .....	45
2.4.1 Protein concentration determination .....	45
2.4.2 SDS-polyacrylamide gel electrophoresis (SDS-PAGE).....	46
2.4.3 Protein overexpression and purification .....	48
2.4.4 Electrophoretic Mobility Shift Assay (EMSA) .....	49
2.5 $\beta$ -glucosidase activity assay for <i>T. thermophilus</i> .....	52
2.6 Microscopy.....	53
<b>3. Results.....</b>	<b>55</b>
3.1 A new genetic modification tool for <i>T. thermophilus</i> .....	55
3.1.1 Toxic effect of substituted indoxyl substrates and its use for counterselection in gene exchange experiments in <i>T. thermophilus</i> .....	55
3.1.2 Possible mechanisms of toxicity of substituted indoxyl substrates .....	60
3.1.3 Toxicity test of substituted indoxyl substrates in other bacteria.....	62
3.2 Chromosomal and megaplasmid partitioning ( <i>par</i> ) loci in <i>T. thermophilus</i> .....	64
3.2.1 Locations, components and genetic structures of <i>parABc</i> and <i>parABm</i> .....	64
3.2.2 Complete deletion of <i>parABc</i> is possible, whereas <i>parBm</i> is essential .....	68
3.2.3 <i>parABm</i> is required for wild-type cell growth, while <i>parABc</i> is not.....	73
3.2.4 <i>parABm</i> is required for maintaining the megaplasmid but not the chromosome, while <i>parABc</i> is not important for maintenance of the both replicons .....	76
3.2.5 <i>In vitro</i> , ParBc binds specifically to <i>parSc</i> , while <i>ParBm</i> does not.....	84
3.2.6. Polar localizations of ParBc-sGFP and ParBm-sGFP in wild-type <i>T. thermophilus</i> cells .....	87
3.2.7 Distinct localization patterns of ParBc-sGFP and ParBm-sGFP in <i>E. coli</i> cells ...	93
3.2.8 <i>parABm</i> is necessary for accurate subcellular localization of the megaplasmid origin region .....	93
3.3 The role of MreB in <i>T. thermophilus</i> .....	95
3.3.1 <i>mreB</i> is deletable in <i>T. thermophilus</i> .....	95
3.3.2 <i>mreB</i> is involved in cell shape maintenance, but not in chromosome segregation in <i>T. thermophilus</i> .....	96
3.4 Separation of two alleles located at one chromosomal gene locus.....	100
3.4.1 Construction of a stable heterozygous strain in <i>T. thermophilus</i> .....	100

---

3.4.2 Allele separation kinetics of the heterozygous strain HL01 .....	102
3.4.3 Distributions of relative DNA contents of daughter cells in <i>T. thermophilus</i> .....	105
<b>4. Discussion .....</b>	<b>109</b>
4.1 Genetic modification of <i>T. thermophilus</i> .....	109
4.1.1 Toxic effect of substituted indoxyl substrates and its use for counterselection during introduction of gene deletions in <i>T. thermophilus</i> .....	109
4.1.2 Possible mechanisms of toxicity and potential broad host range application of substituted indoxyl substrates .....	111
4.2 Chromosomal and megaplasmid partitioning ( <i>par</i> ) systems in <i>T. thermophilus</i> .....	113
4.2.1 Characteristics and functions of the chromosomal <i>par</i> system.....	113
4.2.1.1 Genetic structures and components of the chromosomal <i>par</i> loci .....	113
4.2.1.2 Functions of the chromosomal <i>par</i> loci.....	114
4.2.2 Characteristics and functions of the megaplasmid <i>par</i> system .....	117
4.2.2.1 Genetic structures and components of the megaplasmid <i>par</i> loci.....	117
4.2.2.2 Functions of the megaplasmid <i>par</i> loci.....	118
4.2.3 Chromosomal and megaplasmid <i>Par</i> are two independent systems.....	123
4.3 MreB does not play a role in the chromosome segregation of <i>T. thermophilus</i> .....	125
4.4 Random partitioning of the chromosome copies.....	127
4.4.1 Separation of two alleles at one chromosomal locus is caused by random partitioning of chromosome copies into the daughter cells .....	127
4.4.2 Random partitioning of the chromosome copies favors generation of homozygous gene deletion mutants in <i>T. thermophilus</i> .....	130
<b>5. Summary .....</b>	<b>131</b>
<b>6. Publication list .....</b>	<b>137</b>
<b>7. References.....</b>	<b>138</b>
<b>Appendix: primers used in the study .....</b>	<b>154</b>

## Abbreviations

AP	alkaline phosphatase
Amp	ampicillin
Amp <sup>R</sup>	ampicillin resistant
APS	ammonium persulfate
ATP/ADP	adenosine 5'-triphosphate / Adenosine 5'-diphosphate
BCIP	5-bromo-4-chloro-3-indolyl-phosphate
BCI- $\alpha$ -glu	5-bromo-4-chloro-3-indolyl- $\alpha$ -D-glucopyranoside
BCI- $\beta$ -gal	5-bromo-4-chloro-3-indolyl- $\beta$ -D-galactopyranoside
BCI- $\beta$ -glu	5-bromo-4-chloro-3-indolyl- $\beta$ -D-glucopyranoside
BHI	Brain Heart Infusion Broth
Blm	bleomycin
Blm <sup>R</sup>	bleomycin resistant
bp	base pair
BSA	bovine serum albumin
Cm	chloramphenicol
Cam <sup>R</sup>	chloramphenicol resistant
CFS	6-carboxyfluorescein
Da	Dalton
DAPI	4',6-diamidino-2-phenylindole-dihydrochloride
dd H <sub>2</sub> O	bi-distilled water
DMF	N, N-dimethyl formamid
DNA	deoxyribonucleic acid
DNase	deoxyribonuclease
dNTP	deoxynucleosidetriphosphate
DSM	German Collection of Microorganisms and Cell Cultures
Ec	<i>Escherichia coli</i>
EDTA	ethylene di-amine tetra-acetic acid
h	hour
IPTG	Isopropyl- $\beta$ -D-thiogalactopyranosid
kbp	kilobase pair
Km/kan	kanamycin
Kam <sup>R</sup> / Km <sup>R</sup>	kanamycin resistant
l	liter
LB	Luria-Bertani Broth
M	molar
mA	milliampere
mM	millimolar

min	minutes
ml	milliliter
μ	micro
ng	nanogram
NBT	nitro blue tetrazolium
OD	Optical Density
O/N	overnight
ORF	open reading frame
oriC	origin of replication
oriCc	replication origin of the chromosome
oriCm	replication origin of the megaplasmid
PAGE	polyacrylamide gel electrophoresis
PCR	polymerase chain reaction
PFGE	pulsed field gel electrophoresis
pmol	picomolar
PVP	polyvinylpyrrolidone
RNA	ribonucleic acid
RNase	ribonuclease
rpm	rounds per minute
RT	room temperature
RT-qPCR	reverse transcription quantitative PCR
sec	seconds
SDS	sodiumdodecylsulfate
SSC	saline-sodium citrate buffer
TAE	Tris-Acetate-EDTA buffer
TBE	Tris-Borate-EDTA buffer
TEMED	N,N,N',N'-Tetramethylethylenediamin
ter	terminus of replication
terc	terminus of the chromosome replication
term	terminus of the megaplasmid replication
Tris	tris-hydroxymethyl-aminomethane
Tth	<i>Thermus thermophilus</i>
U	Unit (unit of enzyme activity)
UV	ultraviolet (radiation)
v/v	volume per volume
V	volts
w/v	weight per volume
XGal	5-bromo-4-chloro-3-indolyl-β-D-galactopyranoside
XGlc	5-bromo-4-chloro-3-indolyl-β-D-glucopyranoside

## 1. Introduction

*Thermus* spp is one of the most wide spread genres of thermophilic bacteria, its isolates can be found in natural as well as in man-made thermal environments. By reason of their ancestral origin, the applicability of their enzymes, the ability of thermostable enzymes and their macromolecular complexes to more easily crystallize than their mesophilic counterparts (Vieille *et al.*, 2001; Vassylyev *et al.*, 2002; Malawski *et al.*, 2006; Selmer *et al.*, 2006), extreme thermophiles have promoted great biological interest. Nevertheless, not all extreme thermophiles are applicable as laboratory research models on account of their inherent growth difficulties and the lack of genetic manipulation tools. *Thermus thermophilus* stands as an exception to this rule because of: (i) its ability to grow under laboratory conditions; (ii) its facultative mode of growth, and with high growth rate and good cell yields; (iii) its impressively efficient natural transformation apparatus (Koyama *et al.*, 1990; Friedrich *et al.*, 2002). Numerous methods and genetic tools have been developed to manipulate this species, especially the two model strains HB8 and HB27 (Lasa *et al.*, 1992; de Grado *et al.*, 1998, 1999; Moreno *et al.*, 2003).

*T. thermophilus* is a Gram-negative bacterium that can grow aerobically with high rate at temperatures ranging from 50 °C to 82 °C (Oshima and Imahori, 1971, 1974). It shows orange-yellow colour because of the presence of carotenoids in the membrane. Morphologically, it forms slender rod-shaped cells which tend to form septated filaments in exponential cultures on rich medium (Cava *et al.*, 2009). The whole genome sequence of the two model strains HB8 and HB27 have been sequenced (Henne *et al.*, 2004). The genome of the HB27 strain consists of a chromosome (1.89 Mb) and a megaplasmid (0.23 Mb), while that of the HB8 strain includes a plasmid (9.3 kb) together with a chromosome (1.85 Mb) and a megaplasmid (0.26 Mb) (Henne *et al.*, 2004). In the two strains, the GC content and coding density are both high (69%, 95% respectively) (Henne *et al.*, 2004; Lioliou *et al.*, 2004; Liebl, 2004). The availability of the genome sequences has enabled full accession to the genetic repertoire of *T. thermophilus* and is a prerequisite for in-depth



molecular studies of their extreme thermophile. The ongoing project “Structural and Functional Whole-Cell Project for *T. thermophilus* HB8” is a prominent example of *T. thermophilus* being used as a model organism for structural genomics. The aim of this project is to understand the mechanisms of all the biological phenomena occurring in the HB8 cell by investigating the cellular components at the atomic level on the basis of their three-dimensional (3-D) structures (Yokoyama *et al.*, 2000). So far, at least 1450 ORFs have been heterologously expressed from the 2238 ORFs predicted in the *T. thermophilus* HB8 genome; 944 recombinant proteins have been purified and 682 have been crystallized. Consequently, *T. thermophilus* has become one of the best known organisms at the protein structural genomics level.

### **Genetic transformation and manipulation of *T. thermophilus***

An important property of *T. thermophilus* is its ability to acquire competence for natural genetic transformation, which encourages the study of this organism to a great extent. It has been revealed that the natural competence system is dependent on divalent cations and pH (Hidaka *et al.*, 1994; Koyama *et al.*, 1986), and at least 16 genes are involved in this process (Friedrich *et al.*, 2001, 2002). The 16 proteins encoded by these genes include two DNA translocators (ComEA, ComEC), four pilin-like proteins (PilA1, PilA2, PilA3, PilA4), one leader peptidase (PilD), one traffic-NTPase protein (PilF), one inner membrane protein (PilC), one PilM-homologue, one secretin-like protein (PilQ), and another four proteins (ComZ, PilN, PilO, and PilW) that have no homologues in the protein data banks. Based on these data and those of immunolocalization, Averhoff *et al.* (2004) have proposed a model for the DNA-uptake system of *T. thermophilus*. It is interesting to point out that *T. thermophilus* shows natural transformation capacity throughout the whole growth phase (Koyama *et al.*, 1986) and DNA incorporation in this thermophile rate is strikingly high (in the exponential phase, 40 kb/s and cell) (Schwarzenlander and Averhoff, 2006). Furthermore, the DNA up-take system in *T. thermophilus* does not distinguish DNA from Bacteria, Archaea, or Eukarya, indicating potential interdomain DNA exchanges (Schwarzenlander and Averhoff, 2006).

In order to use *T. thermophilus* as a genetic manipulation model, the development of selection tools after transformation is indispensable. In the initial

period, the total DNA of spontaneous streptomycin resistant mutants was used to determine the transformation capacity of *T. thermophilus* (Koyama *et al.*, 1986), and the selection of the first plasmid was based on the complementation of Leu or Trp auxotrophic mutants (Koyama *et al.*, 1990a, b). One of the breakthroughs in the field of genetic selection tools of *T. thermophilus* was the generation of gene knockout mutants based on insertion of a gene cassette (*kat*) encoding a thermostable kanamycin nucleotidyl transferase (Lasa *et al.*, 1992a). This marker remained the only antibiotic resistance gene marker for *Thermus* until another two thermoadapted antibiotic resistance makers were found, allowing selection with bleomycin and hygromycin (Brouns *et al.*, 2005; Nakamura *et al.*, 2005). The use of these two markers is compatible with a kanamycin resistance background (Cava *et al.*, 2007). However, in spite of being a rapid method for the isolation of direct knockout mutants, the insertion of antibiotic resistant maker blocks further selection procedures and polar effects on downstream genes are possible. To avoid these, alternative strategies have been developed, which allow the generation of marker-free deletion mutants. These usually involve a two-step integration-segregation based on homologous recombination of a plasmid which carries the exchange allele; the integration step is selected with an antibiotic resistance marker and the second step relies on the use of a counterselectable trait. Common examples of counterselection strategies are: inhibition of growth in the presence of sucrose, mediated by the *sacB* gene product (Gay *et al.*, 1985), inhibition of growth in the presence of lipophilic chelators such as fusaric acid, mediated by genes conferring tetracyclineresistance (Maloy and Nunn, 1981), inhibition of growth by purine or pyrimidine analogs, mediated by phosphoribosyl transferases of the purine and pyrimidine base salvage pathways (Peck *et al.*, 2000; Fabret *et al.*, 2002; Bitan-Banin *et al.*, 2003; Pritchett *et al.*, 2004), and the use of a dominant, conditionally lethal *rpsL* allele that confers sensitivity to streptomycin (Russell and Dahlquist, 1989). In *T. thermophilus*, till now, only two counter-selection markers are applicable. The methods are the *pyrE* system, described by Tamakoshi *et al.* (1999) and the system based on the *rpsL1* allele from Blas-Galindo *et al.* (2007). However, the both methods are limited in the *pyrE* and *rpsL1* deletion background. Thus, to facilitate the genetic studies of *T. thermophilus*,

in this study, it was attempted to develop a new counter-selection marker which is applicable in the wild-type background.

Fluorescent proteins have been used as excellent tools to study the cell biology of mesophilic bacteria and eukaryotes (Prescott *et al.*, 2006). However, due to the extreme growth conditions of *T. thermophilus*, the use of fluorescent proteins is limited. Till now, only one green fluorescent protein variant is applicable for *T. thermophilus*. This superfolder GFP (sGFP) variant is from *Aequorea victoria*, it folds efficiently when fused to poorly folded polypeptides (Pedelacq *et al.*, 2006). sGFP also exhibits an improved tolerance to circular permutation and a greater resistance to chemical denaturants. Due to these properties, the functions of sGFP have been tested in *T. thermophilus* by Cava *et al.* (2008). Their results demonstrated that the sGFP variant was able to fold and thus fluoresce properly when expressed in *T. thermophilus* growing at 70 °C. Hence, it becomes practical to use this sGFP as a tool to trace protein localization at high temperature.

### **Genome biology of *T. thermophilus***

Polyploidy means the presence of more than two sets of complete chromosomes in one cell and is found to be ubiquitous in eukaryotes. Polyploid is the result of evolution, and it possesses both advantages and disadvantages (Comai *et al.*, 2005; Semon *et al.*, 2007; Hegarty *et al.*, 2008). In brief, polyploidy renders heterosis effects (hybrid vigour, i.e., an increased performance of the allopolyploid comparing with the inbred parents); also, loss of self-incompatibility leads to the gain of asexual reproduction, and gene redundancy. Gene redundancy can be accompanied by higher resistance against DNA-damaging reagents; may lower the frequency for deleterious recessive mutations becoming homozygous; has potential for gene diversification and the acquisition of new functions. Polyploidy also possesses disadvantages, for instance, a higher frequency of mitotic or meiotic problems leading to aneuploidy and or epigenetic instability.

In comparison with eukaryotes, prokaryotes are generally considered to be monoploid, which means they usually harbor one copy of chromosome per cell. This is best exemplified by the well-studied Gram-negative bacterium *Escherichia coli* and Gram-positive bacterium, *Bacillus subtilis*. *E. coli* is monoploid when grown

under conditions where the doubling time is longer than the time for chromosome replication and segregation (Skarstad *et al.*, 1986; Bremer and Dennis, 1996). However, when *E. coli* is under optimal laboratory growing conditions, replication origins will reinitiate before the previous replication rounds have been terminated, and thus more copies of origins existed than those of termini, and the cell becomes mero-oligoploid (Bremer and Dennis, 1996). The best-studied Gram-positive bacterium, *B. subtilis*, is also monoploid (Webb *et al.*, 1998), as are several other species. On the other hand, there are indeed many bacteria shown to be polyploid. The chromosome copy number of *Micrococcus radiodurans* has been estimated to be 8 (Hansen *et al.*, 1978), *Azotobacter vinelandii* was also shown to be polyploid in which the chromosome copy number could rise up to strikingly high when grown in rich medium (Maldonado *et al.*, 1994). The presence of multiple copies of chromosomes was also reported in several cyanobacterial species (Herdman *et al.*, 1979; Labarre *et al.*, 1989; Tandeau de Marsac, 1994). Recently, Ohtani *et al.* (2010) have shown that *T. thermophilus* strains are also polyploid, the chromosomal and megaplasmid copy numbers of the HB8 strain has been estimated to be four or five. It has not been studied to date how the multiple sets of genomes are regulated in *T. thermophilus*.

### **Machinery for active genome partitioning**

All dividing cells must have mechanisms to ensure that their genomes are faithfully segregated to the daughter cells. While the tubulin-based mitotic apparatus for DNA segregation used by eukaryotes are well established, relatively little is understood regarding the mechanisms that mediate chromosome segregation in prokaryotes, due to the lack of a conspicuous intracellular cytoskeleton and the small cell size of the model organisms. In early years, the seminal replicon model proposed by Jacob *et al.* (1963) suggested that newly replicated sister chromosomes are attached to centrally located sites on the cell membrane that move toward opposite cell poles in parallel with cell elongation. In this model, the process of chromosome segregation is essentially passive which relies on cell elongation. However, more recent evidence has shown that bacterial chromosomes are actively segregated which is independent of cell growth (Glaser *et al.*, 1997; Gordon *et al.*, 1997; Webb *et al.*,

1997, 1998; Viollier *et al.*, 2004). These observations indicate that cytoskeletal proteins are also present in prokaryotic cells that form mitotic-like apparatuses providing force for active chromosome segregation (Sharpe and Errington 1999; Gerdes *et al.*, 2004).

#### *DNA polymerase-, RNA polymerase-, and MreB-mediated systems*

Several factors have been proposed which may contribute to the dynamic movements of bacterial chromosomes (for reviews, see Errington *et al.*, 2005; Leonard *et al.*, 2005). In *B. subtilis*, it has been observed that the DNA replication machinery seems to be localized at the cell center and forms like a stationary “factory” (Lemon and Grossman, 1998). This observation has inspired the proposal that DNA polymerase can provide force for the bidirectional segregation (Lemon and Grossman, 2000). Likewise, RNA polymerase, interacting with directionally biased genes near the origin, has been suggested to afford both incentive force and directionality for segregation (Dworkin and Losick, 2002; Kruse *et al.*, 2006). The above two models seem to well interpret the situations in *B. subtilis* and *E. coli* in which the DNA replicates in the middle cell and segregates symmetrically to the 1/4 and 3/4 of cell positions, while it is impossible to directly apply them to the asymmetric segregation pattern that occurs in *Caulobacter crescentus* (Mohl and Gober, 1997; Viollier *et al.*, 2004) and *Vibrio cholerae* (Fogel and Waldor, 2005). In both of these organisms, the origin region is located close to one pole (the “old” pole) early in the cell cycle, and after replication, one copy remains at that pole while the other traverses the entire length of the cell to the opposite (“new”) pole. In consistence with this segregation process, later, it has been shown that the DNA replication machinery of *C. crescentus* positioned at the old pole initially, and then after replication, it made slow progression from cell pole to mid-cell (Jensen *et al.*, 2001). Except for DNA and RNA polymerases, in recent years, there is also certain evidence showing that MreB may provide force for active DNA segregation. *In vivo*, MreB assembles into actin-like filaments and is helically located underneath the cytoplasmic membrane (Jones *et al.*, 2001; Figge *et al.*, 2004; Kruse *et al.*, 2005; Shih *et al.*, 2005). Nearly all rod-shaped bacteria encode MreB homolog, and numerous experiments have shown that MreB is involved in cell morphology maintenance (Jones *et al.*, 2001;

Figge *et al.*, 2004; Dye *et al.*, 2005; Formstone and Errington, 2005; Kruse *et al.*, 2005). The role of MreB in DNA segregation is still in debate, there is some evidence showing that it is required for chromosome segregation in *B. subtilis* (Defeu Soufo and Graumann, 2003), *C. crescentus* (Gitai *et al.*, 2005) and *E. coli* (Kruse *et al.*, 2003, 2006); by contrast, evidences excluding MreB as an active chromosome segregation factor are also present (Formstone and Errington, 2005; Hu *et al.*, 2007). *T. thermophilus* also expresses a MreB homolog from its chromosome. Although the MreB function has been studied in other model bacterial species, its role in *T. thermophilus* is completely unknown. Therefore, in this study, one of the intentions was to study the potential role of MreB regarding chromosome segregation.

### *Par-mediated system*

Partitioning (*par*) genes have been known for a long time to play a pivotal role in the maintenance of certain low-copy plasmids. Plasmid *par* systems are composed of three components: an ATPase (ParA), a DNA-binding protein (termed ParB), and a centromere-like site (*parS*). ParB binds its *parS* and extends along the DNA, forming a large nucleoprotein complex. Formation of this complex and its interaction with ParA filaments were suggested to be essential for efficient plasmid segregation (Ebersbach and Gerdes 2005; Leonard *et al.*, 2005). Plasmids with disrupted *par* loci would no longer localize to the particular cell regions and were prone to be eliminated from the host cell (Austin and Abeles, 1983; Ogura and Hiraga, 1983; Niki and Hiraga, 1997; Li *et al.*, 2004). The ParA ATPase encoded by *par* loci can be divided into two groups: type I ParAs are P-loop ATPases containing the conserved Walker-box ATP-binding motif, while type II ParAs are actin-like ATPases (Gerdes *et al.*, 2000). Type I and II ParAs are found in different plasmid families, but only type I *par* loci have been identified on bacterial chromosomes (Gerdes *et al.*, 2000). P-loop ATPase ParAs can be subdivided into two types: those possessing an N-terminal DNA-binding helix-turn-helix (HTH) motif and those lacking this motif. These two subtypes are referred as Type Ia and Type Ib (Gerdes *et al.*, 2000) or as large and small ParAs (Gerdes *et al.*, 2010). *par* loci encoding large ParAs also encode large ParBs and are found only on plasmids, whereas small ParAs lacking an N-terminal DNA-binding domain are present on many plasmids and most bacterial

chromosomes (Livny *et al.*, 2007). *In vitro*, both type I and type II ParAs form filaments, in an ATP-dependent manner (Møller-Jensen *et al.*, 2002; Barilla *et al.*, 2005; Lim *et al.*, 2005). Type II ParAs seem to segregate plasmids by polymerizing between plasmid pairs and “pushing” them apart toward the poles (Møller-Jensen *et al.*, 2003). How type I ParAs mediate plasmid segregation is still somehow obscure. Some experiments showed that Type I ParAs could oscillate back and forth in the cell (Ebersbach and Gerdes, 2001; Lim *et al.*, 2005; Adachi *et al.*, 2006). Recently, Ringgaard *et al.* (2009) have proposed a model for Type I ParA-mediated plasmid movement based on the study of pB171 ParA movement, and it suggests that ParAs move the plasmid by a pulling mechanism (Fig. 1).

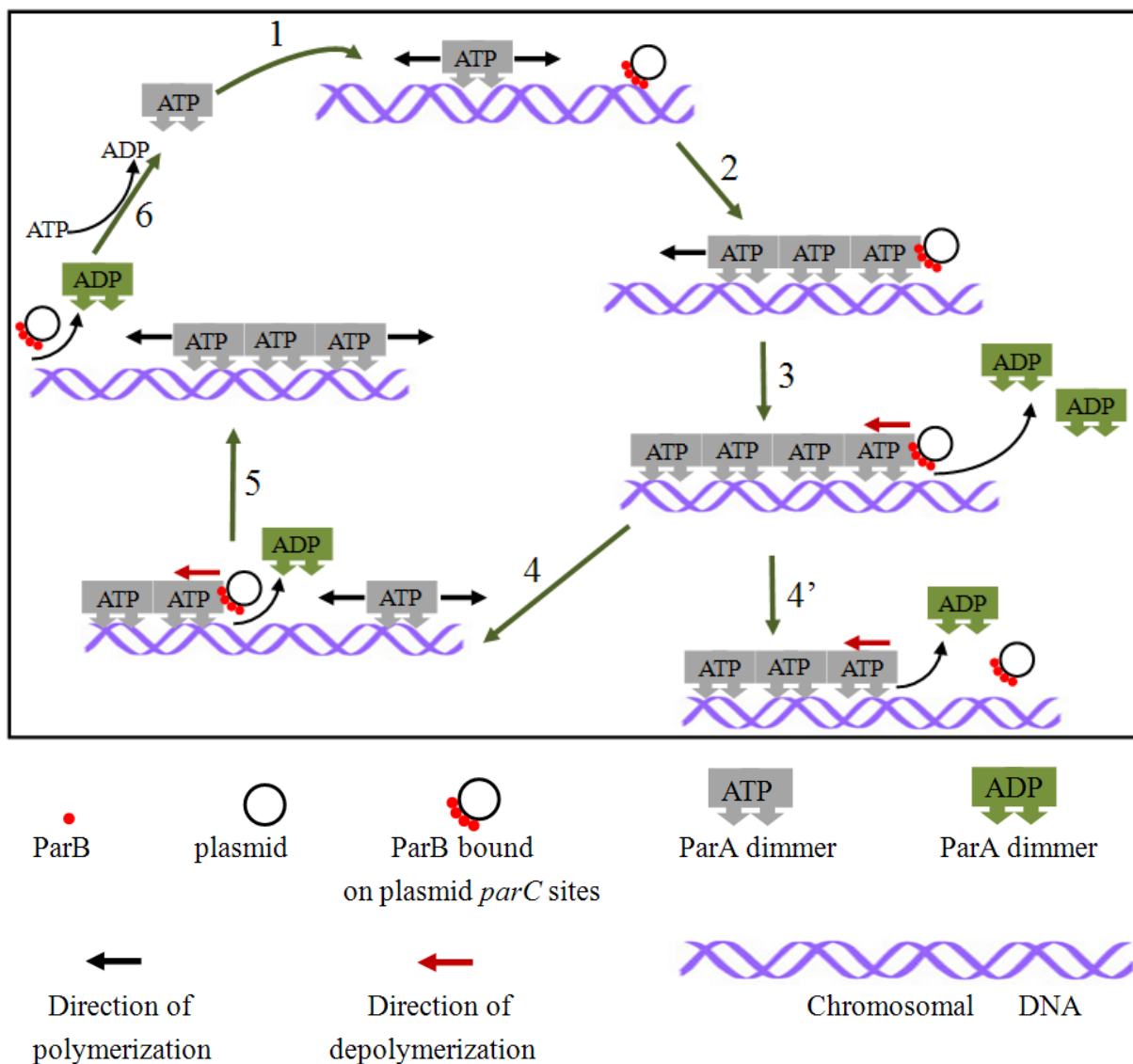


Fig. 1. A molecular model of the ParA pulling mechanism modified from Ringgaard *et al.* (2009) and

Gerdes *et al.* (2010). ParA-ATP dimers bind cooperatively to nucleoid DNA, thereby forming large ParA filaments. Filaments form from a nucleating core, then rapid polymerization proceeds (1). A growing filament contacts a plasmid via ParB bound to *parC* centromere DNA (2). The ATPase activity of ParA-ATP at the end of the filament is stimulated by ParBs bound to *parC* on the plasmid (3). Through this reaction, ParA-ATP is converted to its ADP form and released from the DNA, leaving a new ParA-ATP filament end that is accessible for interaction with the partition complex. When the ParA filaments are depolymerized, the plasmid can either detach (4') or remain attached to the end of the depolymerizing ParA filament (4). The moving plasmid leaves behind it a ParA-free nucleoid zone (5). Eventually, the ParA-ATP subunits released by ParB/*parC* assemble into a new filament in this zone that polymerizes toward the plasmid from the opposite side. After contact forms, this filament will move the plasmid to the opposite direction. In this way, a plasmid will jiggle around its position in between two other plasmids or between a plasmid and the nucleoid end. Finally, free ParA-ADP is renovated to ParA-ATP and the cycle repeats (6).

Most bacterial chromosomes encode orthologs of plasmid partitioning (Par) proteins near their origins (Gerdes *et al.*, 2000). Chromosomal centromere-like sites are usually denoted as *parS*. The first ParB bound chromosomal *parS* sites were discovered in *B. subtilis*. In *B. subtilis*, 10 pseudopalindromic 16-bp sequences were identified in the 20% origin-proximal region of its chromosome, among which, 8 were shown to be bound by ParB *in vivo* (Lin and Grossman, 1998; Breier and Grossman, 2007), and the presence of one such site could avoid the loss of an otherwise unstable plasmid from the host cell in a ParAB-dependent manner. Thus, the 16-bp pseudopalindromic sequences were formulated as 5'-TGTTNCACGTGAAACA-3'. Recently, this 16-bp sequence is found in a large variety of bacteria via a comprehensive bioinformatics analysis, and in most cases they are located in the origin-proximal region (Livny *et al.*, 2007; Gerdes *et al.*, 2010). Normally, the corresponding *parAB* genes can also be identified in the chromosomes encoding *parS* sites. Only Archaea, two branches of  $\gamma$ -proteobacteria (including *E. coli*), and one branch of *Firmicutes* (including *Mycoplasma*) do not contain obvious *parABS* loci, arguing that these loci evolved early in the bacterial kingdom and that their absence may reflect gene loss (Livny *et al.*, 2007; Gerdes *et al.*, 2010).

The crucial role of *par* loci in plasmid partitioning has been well-studied, whereas the function of their chromosomal counterparts is less clear. According to the published data, it seems that the function of chromosomal *par* loci is pleiotropic, and their role in chromosome segregation is still disputable. It has been shown that in *B.*



*subtilis*, the chromosomal *parAB* orthologs are not essential genes, and are required for chromosome replication and segregation, chromosome origin localization and separation, cell division, and developmental gene regulation (Ireton *et al.*, 1994; Sharpe and Errington, 1996; Lee *et al.*, 2003; Wu and Errington, 2003; Ogura *et al.*, 2003; Lee and Grossman, 2006); the *parAB* genes in *C. crescentus* are essential, depletion or overexpression of them result in cell-cycle progression, cell division and chromosome segregation defects (Mohl and Gober, 1997; Mohl *et al.*, 2001); *par* loci in *Mycobacterium smegmatis* are involved in chromosome segregation and cell growth (Jakimowicz *et al.*, 2007a); in *Pseudomonas aeruginosa*, they seem to participate in the processes of chromosome organization and segregation, cell growth, and motility (Bartosik *et al.*, 2004; Lasocki *et al.*, 2007); in *Pseudomonas putida*, chromosome segregation and cell morphology are affected in *parAB* mutants (Godfrin-Estevenson *et al.*, 2002; Lewis *et al.*, 2002).

*V. cholerae* has two circular chromosomes (chrI and chrII), and it seems their segregations are governed by different mechanisms. Their origin regions have distinct subcellular distributions and dynamics. In newborn cells, the origin of chrI (*oriCIvc*) is polar localized, while that of chrII (*oriCIIvc*) is mid-cell localized (Fogel and Waldor, 2005; Fiebig *et al.*, 2006). Both of the chromosomes contain their own *parAB* genes located near to the replication origins (Heidelberg *et al.*, 2000). Phylogenetic analyses suggest that the ParAB1 proteins of chrI show homology to other chromosome-encoded Par proteins, whereas the ParAB2 of chrII are more close to plasmid and phage Par proteins (Yamaichi *et al.*, 2000; Gerdes *et al.*, 2000), and ParB1 and ParB2 only bind to their cognate *parS* sites (Yamaichi *et al.*, 2007). In *V. cholerae*, the role in chromosome segregation of *parABS1* and *parABS2* has been evaluated. A *parA1* mutant does not have a perceptible cell growth defect and does not lose chrI or chrII, but provokes mislocalization (less-polar) of the origin region of chrI (Fogel and Waldor, 2006; Saint-Dic *et al.*, 2006). The *parAB2* are essential, a *parAB2* deletion mutant yields a high frequency of cells lacking chrII, but containing chrI; cells containing only chrI divide once and then show condensed nucleoid, hypertrophic, and undividing. Thus, it seems that ParAB2 can promote accurate subcellular localization and maintenance of chrII but not chrI, and there appears to be

no redundancy in the mechanisms that contribute to chrII segregation in *V. cholerae*. Since there was no detectable mislocalization of *oriCIvc* in the *parAB2* background and no *oriCIIvc* mislocalization in the *parA1* background, it seems the Par systems of the two chromosomes function independently of one another (Fogel and Waldor, 2006; Saint-Dic *et al.*, 2006).

Although the chromosomal Par systems have been studied to some extent in the classic model organisms, the situation in other bacteria remains largely unknown, not to mention in bacteria containing multiple chromosomes. In addition to *V. cholerae*, there is only one study related to the *par* loci in bacteria possessing multiple chromosomes. *Burkholderia cenocepacia* has three chromosomes and a low-copy-number plasmid. Dubarry *et al.* (2006) identified *parS* sites on the four replicons, and showed the *parABS* systems on these four replicons are independent from each other.

As mentioned, *T. thermophilus* has arised as a model organism for studying thermophilic bacteria, its genome contains a chromosome and a megaplasmid which are both polyploid. There are no reports in the literature regarding the chromosome and megaplasmid segregation in this organism. In *T. thermophilus*, the *parAB* genes are also present in both chromosome and megaplasmid (termed *parABc* and *parABm* in the following text). No reports have referred to the megaplasmid *par* loci, and only two studies have involved the chromosomal *par* loci, which deal with the ParAc and ParBc protein structures (Leonard *et al.*, 2004, 2005). The X-ray crystal structure of ParBc has been solved: it is a DNA-binding protein with structural similarity to the helix-turn-helix (HTH) motif of the lambda repressor DNA-binding domain. Its C-terminal domain seems to be exclusively dimeric, and thus the C-terminus is properly serving as a dimerization domain (Leonard *et al.*, 2004). Biochemical and structural analysis of ParAc has shown that the protein is a dynamic molecular switch that is capable of forming an ATP-dependent “sandwich” dimer (Leonard *et al.*, 2005). Nevertheless, the biological functions of the Parc and Parm systems in *T. thermophilus* are still not revealed. Therefore, one of the intentions of the current work was to obtain certain understanding of the properties and functions of the two systems in *T. thermophilus*, thereby acquiring some preliminary information about the

chromosome and megaplasmid segregation patterns.

### **Mechanisms for Heterozygosity converting to homozygosity in *T. thermophilus***

Ohtani *et al.* (2010) have shown that a heterozygous *T. thermophilus* strain containing two different antibiotic markers at the same chromosomal locus, tend to lose one of the two markers gradually when grown in antibiotic-free medium. In the former work of our group, this phenomenon was also noticed. However, the mechanisms through which the heterozygosity converts to homozygosity is not clear. And another interesting point is that there seems to be a contradiction between polyploidy and the ease with which gene deletion mutants are generated, for example by the use of the *kat* cassette. In a polyploid cell, integration of the selection marker in one of the genome copies would lead to marker-caused resistance of the whole cell. Therefore, it is conceivable that the resistant colonies obtained in marker insertion experiments could be heterozygous at the target locus. On the other hand, there are numerous examples of genes in both *T. thermophilus* strains which have been deleted or disrupted, without the complications expected in a polyploid organism like intermediate phenotype and instability of the mutations (Kato *et al.*, 1992; Fernández-Herrero *et al.*, 1995; Castán *et al.*, 2001; Friedrich *et al.*, 2002; Agari *et al.*, 2008;). In our experience, when a non-essential locus is targeted with a DNA fragment which carries the *kat* cassette flanked by sequences from both sides of that locus, practically all of the kanamycin resistant colonies obtained are apparently homozygous gene replacement mutants for that locus.

In allusion to the above two unresolved puzzles, i.e., through which way the heterozygous *T. thermophilus* cells turned into homozygous cells, and the contradiction between being polyploid and the ease of obtaining knock-out mutants, two possibilities were proposed: (i) In the presence of selection pressure, gene conversion, or the non-reciprocal exchange of information between homologous sequences, would lead to an equalization of the genomes within one cell and would result in a homozygosity in the above examples. A genetic manifestation of gene conversion can be obtained when a heterozygous strain is cultivated in the absence of selection pressure for any of the two alleles. In case gene conversion occurs, rapid segregation of the alleles is observed and the heterozygous state is lost. It has been

shown recently that allele equalization via gene conversion exists in polyploid archaea (Lange *et al.*, 2011). (ii) Another possible reason for allele segregation is random separation of the genome copies in the daughter cells at cell division. While both processes are expected to lead to a loss of the heterozygous state (change in genotype frequency), gene conversion is in addition accompanied by a change in the average fraction of each genome type (change in allele frequency) in the whole population.

### **The intentions of the current work**

(I) *T. thermophilus* is now widely used as a model organism to study the molecular nature of a thermophilic lifestyle. For efficient genetic manipulation of *T. thermophilus*, the development of selection tools after transformation is requisite. The method most often used for isolation of directed knockout mutants in *T. thermophilus* is based on the insertion of antibiotic resistance markers. This gene exchange approach has disadvantages, as the antibiotic resistance marker cannot be reused and polar effects of downstream genes are possible. Alternative strategies based on counter-selection principle permitting generation of scar-less deletion mutants were developed. However, until now, only two counter-selection markers are applicable for *T. thermophilus*, i.e. *pyrE* and *rpsL1* allele based systems, which were both relied on prior genetic modification of either *pyrE* or *rpsL* allele. Thus, to facilitate the genetic studies of *T. thermophilus*, in this work, one of the intentions was to develop a new marker-free gene deletion strategy which was expected to be broadly applicable (e.g., in wild-type background).

(II) The plasmid partitioning (Par) system composed of ParA, ParB, and *parS* site acts to actively segregate plasmid molecules to daughter cells and thereby ensure plasmid maintenance. Orthologs of the ParAB proteins are present on the chromosomes of most bacteria, however, their role in chromosome segregation is still poorly understood. MreB is a chromosomally encoded actin-like protein whose role in cell morphology maintenance is well-studied in rod-shape bacteria. Recently, MreB has also been suggested to provide force for active chromosome segregation in some bacteria (e.g., *E. coli*, *B. subtilis*, *C. crescentus*). For *T. thermophilus*, currently nothing is known about how the polyploid cells partition chromosome and

megaplasmid copies into daughter cells. Both the chromosome and megaplasmid encode *par* gene homologues, and the chromosome also contains a *mreB* gene homologue. In the current work, it was attempted to investigate the roles of these mitotic-like genome partitioning machineries (Par and MreB systems) in the *T. thermophilus* chromosome and megaplasmid segregation processes, thereby obtaining a fundamental understanding of the genome segregation in *T. thermophilus*.

Since the heterozygous *T. thermophilus* cells containing two different alleles at one chromosomal locus can convert to homozygous cells, and random partitioning of chromosome copies to the daughter cells would be one potential mechanism leading to this effect, another intention of the current work was to provide evidence for this hypothesis.

## 2. Materials and methods

### 2.1 Bacteria strains and growth media

#### 2.1.1 Strains and plasmids

The main bacterial strains used in the current work are described in Table 1. In Table 2, the basic plasmid vectors and plasmids are summarized.

Table 1. Strains used.

Strain	Description*	Reference
<i>T. thermophilus</i> strains		
HB27	wild type (DSM 7039)	Oshima and Imahori, 1974
$\Delta bgl$	HB27 derivative, $\beta$ -glucosidase synthesis deficient	this study
$\Delta 340$	$\Delta bgl$ derivative with markerless deletion of ORFs TT_C0340-0341	this study
TL-1	HB27 derivative, carotenoid synthesis deficient, otherwise is considered as wild type	our group, unpublished data
$\Delta parABc$	HB27 derivative with <i>parABc</i> replaced by <i>kat</i>	this study
$\Delta parAmN-1$	HB27 derivative with the N-terminal of <i>parAm</i> replaced by <i>blm</i> in the <i>parABm</i> transcription opposite direction	this study
$\Delta parAmN-2$	HB27 derivative with the N-terminal of <i>parAm</i> replaced by <i>blm</i> in the <i>parABm</i> transcription co-linear direction	this study
TMP0	HB27 derivative carrying pMK18 vector	this study

TMP01	HB27 derivative permitting overexpression of ParAm	this study
TMP02	HB27 derivative permitting overexpression of ParBm	this study
TL-1/parBc-sGFP	TL-1 derivative permitting expression of ParBc-sGFP	this study
TL-1/ParBm-sGFP	TL-1 derivative permitting expression of ParBm-sGFP	this study
$\Delta mreB::kat$	HB27 derivative with <i>mreB</i> replaced by <i>kat</i>	this study
HL01	HB27 derivative carrying both <i>kat</i> and <i>blm</i> at the <i>pyrE</i> gene locus	this study
<i>E. coli</i> XL-1 Blue	<i>recA<sup>-</sup>, thi, hsdR1, supE44, relA1, lacF<sup>'</sup>, proAB, lacI<sup>q</sup>, lacZ<math>\Delta</math>M15, Tn10[Tet]</i>	Bullock <i>et al.</i> , 1987
<i>E. coli</i> Rosetta 2 (DE3)	F <sup>-</sup> <i>ompT hsdS<sub>B</sub>(r<sub>B</sub><sup>-</sup> m<sub>B</sub><sup>-</sup>) gal dcm</i> (DE3) pRARE (Cam <sup>R</sup> )	Novagen
<i>B. subtilis</i> 168	type strain (DSM 402)	Spizizen, 1958

\* Cam<sup>R</sup>, chloramphenicol resistant.

Table 2. Plasmids used.

Plasmids	Description*	Reference
pUC18	high-copy-number cloning vector, <i>ori</i> pUC, Amp <sup>R</sup>	Yanisch-perron <i>et al.</i> , 1985
pCR2.1-TOPO	high-copy-number cloning vector, <i>ori</i> pUC, Km <sup>R</sup>	Invitrogen
pJET 1.2	high-copy-number cloning vector, Amp <sup>R</sup>	Thermo Scientific
pMK18	<i>E. coli</i> / <i>T. thermophilus</i> shuttle vector, <i>Tth</i> ( <i>repA</i> ), <i>Ec</i> ( <i>oriE</i> ), Km <sup>R</sup>	de Grado <i>et al.</i> , 1999

## 2. Materials and methods

---

---

pMB18	<i>E. coli</i> / <i>T. thermophilus</i> shuttle vector, <i>Tth</i> ( <i>repA</i> ), <i>Ec</i> ( <i>oriE</i> ), <i>Blm</i> <sup>R</sup>	our group
pTΔ42	allele exchange vector for generating $\Delta bgl$ , <i>ori</i> pUC, <i>Km</i> <sup>R</sup>	this study
pTKO-4	a non-replicative <i>T. thermophilus</i> vector, <i>ori</i> pUC, <i>Km</i> <sup>R</sup>	this study
pTKO-Δ340	allele exchange vector for generating $\Delta 340$ , <i>ori</i> pUC, <i>Km</i> <sup>R</sup>	this study
pUC-Δ <i>parABc::kat</i>	allele exchange vector for generating $\Delta parABc$ , <i>ori</i> pUC, <i>Km</i> <sup>R</sup>	this study
pUC-Δ <i>parABm::blm</i>	allele exchange vector for generating $\Delta parABm$ , <i>ori</i> pUC, <i>Blm</i> <sup>R</sup>	this study
pUC-Δ <i>parAmN-1</i>	allele exchange vector for generating $\Delta parAmN-1$ , <i>ori</i> pUC, <i>Blm</i> <sup>R</sup>	this study
pUC-Δ <i>parAmN-2</i>	allele exchange vector for generating $\Delta parAmN-2$ , <i>ori</i> pUC, <i>Blm</i> <sup>R</sup>	this study
pUC-Δ <i>parBm::blm</i>	allele exchange vector for generating $\Delta parBm$ , <i>ori</i> pUC, <i>Blm</i> <sup>R</sup>	this study
pMK- <i>parAm</i>	pMK18 derived vector, allowing overexpression of ParAm in <i>Tth</i>	this study
pMK- <i>parBm</i>	pMK18 derived vector, allowing overexpression of ParBm in <i>Tth</i>	this study
pET21a	expression vector, PT <sub>7</sub> , lacI, pBR322 <i>ori</i> , Amp <sup>R</sup>	Novagen
pET21a- <i>parBc</i>	pET21a derived vector, allowing overexpression of ParBc in <i>Ec</i>	this study
pET21a- <i>parBm</i>	pET21a derived vector, allowing overexpression of ParBm in <i>Ec</i>	this study
pMK <i>sgfp</i>	pMK18 derived vector, allowing expression of sGFP in <i>Ec</i> and <i>Tth</i>	this study

---



---

pMK <i>parBc-sgfp</i>	pMK18 derived vector, allowing expression of <i>parBc-sGFP</i> in <i>Ec</i> and <i>Tth</i>	this study
pMK <i>parBm-sgfp</i>	pMK18 derived vector, allowing expression of <i>parBm-sGFP</i> in <i>Ec</i> and <i>Tth</i>	this study
pUC- $\Delta$ <i>mreB::kat</i>	allele exchange vector for generating $\Delta$ <i>mreB</i> in <i>Tth</i>	this study
pCT3FK	vector used for construction of the <i>Tth</i> heterozygous strain HL01	Angelov <i>et al.</i> , 2008
pJ- <i>pyrFE</i>	intermediate vector for generating pJ- $\Delta$ <i>pyrE::blm</i>	this study
pJ- $\Delta$ <i>pyrE::blm</i>	vector used for construction of the <i>Tth</i> heterozygous strain HL01	this study

---

\* *Tth*, *T. thermophilus*; *Ec*, *E. coli*; Amp<sup>R</sup>, ampicillin resistant; Blm<sup>R</sup>, bleomycin resistant; Km<sup>R</sup>, kanamycin resistant; *Tth* (*repA*), replicaton origin for *Tth*; *Ec* (*oriE*), replication origin for *Ec*; *ori* pUC, replication origin for pUC18.

The detailed plasmid construction methods are as follows:

For construction of the plasmid pT- $\Delta$ 42, a 3.3 kbp region containing the *T. thermophilus* HB27 *bgl* gene (TT\_P0042) and flanking sequences was amplified by PCR with primers 42.F and 42.R (primer sequences are listed in Table S1) and cloned in the pCR2.1-TOPO vector (Invitrogen, Carlsbad, USA). Next, two BglII restriction sites were introduced in this vector at nucleotide positions 13 and 1289 relative to the start codon of the *bgl* gene by site-directed mutagenesis, using the oligonucleotides 42m-Bgl.F and 42m-Bgl. R (Change-IT Multiple Mutation Site Directed Mutagenesis Kit, Affymetrix, Santa Clara, USA). Restriction with BglII followed by vector re-ligation gave pT- $\Delta$ 42, where the complete TT\_P0042 ORF was deleted (amino acid positions 3 to 430). For the construction of pTKO-4, the *kat* and *bgl* sequences were amplified from pMK18 and HB27 genomic DNA, respectively using primers that generate sufficient overlap between them to permit cloning by Gibson assembly (Gibson *et al.*, 2009) (New England Biolabs). The three-fragment Gibson assembly reaction consisted of the *kat* and *bgl* PCR products and the SapI digested pUC18, giving pTKO-4. The allelic exchange vector

pTKO- $\Delta 340$  was obtained by first generating the  $\Delta 340$  allele by PCR, cloning of the PCR product in pCR2.1-TOPO and site-directed mutagenesis by a strategy similar to the one used for the pT- $\Delta 42$ , leading to the deletion of the sequence corresponding to *T. thermophilus* HB27 chromosome nucleotide positions 323,715 to 325,194. The 1295 bp *AvrII* fragment from pT- $\Delta 340$ , containing upstream and downstream sequences of ORFs TT\_C0340-0341, was then cloned in the *XbaI* site of pTKO-4, yielding pTKO- $\Delta 340$ .

The plasmid pUC- $\Delta parABc::kat$  was an allele exchange vector for generating  $\Delta parABc$  in *T. thermophilus* HB27. The two flanking regions the *parABc* genes, and *kat* were respectively PCR amplified from *T. thermophilus* HB27 genomic DNA and pMK18 plasmid DNA, using primer pairs *parABc*-1-F/*parABc*-1-R, *parABc*-2-F/*parABc*-2-R, *kat*-1-F/*kat*-1-R, the primers generated PCR fragments containing sufficient overlaps between each other to permit cloning by Gibson assembly (Gibson et al., 2009) (New England Biolabs). The four-fragment Gibson assembly reaction was consisted of the purified PCR products of the two flanking regions, *kat* and *XbaI* digested pUC18. The following plasmids were all constructed via Gibson assembly. The plasmid pUC- $\Delta parABm::blm$  was an allele exchange vector attempted to generate  $\Delta parABm$  in *T. thermophilus*. The *blm* cassette was used as a selection marker (chemically synthesized using sequence data from Brouns *et al.* (2005), and cloned in pMB18), and the primers used for amplification of the *parABm* flanking regions, and *blm* were *parABm*-1-F/*parABm*-1-R, *parABm*-2-F/*parABm*-2-R, *blm*-1-F/*blm*-1-R, respectively. The plasmid pUC- $\Delta parAmN-1$  was an allele exchange vector to replace the N-terminal region of *parAm* with the *blm* cassette opposing *parABm* transcription direction in *T. thermophilus* (mutant  $\Delta parAmN-1$ ). The two flanking regions of *parAmN* and *blm* were PCR amplified by primer pairs *parAmN*-1-F/*parAmN*-1-R, *parAmN*-2-F/*parABm*-2-R, *blm*-2-F/*blm*-2-R, respectively, and the fragments were introduced in to *XbaI* digested pUC18. The plasmid pUC- $\Delta parAmN-2$  was designed to replace the N-terminal region of *parAm* with *blm* co-linear with the *parABm* transcription direction in *T. thermophilus* (mutant  $\Delta parAmN-2$ ). The cloning method and flanking regions were the same as those of pUC- $\Delta parAmN-1$ , except for *blm*

was PCR amplified by different primer pairs (blm-3-F/blm-3-R). The plasmid pUC- $\Delta$ parBm::blm was attempted to exchange parBm with blm in *T. thermophilus*. The primer pairs for amplifying the two flanking regions of parBm, and blm were parABm-1-F/parBm-1-R, parBm-2-F/parBm-2-R, and blm-4-F/blm-4-R, respectively. The three fragments were introduced into XbaI digested pUC18. The plasmids pMK-parAm and pMK-parBm were replicative vectors derived from pMK18, they permitted overexpressions of ParAm and ParBm in *T. thermophilus*, respectively (strains TMP01 and TMP02, respectively). The backbone pMK18 was PCR amplified by primers pMK-1-F/pMK-1-R, and the parAm, parBm coding sequences with stop codons and native RBS regions were PCR amplified using primers parAm-F/parAm-R, parBm-1-F/parBm-1-R, respectively. The plasmid pUC- $\Delta$ mreB::kat was an allele exchange vector for generating  $\Delta$ mreB in *T. thermophilus* HB27. The primer pairs for amplifying the two flanking regions of mreB, and kat were mreB-1-F/mreB-1-R, mreB-2-F/mreB-2-R, and kat-2-F/kat-2-R, respectively. The three fragments were introduced into XbaI digested pUC18.

The plasmids pET21a-parBc and pET21a-parBm were pET21a based expression vectors permitting the expression of recombinant ParBc and ParBm proteins under the control of PT<sub>7</sub> promoter in *E. coli*, respectively. The parBc and parBm fragments were PCR amplified by primer pairs parBc-F/parBc-R, parBm-2-F/parBm-2-R, respectively. The corresponding vector was obtained by assembling parBc or parBm fragment carrying 5' and 3' overlaps, into XhoI, NdeI linearized pET21a by Gibson assembly.

The plasmid pMKsgfp was derived from pMK18, in which the sgfp coding sequence (chemically synthesized using sequence data from Cava *et al.* (2008)) was transcriptionally fused to the kat cassette of pMK18. The plasmids pMKparBc-sgfp and pMKparBm-sgfp were replicative vectors allowing expressions of ParBc-sGFP and ParBm-sGFP in *T. thermophilus* and *E. coli* cells, respectively. For C-terminal fusion, the pMKsgfp construct was used, the backbone sequence was PCR amplified from the positions relative to the second codon of sgfp and the stop codon of kat (primers pMKfp-F and pMKfp-R). Except for the stop codon sequences, the full lengths and the native RBS regions of parBc, parBm genes were PCR amplified with

primers creating sufficient overlaps of the pMK.*sgfp* backbone (parBcfp-F/parBcfp-R and parBmfp-F/parBmfp-R, respectively), and the fusions were performed by Gibson assembly. For better protein folding purpose, codons encoding four glycine residues (poly-glycine linker) were introduced between *parB* and *sgfp*. The ParB-sGFP fusions were expressed under the *kat* promoter.

The plasmid pCT3FK was an *E. coli*/*T. thermophilus* shuttle fosmid vector (without insert) derived from the fosmid pCC1FOS (CopyControl Fosmid Library Production Kit, Epicentre) (Angelov *et al.*, 2008). It contained *kat* cassette sandwiched by the two flanking regions of the chromosomally located *pyrE* gene, and used for the construction of the *T. thermophilus* heterozygous strain HL01. For the construction of the plasmid pJ- $\Delta$ *pyr::blm*, the 2.3 kbp PCR-amplified *pyr* region was cloned in pJET1.2, followed by introduction of two NdeI sites by mutagenesis (Change-IT Multiple Mutation Site Directed Mutagenesis Kit, Affymetrix, Santa Clara, USA) at positions -3 and +556 relative to the start codon of *pyrE*, giving pJ-*pyrFE*. The *pyrE* gene in pJ-*pyrFE* was replaced by the *blm* resistance marker by digesting pJ-*pyrFE* with NdeI, DNA end-blunting (Quick Blunting Kit, NEB, Ipswich, USA) and ligation of *blm*-carrying DNA fragment which was blunted the same way. It was used for the construction of the *T. thermophilus* heterozygous strain HL01.

### 2.1.2 Growth media

Liquid media were prepared in bidistilled water or high-carbon mineral water (purania, DRINKPOOL GmbH, Germany) and autoclaved at 120 °C for 20 min. Solid media were prepared with the addition of 18 g/l bacteriological agar (Roth, Karlsruhe, Germany) before autoclaving. Substrates that are sensitive to autoclaving such as antibiotics or sugars were sterilized by filtration (0.2 µm, Sartorius Stedim, Aubagne, France) and added to the media after autoclaving at a medium temperature lower than 60 °C .

For *E. coli* and *B. subtilis* strains

LB medium (Sambrook *et al.*, 1989):

Tryptone 10 g

Yeast extract 5 g

NaCl 5 g

dd H<sub>2</sub>O up to 1000 ml

When required, antibiotics, IPTG were added after autoclaving at concentrations described in Table 3.

Table 3. Media additives for LB medium.

Additive	Abbr.	Stock solutions *	Working concentration
Ampicilin	Amp	100 mg/ml in water	100 µg/ml
Bleomycin	Blm	10 mg/ml in water	3 µg/ml
Kanamycin	Km	50 mg/ml in water	20 µg/ml
Chloramphenicol	Cm	25 mg/ml in ethanol	12 µg/ml
Isopropyl- β-d -thiogalactopyranosid	IPTG	100 mM in water	1 mM

\*The stock solutions were sterilized by filtration, aliquoted in 1.5 ml volumes and stored at -20 °C.

For *T. thermophilus*

TB medium:

Trypticase peptone 8 g

Bacto yeast extract 4 g

NaCl 3 g

Mineral H<sub>2</sub>O (purania, DRINKPOOL GmbH, Germany) up to 1000 ml

The pH was adjusted to 7.5 with Sodium hydroxide (NaOH) and hydrochloric acid (HCl). When required, antibiotics, substrates were added after autoclaving at concentrations described in Table 4.

Table 4. Media additives for TB and SH media.

Additive	Abbr.	Stock solution	Working concentration
Bleomycin	Blm	10 mg/ml in water	15 µg/ml
Kanamycin	Km	50 mg/ml in water	20 µg/ml
5-bromo-4-chloro-3-indolyl β-d-glucopyranoside	XGlc/ BCI-β -glu	50 mg/ml in DMF	50-500 µg/ml
5-bromo-4-chloro-3-indolyl β-d-galactopyranoside	XGal	50 mg/ml in DMF	50 µg/ml

SH medium:

- Required solutions

100 µg/ml Biotin: prepared in dd H<sub>2</sub>O, sterilized by filtration

1 mg/ml Thiamin: prepared in dd H<sub>2</sub>O, sterilized by filtration

0.05 M Molybdenum solution: 1.2 g Na<sub>2</sub>MoO<sub>4</sub> · 2H<sub>2</sub>O prepared in 100 ml dd H<sub>2</sub>O, sterilized by filtration

0.05 M Vanadium solution: 0.1 g VOSO<sub>4</sub> · 3H<sub>2</sub>O prepared in 100 ml dd H<sub>2</sub>O, sterilized by filtration

0.025 M Manganese solution: 0.5 g MnCl<sub>2</sub> · 4H<sub>2</sub>O prepared in 100 ml 0.01 N HCl

Copper/Zinc solution: 60 mg ZnSO<sub>4</sub> · 7H<sub>2</sub>O, 15 mg CuSO<sub>4</sub> · 5H<sub>2</sub>O, prepared in 100 ml dd H<sub>2</sub>O, sterilized by filtration

Solution B: 12.5 g MgCl<sub>2</sub> · 6H<sub>2</sub>O, 2.5 g CaCl<sub>2</sub> · 2H<sub>2</sub>O, prepared in 100 ml dd H<sub>2</sub>O, autoclaved at 121 °C, 20 min, stored at 4 °C

Solution C: 6.0 g FeSO<sub>4</sub> · 7H<sub>2</sub>O, 0.8 g CoCl<sub>2</sub> · 6H<sub>2</sub>O, 20 mg NiCl<sub>2</sub> · 6H<sub>2</sub>O, prepared in 100 ml 0.01 NH<sub>2</sub>SO<sub>4</sub>

20% Sucrose solution: 20 g sucrose prepared in 100 ml dd H<sub>2</sub>O, sterilized by filtration

- Medium preparation

K<sub>2</sub>HPO<sub>4</sub> 0.75g

KH<sub>2</sub>PO<sub>4</sub> 0.25 g

NaCl 2.0 g

(NH<sub>4</sub>)<sub>2</sub>SO<sub>4</sub> 2.5 g

Casamino acids 5.0 g

100 µg/ml Biotin 1.0 ml

1 mg/ml Thiamin 1.0 ml

Added 800 ml dd H<sub>2</sub>O, adjusted pH to 7.2

Added 0.05 M Molybdenum solution 100 µl, 0.05 M Vanadium solution 100 µl,  
0.025 M Manganese solution 100 µl, Copper/Zinc solution 100 µl

Added dd H<sub>2</sub>O up to 974 ml

Autoclaved at 121 °C, 20 min

Added 25 ml 20% Sucrose solution, 1 ml Solution B, and 100 µl Solution C

For the bacterial species listed in Table 6

HD medium:

Peptone 10 g

Yeast extract 5 g

Glucose 5 g

NaCl 8 g

dd H<sub>2</sub>O up to 1000 ml

The pH was adjusted to 7.5 with Sodium hydroxide (NaOH) and hydrochloric acid (HCl). The substrates BCI-β-glu, BCI-β-gal, BCI-α-glu and BCIP were supplemented at 0, 100 and 500 µg/ml.

BHI/NaCl:

BHI powder (Sigma) 37 g

dd H<sub>2</sub>O up to 1000 ml

The substrates BCI-β-glu was supplemented at 0, 100 and 500 µg/ml.

### 2.1.3 Growth conditions

*E. coli*, *B. subtilis*, and *T. thermophilus* were cultured in both liquid and on solid

meida. *E. coli* cultures used for mini-plasmid preparation were inoculated from single colonies and grown in 5 ml standard test tubes. *T. thermophilus* cultures for normal DNA manipulation and microscopy were grown in 15 ml falcon tubes; for growth curve measurements, they were grown in 100 ml Erlenmeyer flasks with culture volumes of 30 mls. *B. subtilis* liquid cultures were all grown in standard test tubes. For optimal aeration, the cultures in Erlenmeyer flasks were incubated on a flat-deck rotary shaker while the test tubes and falcon tubes were agitated on racks with fixed 40 degree angle to the shaking surface at 180 rpm. For the cultivations of organisms on solid media, 92 mm disposable plastic plates were used (Sarstedt, Nümbrecht, Germany), prepared as follows: 1.8% (w/v) agar was added to the liquid media before autoclaving. After autoclave, the media containing agar were left to cool down to 60 °C, and if necessary, supplemented with additives before pouring into sterile plates. Dependent on need, *E. coli* and *B. subtilis* cultures were incubated at 37 °C or 30 °C. *T. thermophilus* cultures were incubated at 70 °C, except for the case when antibiotics were supplemented in the media (60 °C). Furthermore, *T. thermophilus* agar plates were wrapped up air-tightly to prevent them from drying out.

### 2.1.4 Storage of strains and control of purity

Frequently used *E. coli* and *T. thermophilus* strains were maintained on LB and TB agar plates respectively, which could be stored at 4 °C up to 2 months. For long-term storage, bacterial strains were stocked at -70 °C as glycerol cultures. In detail, 0.7 ml of fresh overnight culture grown in complex media in the presence of selective pressure if required, was mixed with an equal volume of 50% (w/v) autoclaved glycerol. In this manner, although with moderate viability loss, the stock cultures were stable over years. Before using the strains from glycerol stocks, their purity was checked. To this end, the strains were streaked on both selective and non-selective agar plates and checked for the uniformity of the colonies. The plasmid-containing strains were additionally checked by plasmid preparation and analytical restrictions.



## 2.2 DNA manipulations

### 2.2.1 General techniques

Before DNA manipulation, the potential DNA-degrading enzymes of the tools and solutions should be inactivated. Vessels and solutions were autoclaved (20 min, 120 °C), tools that are not autoclavable were first rinsed with 70% (w/v) ethanol and subsequently with sterile dd H<sub>2</sub>O. Non-autoclavable or heat-unstable substances (e.g. lysozyme, proteinase K) were dissolved in sterile buffers or water.

### 2.2.2 DNA isolation, purification and quality evaluation

#### 2.2.2.1 Plasmid DNA isolation from *E. coli*

*E. coli* cultures for plasmid preparation were cultivated in 5 ml LB media with antibiotics. The cells from 4 ml culture were pelleted at the bottom of 2 ml reaction tubes by centrifugation in RT (13000 rpm/min, 5 min). The pellet was completely resuspended in 250 µl resuspension buffer (P1). 250 µl lysis buffer (P2) was added into the cell suspension and mixed gently by inverting the tube for several seconds or until the mixture was clear to ensure an efficient cell lysis. Rapidly added 350 µl of the neutralization solution (P3) to the samples and mixed gently by inverting the tubes, and followed by centrifugation (13000 rpm/min, 10 min, RT). The supernatant containing the plasmid DNA was mixed with 0.7 volume of isopropanol, and incubated 15 min on ice (alternatively, 20 min at -20 °C). The precipitated DNA was further pelleted by centrifugation (13000 rpm/min, 15 min, 4 °C). The pellet was washed twice with 70% (v/v) ethanol and centrifuged shortly (13000 rpm/min, 1 min, RT) before decanting the ethanol. The remaining ethanol was carefully pipetted out and the pellet was dried for 5-10 min to allow the evaporation of the remaining ethanol. The plasmid DNA used for transformation of *T. thermophilus* cells or sequencing, was purified by AccuPrep Plasmid Extraction Kit (Bioneer, Daejeon, Korea). The purification procedure was performed according to the manufacturer's instructions. The isolated plasmids were analyzed by restriction digestion and agarose gel electrophoresis.

#### **2.2.2.2 Genomic DNA isolation**

Genomic DNA of *T. thermophilus* cells was isolated using Master Pure™ Complete DNA & RNA Purification Kit (Epicentre, Madison, USA) according to the manufacturer's guides. Briefly, 4 ml overnight well-grown culture was used for cell pellet collection, after cell lysis, elimination of proteins and other cell components was processed, the DNA in the supernatant was precipitated by 0.7 volume of isopropanol followed by incubation at -20 °C for 20 min, and centrifugation at 4 °C (13000 rpm/min, 15 min). The DNA pellet was washed twice with 70% (v/v) ethanol, after brief centrifugation (13000 rpm/min, 1 min, RT), the ethanol was decanted, and the pellet was left for drying before dissolved with 50 µl of sterile dd H<sub>2</sub>O. The quality and amount of the isolated DNA were checked by agarose gel electrophoresis and spectrophotometric method (Nanodrop ND-1000, PeQlab, Erlangen, Germany).

#### **2.2.2.3 DNA isolation from agarose gels**

The procedure allowing isolation of target DNA fragment from a mixture of linear DNA molecules by agarose gel extraction is as following text described. DNA restriction mixtures or PCR products were first separated slowly on agarose gels, which permit target fragments to separate from others because of the differed molecular sizes. After staining the gel with ethidium bromide, parts of the gel containing the target fragments were sliced out and subjected to DNA isolation with the QIAquick Gel Extraction Kit (QIAGEN, Hilden, Germany). The extraction procedure was performed based on the manufacturer's instructions and the DNA was eluted with 30-50 µl of sterile dd H<sub>2</sub>O by centrifugation (13000 rpm/min, 2 min, RT). The purity and the concentration of the isolated fragments were checked on analytical agarose gels and spectrophotometric method.

#### **2.2.2.4 Direct PCR product purification**

In the cases that the PCR products shown highly pure bands on agarose gels, direct PCR product purification was implemented. The process was performed by AccuPrep PCR Purification Kit (Bioneer, Daejeon, Korea) obeying the instructions provided by the manufacturer. Before applying the purified PCR products, their

purity and concentration were also analyzed.

#### **2.2.2.5 DNA analysis using agarose gel electrophoresis**

For normal DNA electrophoresis, the horizontal mini gel apparatus (Pharmacia) holding a gel size of 10 x 6.6 x 0.8 cm was used. The matching combs could create 16 or 25 slots per gel. The agarose concentration in the gel could vary from 0.8 to 3.0% (w/v), hinging on the sizes of the target DNA fragments. Before loading to the gel pockets, samples were mixed in a ratio of 5:1 with 6 x Loading Dye (Thermo Scientific, St. Leon-Rot, Germany). 1 kb or 50 bp DNA ladder (Thermo Scientific, St. Leon-Rot, Germany) was used to weigh the correct sizes of the target DNA fragments. The running buffer of electrophoreses was 1 x TAE buffer that was diluted from 50 x stocking solution, and a constant voltage of 100 V (BioRad Power Pac 300 power supply) was applied for running. For visualization of the DNA, the gels were stained in an ethidium bromide solution (1.5 µg/ml in water) for 5-10 min, followed by rinsing with dd H<sub>2</sub>O. The DNA was visualized under UV light and the gel documentation was performed by a gel documentation device (AlphaImager Mini, Biozym, Oldendorf, Germany) and the corresponding software.

##### 50 x Tris-acetate-EDTA (TAE) buffer

Tris base 242 g

Glacial acetic acid 57.1 ml

EDTA 18.6 g

dd H<sub>2</sub>O up to 1000 ml

#### **2.2.2.6 DNA quantification**

The concentration of DNA was determined by spectrophotometric method (Nanodrop ND-1000, PeQlab, Erlangen, Germany). Alternatively, agarose gel electrophoresis was also used for quantification by measuring and comparing the bands' intensity of the target fragments and those of the marker bands which have defined concentrations (Image J, NIH, USA). This quantity estimation method was also used for the direct comparison of the DNA amounts in different samples.

### 2.2.2.7 DNA sequencing

To verify the accuracy of DNA sequences, DNA samples were sent for sequencing (GATC Biotech, Germany). The resulting sequences were analyzed by comparing with the reference sequences using Clone Manager 9.0 (Scientific & Educational Software, USA)

### 2.2.3 Enzymatic modification of DNA

#### 2.2.3.1 Restriction

In the case that the DNA constructs were only used for analyzing purpose, small scale of analytical digestion reactions were set up.

##### Analytical digestion reaction

DNA solution x  $\mu$ l (up to 1  $\mu$ g)

10 x reaction buffer 1  $\mu$ l

Restriction enzyme x  $\mu$ l (2-5 U)

dd H<sub>2</sub>O up to 10  $\mu$ l

The digestion reactions were incubated at the optimal temperatures suggested for the restriction enzymes, thereby rendering efficient digestions. Normally, the digestions were processed for 2 h before being analyzed by agarose gel electrophoresis.

If the fragments from the digestion reactions were used for further cloning procedures, the reaction systems were scaled up as follows:

##### Preparative digestion reaction

DNA solution x  $\mu$ l (up to 10  $\mu$ g)

10 x reaction buffer 5  $\mu$ l

Restriction enzyme x  $\mu$ l (10-25 U)

dd H<sub>2</sub>O up to 50  $\mu$ l

The digestion reactions were performed at the enzymes' optimal temperatures. For a complete digestion, 4-16 h should be consumed. When performed digestions with two enzymes, the universal double digestion buffer system was applied (Thermo Scientific, St. Leon-Rot, Germany), or the DNAs were digested sequentially with

purification and buffer changes between the steps.

### 2.2.3.2 Dephosphorylation of linearized DNA

To avoid recircularization during ligation, dephosphorylation of cloning vector DNA was necessary. Alkaline phosphatase catalyzed the release of 5'- and 3'-phosphate groups from DNA. After digestion and preparative agarose gel purification, the linearized vector DNA was exposed to Fast AP Thermosensitive Alkaline Phosphatase (Thermo Scientific, St. Leon-Rot, Germany). The reaction mixtures were set up as the instructions provided by the manufacturer, followed by incubation at 37 °C for 10-20 min. After heat inactivated the enzyme at 75 °C for 5 min, the dephosphorylated vector DNAs were directly used for further ligation step.

### 2.2.3.3 Ligation

The ligation of DNA fragments into plasmid vector was accomplished by bacteriophage T4 ligase. Since the intramolecular religation between the two ends of one DNA molecule might also occur, the molar ratio between foreign DNA fragment (insert) and the linearized vector was adjusted. In normal case, the molar concentration of the insert DNA should exceed that of the vector DNA at least 3-fold. Based on the manufacturer's instructions (Thermo Scientific, St. Leon-Rot, Germany), the ligation reaction was prepared as follows:

#### Ligation reaction

Linear vector DNA    x  $\mu$ l (20-100ng)

Insert DNA    x  $\mu$ l (3:1 molar ratio over vector DNA)

10 x T4 DNA ligase buffer    2  $\mu$ l

T4 ligase    1  $\mu$ l

dd H<sub>2</sub>O    up to 20  $\mu$ l

The ligation was incubated at 16 °C up to 16 h.

### 2.2.3.4 Gibson Assembly of DNA fragments

Another used method that permit introduction of foreign DNA fragments (inserts) into linearized vector DNA was Gibson assembly (Gibson *et al.*, 2009) (New England Biolabs). Gibson assembly efficiently joins DNA fragments containing overlapping

sequences at 5'- or 3'- end in a single reaction isothermally (Gibson *et al.*, 2009), therefore, it permits successful assembly of multiple DNA fragments, regardless of fragment length or end compatibility. According to the manufacturer's instructions, Gibson assembly mixture was prepared on ice as follows:

### 2-4 fragment assembly

Total amount of fragments 0.02-0.2 pmols\*

2 x Gibson Assembly Master Mix 10  $\mu$ l

dd H<sub>2</sub>O up to 20  $\mu$ l

\* 50-100 ng of vectors with 2-3 fold excess of inserts

The reaction mixture was incubated at a thermocycler at 50 °C for 1 h. Following incubation the mixture was stored on ice or -20 °C for subsequent transformation.

### **2.2.4 *In vitro* DNA amplification**

For cloning and analytical purposes, PCR reactions were used for the *in vitro* amplification of DNA fragments. The normal primers used for amplification were designed to have between 19 to 22 bp homology with the target sequence and GC contents between 40 and 60% if possible. The primers used for Gibson assemblies contained additional 18 to 22 bp sequence for generation of overlaps for the amplicons. The primers used were synthesized by Eurofins MWG Operon (Ebersberg, Germany). All primers used are listed in the Appendix Table.

#### **2.2.4.1 Analytical PCR**

To confirm the genotypes of bacterial strains or to check different DNA constructs, analytical PCR reactions were performed, and *Taq* DNA polymerase was used (Dream *Taq* DNA polymerase, Thermo Scientific, St. Leon-Rot, Germany). The PCR reactions were set up in 0.2 ml plastic tubes, the reaction volumes were between 20 and 50  $\mu$ l. Reaction mix was prepared as follows :

#### Analytical PCR reaction (50 $\mu$ l reaction system)

10 x Dream *Taq* buffer 5  $\mu$ l

dNTP mix (2 mM each) 5  $\mu$ l

primer A (10 pmol/ $\mu$ l) 5  $\mu$ l  
primer B (10 pmol/ $\mu$ l) 5  $\mu$ l  
Dream *Taq* polymerase 0.5  $\mu$ l  
Template DNA 1  $\mu$ l  
dd H<sub>2</sub>O 28.5  $\mu$ l

PCR conditions

Initial denaturation 95 °C, 3 min  
Three-step cycles (30 x):  
Denaturation 95 °C, 30 sec  
Annealing T<sub>m</sub>-5, 30 sec  
Extension 72 °C, 1 min/kb  
Final extension 72 °C, 10 min  
Store 4 °C

The obtained PCR products were analyzed by agarose gel electrophoresis.

**2.2.4.2 Preparative PCR**

For generation of high-fidelity PCR fragments aimed for cloning, preparative PCR reactions were performed, and *pfu* DNA polymerase was used (Thermo Scientific, St. Leon-Rot, Germany). *Pfu* DNA polymerase exhibits 3' to 5' exonuclease (proofreading) activity that enables the polymerase to correct nucleotide incorporation errors. The *pfu*-PCR reaction procedure was:

Preparative PCR reaction (50  $\mu$ l reaction system)

10 x *Pfu* buffer with MgSO<sub>4</sub> 5  $\mu$ l  
dNTP mix (2 mM each) 5  $\mu$ l  
primer A (10 pmol/ $\mu$ l) 5  $\mu$ l  
primer B (10 pmol/ $\mu$ l) 5  $\mu$ l  
*Pfu* polymerase (2.5 u/ $\mu$ l) 1  $\mu$ l  
Template DNA 1  $\mu$ l  
dd H<sub>2</sub>O 37  $\mu$ l

### PCR conditions

Initial denaturation 95 °C, 3 min

Three-step cycles (30 x):

Denaturation 95 °C, 30 sec

Annealing  $T_m-5$ , 30 sec

Extention 72 °C, 2 min/kb

Final extension 72 °C, 10 min

Store 4 °C

The obtained PCR products were analyzed by agarose gel electrophoresis and further subjected to purification and cloning as described.

### **2.2.4.3 Quantitative PCR**

Real-time quantitative PCR to quantify genome copy number was essentially performed according to the method described (Breuert *et al.*, 2006). The aim of this method is to determine the average DNA molecule number in a cell lysate. The general line is: harvest cells and lyse them completely; dilutions of the cell lysates are used directly as templates in Real-time PCR assays; average genome copy number of the cell lysate is quantitated by comparing the results with a standard curve created from dilution series of a PCR product with known concentration.

The amplification loci were chosen based on need, a standard curve was required for each chosen locus. For generation of a standard curve, an approximately 1 kbp standard fragment of the target locus was PCR amplified using isolated DNA as template. The fragment was then purified from a preparative agarose gel and photometrically quantified. The molar concentration of the fragment was calculated based on the DNA concentrations and the sequences. A series of dilutions containing defined numbers of standard molecules were prepared, and 5  $\mu$ l aliquots were used as templates for real-time PCR. The cell cultures prepared for genome copy number quantification were reinoculated for three times to ensure they were exponentially growing cells. Cell extracts for qPCR were prepared by harvesting defined cell numbers (determined by spectrophotometric method and Neubauer counting chamber) from exponentially growing cultures, and resuspending in 250  $\mu$ l cell lysis buffer (Epicentre Biotechnologies, Hesisch Oldendorf, Germany), the cell lysis



efficiency was considered when analyzed the total cell numbers in the reactions. After dialysis, a series of dilutions were prepared from the cell lysates, and aliquots were used as templates. To ensure the amplification efficiency was the same between using genomic DNA as templates and standard PCR products as templates, dilution serials of PCR standards were added to the cell lysates to verify the efficiency. No template control group was also included. For qPCR, the sizes of the target amplicons were between 100 and 200 bp, and qPCR Mastermix plus with fluorescein (Eurogentec, Köln, Germany) was used. The PCR was performed in "iCycler" thermal cycler (Bio-Rad, Germany), and the conditions were 95 °C 10 min, 40 cycles with 15 sec 95 °C, 30 sec 60 °C, 30 sec 72 °C followed by 55 °C 1 min and a melt curve analysis from 55 °C to 95 °C in 0.5 °C steps. Three independent experiments were carried out for each dilution serial. Standard curves were constructed from the  $C_t$  values of the standards and were later used to quantitate the genome copy numbers in the cell lysates.

### **2.2.5 Southern hybridization**

Southern hybridization was used for verifying the genotype of the bacterial strains. The general procedure of Southern blot was based on Molecular Cloning (Sambrook and Russel, 2001). Specific steps are shown as follows:

- Required solutions

Depurination solution: 0.15 M HCl

Denaturation solution: 1.5 M NaCl, 0.5 M NaOH

Neutralization solution: 1.5 M NaCl, 0.5 M Tris-HCl (pH 7.2), 1 mM EDTA

20 x SSC, pH 7.0 (transferring buffer): 3 M NaCl, 0.3 M sodium citrate

50 x Denhardt's solution: 1% (w/v) BSA, 1% (w/v) Ficoll™, 1% (w/v) PVP (polyvinylpyrrolidone) (Life Technologies)

Pre-hybridization solution: 6 x SSC, 5 x Denhardt's solution, 50% formamide, 0.5% SDS

- Genomic DNA digestion

For Southern hybridization purpose, considerable amount of high-quality

genomic DNA was required. The restriction enzyme was selected based on specific need. The digestion mixture was set up with a 30  $\mu$ l reaction volume:

Genomic DNA digestion reaction for Southern hybridization

Genomic DNA solution    x  $\mu$ l (10-15 $\mu$ g)

10 x reaction buffer    3  $\mu$ l

Restriction enzyme    x  $\mu$ l (25-50 U)

dd H<sub>2</sub>O    up to 30  $\mu$ l

In order to obtain a complete digestion, the reaction mixture was incubated at the optimal temperature for the enzyme activity for 14-16 h.

- Agarose gel electrophoresis

The agarose gel for blotting should be much thicker to avoid damage. After complete digestions, the genomic DNA probes were mixed with 6 x DNA loading Dye (5:1 ratio), accompanying with DNA markers, they were loaded in the slots of a 0.8% agarose gel individually. The gel was run with a constant voltage of 80 V for 2 h, which allowed an efficient fragment-separation.

- Southern blotting

The transferring of the separated DNA from the agarose gel to a nylon membrane was processed by a Vacuum Blotter guided by the user manual (Bio-Rad Life Science). The nylon membrane used (SensiBlot plus nylon membrane, Thermo Scientific, St. Leon-Rot, Germany) was cut with a size slightly larger than the agarose gel. The following steps were followed for DNA pre-treatment, blotting, and fixation. The solutions used were poured on the top of the gel:

(1) Depurination of the DNA with 0.15 M HCl, until the blue bromophenol colour turned into yellow (10-20 min).

(2) Rinsed the gel with dd H<sub>2</sub>O, twice.

(3) Denatured the DNA with denaturation solution for 15 min, twice.

(4) Rinsed the gel with dd H<sub>2</sub>O, twice.

(5) Neutralized the DNA with neutralization solution for 15 min, twice.

(6) 20 x SSC was used for DNA transferring, and the blotting procedure was last for 2 h with addition of the solution every 20 min to avoid drying out.

(7) After blotting, the DNA was further fixed on the membrane under UV light for 1-2 min, and the membrane was used directly for hybridization or stored at -20 °C for later use.

- Generation of labeled probes

The DNA template for probe labeling was PCR amplified with a size between 0.4-1.2 kbp. After purification and quantification, the fragment was labeled via random-primed method (Biotin Decalabel DNA labeling Kit, Thermo Scientific, St. Leon-Rot, Germany). The labeling process was performed in a 1.5 ml microcentrifuge tube according to the manufacturer's protocol:

DNA template (100 ng-1µg) x µl

Decanucleotide in 5 x Reaction Buffer 10 µl

dd H<sub>2</sub>O up to 44 µl

Vortexed the tube and spined down in a microcentrifuge for 3-5 s. Boiled the tube in a boiling water bath for 5-10 min, and quickly spined down followed by cooling on ice.

Added the following components in the same tube:

Biotin Labeling Mix 5 µl

Klenow fragment, exo- (5 U) 1 µl

Mixed thoroughly and spined down in a microcentrifuge for 3-5 s. Incubated the reaction at 37 °C for at least 5 h, up to 20 h could increase the yield of labeled DNA.

Stopped the reaction by addition of 1 µl of 0.5 M EDTA, pH 8.0. The labeled DNA was used directly for hybridization or stored at -20 °C.

- Hybridization

The prepared DNA-containing nylon membrane was placed into a hybridization tube, added 10 ml pre-hybridization solution and pre-hybridize for 1 h at 42 °C with rotation in a hybridization oven (Hybrid 2000, Helmut Saur, Reutlingen, Germany). Denatured the labeled probe in a boiling water bath for 5-10 min followed by

chilling on ice for 5 min, and pipetted into the pre-hybridization solution with caution to avoid splashing to the membrane. The hybridization was performed at 42 °C with rotation for up to 16 h. The reaction was stopped by discarding the hybridization solution and proceeding by membrane washing. The following washing steps were carried out:

Twice in 2 x SSC + 0.1% SDS for 10 min at RT

Twice in 0.1 x SSC + 0.1% SDS for 10 min at 65 °C

- Signal detection

The biotin-labeled probe-target hybrids were detected with alkaline phosphatase-conjugated streptavidin (Biotin Chromogenic Detection Kit, Thermo Scientific). The principle of this detection is, alkaline phosphatase (AP) conjugated streptavidin binds to the biotin-labeled probe-target hybrids, and results in the formation of an insoluble blue precipitate would appear as a well-defined spot or band at the reaction site on the membrane. The detection procedure was performed exactly as the protocol provided by the manufacturer (Biotin Chromogenic Detection Kit, Thermo Scientific, St. Leon-Rot, Germany).

- Signal documentation

The documentation of signals appeared on Southern hybridization membrane was processed by scanning with a scanner (ScanMaker 1000X1 Microtek, Willich, Germany) and its corresponding software.

### 2.2.6 Pulsed field gel electrophoresis

The method pulsed-field gel electrophoresis (PFGE) was used to separate chromosome and megaplasmid of *T. thermophilus* strains. Essentially, the protocol used was based on Herschleb *et al.* (2007). Specific steps are as follows:

- Required solutions

TE buffer: 10 mM Tris, 1 mM EDTA (pH 8.0)

NDSK buffer: 0.5 M EDTA, 1% (w/v) N-laurylsarcosine (Sigma), 1 mg/ml Proteinase K (Epicentre Biotechnologies)

TNE buffer: 10 mM Tris, 200 mM NaCl and 100 mM EDTA (pH 7.2)

EC lysis buffer: 6 mM Tris-HCl (pH 7.6), 1 M NaCl (w/v), 100 mM EDTA, 0.5% (w/v) Brij-58 (polyoxyethylene 20 cetyl ester; Sigma), 0.2% (w/v) deoxycholate, 0.5% (w/v) N-laurylsarcosine, 1 mg/ml lysozyme (Sigma), 20 mg/ml RNase

0.5 x TBE buffer: 44.5 mM Tris-borate, 1 mM EDTA (pH 8.3)

- Preparation of agarose inserts

(1) Quantitated the cells by spectrophotometric readings, for *T.thermophilus*, ~  $1 \times 10^9$  cells were present when OD<sub>600</sub> was approximately 1.0.

(2) Pelleted cells by centrifuging at 4000 rpm/min for 10 min at 4 °C.

(3) Washed the cells in TNE buffer once, kept the samples on ice during wash. For each insert, approximately  $2 \times 10^9$  cells were required. Calculated cell concentration and resuspension volume accordingly.

(4) Melted 2% clean-cut agarose (Bio-Rad) in a water bath, and equilibrated to 60 °C, gently mixed the cells with an equal amount of agarose.

(5) Pipetted the agarose/cell suspension into a casting mold, taking care to avoid air bubbles. Allowed the molds to set at 4 °C until the agarose had gelled.

(6) Unmolded the solidified inserts, and incubated the insert in EC lysis buffer overnight at 37 °C to create spheroplasts, disrupt membranes and digest other cellular debris.

(7) Drained the buffer from the tube and replace with NDSK buffer, and incubate an additional two nights in NDSK at 50 °C.

- Casting and running a pulsed field gel

For pulsed field gel running, the CHEF-DR<sup>®</sup> III variable angle system was used (Bio-Rad), the gel casting and running were performed according to the protocol provided by the manufacturer. The 21 x 14 cm gel casting stand was used, and 150 ml 1% PFGE certificated agarose (Biozym Gold Agarose) prepared in 0.5 x TBE was used for one gel. The gels were run in 0.5 x TBE for 24 h under the following conditions: 6 V/cm, 120 degree included angel, 8-50 sec switch time ramp, 14 °C.

The gel documentation was performed by a gel documentation device (AlphaImager Mini, Biozym, Oldendorf, Germany) and the corresponding software.

### 2.2.7 Transformation

#### 2.2.7.1 Transformation of *E. coli*

The *E. coli* competent cells were prepared based on Inoue *et al.* (1990) with modifications, and finally resuspended in a solution containing  $\text{Ca}^{2+}$ ,  $\text{K}^+$  and  $\text{Mn}^{2+}$ , and aliquoted with a volume of 100  $\mu\text{l}$  before storing at  $-70\text{ }^\circ\text{C}$ . The transformation was accomplished by incubation of DNA and chilled competent cells, followed by a short heat shock treatment. Before adding DNA, the competent cell aliquot was completely thawed on ice for 10 min. Added DNA with a volume no more than 10% of the total volume, gently flipped the tube and immediately incubated on ice for 30 min, followed by a short heat shock at  $42\text{ }^\circ\text{C}$  for 60 sec and re-chilled on ice for 5 min. Then the transformation reaction was mixed with 700  $\mu\text{l}$  of prewarmed ( $37\text{ }^\circ\text{C}$ ) LB medium and recovered for 1 h at  $37\text{ }^\circ\text{C}$  before plating on selective plates.

#### 2.2.7.2 Transformation of *T. thermophilus*

Take advantage of the natural competence ability of *T. thermophilus*, transformation of *T. thermophilus* was performed as directly adding DNA into cell culture followed by incubation (De Grado *et al.*, 1999). Specifically, one single colony was inoculated into 5 ml TB medium, addition with antibiotic if necessary. After O/N growth, 10% of the cell culture was reinoculated into 4.5 ml fresh TB medium and, grew under optimal temperature until  $\text{OD}_{600}$  reached 0.7-0.8. 500  $\mu\text{l}$  of the exponentially growing cell culture was mixed with 500  $\mu\text{l}$  fresh TB medium, followed by incubating for 1 h at optimal temperature. Added 1-10  $\mu\text{g}$  of DNA to the 1 ml cell culture and incubated the mixture under growing conditions for 2 h before plating on selection plates.

### 2.3 RNA manipulations

For RNA manipulations, all the vessels and solutions should be autoclaved twice (20 min,  $120\text{ }^\circ\text{C}$ ) to completely inactivate RNase.

### 2.3.1 RNA isolation

RNA of *T. thermophilus* cells was isolated using Master Pure™ Complete DNA & RNA Purification Kit (Epicentre, Madison, USA) according to the manufacturer's guides. The quality and amount of the isolated RNA were checked by agarose gel electrophoresis and spectrophotometric method (Nanodrop ND-1000, PeQlab, Erlangen, Germany).

### 2.3.2 Reverse transcription-polymerase chain reaction (RT-PCR)

For RT-PCR, cDNA synthesis for the subsequent qPCR was performed using the Maxima First Strand cDNA Synthesis Kit (Thermo Scientific, St. Leon-Rot, Germany) based on the manufacturer's protocol. Controls with all the components apart for enzymes were always set up for each experiment. The product of the first strand cDNA synthesis was diluted and used directly in the following qPCR (Chapter 2.2.4.3). 5 µL of the 1:2 or 1:5 diluted RT mixture was used as template for subsequent qPCR in a 25 µL total volume.

## 2.4 Protein manipulations and biochemical methods

### 2.4.1 Protein concentration determination

For determination of protein concentrations in solutions, a modified Bradford assay method was adopted (Bradford, 1976). To this aim, initially, a standard curve depicting the protein concentrations and the corresponding absorption values at a wavelength of 595 nm was created by using a series of BSA protein solutions with defined concentrations (0-10 µl/ml). For measuring, 10 µl of appropriately diluted protein samples were added to the bottom of the 1 ml disposable plastic cuvettes (Sarstedt, Nümbrecht, Germany), the reactions were started with the addition of 990 µl of the Bradford reagent (Thermo Scientific, St. Leon-Rot, Germany). After incubation at RT for 5 min, the absorption at 595 nm wavelength was measured with an Ultrospec 2100 pro spectrophotometer (GE Healthcare) by using pure Bradford reagent as a reference. The protein concentrations of the samples were then calculated based on the OD<sub>595</sub> values and the standard curve.

### 2.4.2 SDS-polyacrylamide gel electrophoresis (SDS-PAGE)

To visualize the proteins in cell crude extracts or in protein solutions after purification, sodium dodecyl sulphate polyacrylamide gel electrophoresis was performed. In this gel electrophoresis, the proteins are separated based on their different molecular weights.

- Required solutions

40% (w/v) Acrylamide-bis (29: 1): ready-for-use (Roth, Karlsruhe, Germany)

0.5 M/1 M Tris-HCl (pH 6.8): prepared in dd H<sub>2</sub>O, after autoclave, stored at 4 °C

1.5 M Tris-HCl (pH 8.8): prepared in dd H<sub>2</sub>O, after autoclave, stored at 4 °C

10% (w/v) SDS: dissolved in dd H<sub>2</sub>O, stored at RT

2% (w/v) bromophenol blue: dissolved in dd H<sub>2</sub>O, stored at -20 °C

#### 4 x sample buffer

1 M Tris-HCl (pH 6.8) 2.4 ml

100% glycerol 4 ml

SDS 0.8 g

Beta-mercaptoethanol 0.5 ml

2% (w/v) bromophenol blue 0.2 ml

dd H<sub>2</sub>O up to 10 ml

The buffer was aliquoted (100 µl) and stored at -20 °C.

#### 10 x running buffer

Tris-HCl (pH 8.4) 30.3 g

Glycine 144.1 g

SDS 10 g

dd H<sub>2</sub>O up to 1000 ml

#### Coomassie staining buffer

Coomassie blue R 250 5 g

Isopropanol 250 ml

acetic acid 100 ml



dd H<sub>2</sub>O up to 1000 ml

Destaining solution

acetic acid 100 ml

dd H<sub>2</sub>O up to 1000 ml

A minigel electrophoresis apparatus (mini-PROTEAN II; BioRad) was used for SDS-PAGE gel preparation and running. For gel preparation, the 7.3 cm x 10.2 cm glass plates and the 0.75 mm combs were used. The protein samples were run in a two-gel system, stacking gel and separating gel, prepared as follows:

Separating gel (10 ml), final Acrylamide-bis concentration 12.5%

40% (w/v) Acrylamide-bis (29:1) 1.565 ml

Separating gel buffer (1.5 M Tris-HCl, pH 8.8) 1.250 ml

dd H<sub>2</sub>O 2.135 ml

10% (w/v) SDS 50  $\mu$ l

TEMED 15  $\mu$ l

10% (w/v) APS (freshly-prepared) 30  $\mu$ l

Stacking gel (5 ml), final Acrylamide-bis concentration 5%

40% (w/v) Acrylamide-bis (29:1) 0.625 ml

Stacking gel buffer (0.5 M Tris-HCl, pH 6.8) 1.250 ml

dd H<sub>2</sub>O 3.075 ml

10% (w/v) SDS 50  $\mu$ l

TEMED 7.5  $\mu$ l

10% (w/v) APS (freshly-prepared) 15  $\mu$ l

The components for each type of gel were added as the above order, after properly mixed, the separating gel mixture was pipetted into gel chambers immediately (approximately 3.25 ml/chamber) followed by covering with a small volume of dd H<sub>2</sub>O. When the gel was polymerized, removed the water layer and poured the stacking gel mixture on the top of the separating gel. The 0.75 mm plastic comb was placed into the stacking gel. After stacking gel polymerization, the gel-containing glass plates were placed into the electrophoresis chamber, poured

appropriate volume of 1 x running buffer and removed the comb. The protein-containing solutions were mixed with 4 x sample buffer by a ratio of 3:1, and heat-treated at 98 °C for 5 min (protein denaturation), followed by chilling on ice for 5 min. For gel electrophoresis, 10 µg protein was applied for each lane. The gel was run with a constant current of 15 mA/gel in 1 x running buffer, when the samples reached the separating gel, the current was increased to 30 mA/gel, and proceeded running until the bromophenol blue band reached the bottom of the gel. The gel was then subjected to staining. The gel staining was performed in Coomassie staining solution with mildly shaking on a shaker for at least 30 min. After decanting the staining solution, the gel was rinsed once with destaining solution, and kept destaining with agitation for several hours. The documentation of the gel was performed by scanning (ScanMaker 1000XI Microtek, Willich, Germany). Page Ruler Prestained Ladder (Thermo Scientific, St. Leon-Rot, Germany) run beside the samples was used to evaluate the correctness of the expected sizes.

### 2.4.3 Protein overexpression and purification

The pET21a-based vectors containing the target genes were obtained from the *E. coli* cloning strain XL-1 blue, and followed by transformation into the expression strain Rosetta 2 (DE3). After that, single colonies from the transformation plates were used for protein expression cultivation. The preculture was grown in 30 ml of LB medium supplemented with chloramphenicol and ampicillin at 37 °C. Afterwards, it was reinoculated into 1000 ml fresh LB medium (plus chloramphenicol and ampicillin) with a starting OD<sub>600</sub> of approximately 0.1, followed by growing at 37 °C with shaking. When the OD<sub>600</sub> reached a value between 0.7 and 0.8, the protein expression was induced by addition of IPTG with a final concentration of 1 mM, and induction was processed by incubating the culture with agitation at 30 °C for 4 h. After induction, the cells were harvested and lysed by ultrasonication with an amplitude of 40 µm and a duty cycle of 0.4-0.5 (UP200S, Hilscher, Teltow, Germany), during which, the vessels containing the cell solutions were incubated on ice-water bath. After sonication, the crude cell extracts were centrifugated under 4 °C with a speed of 10000 rpm/min for 30 min, and the supernatants were subjected for further purification processes. The His-tagged proteins were purified by Protino

Ni-IDA Packed 2000 Columns as the manufacturer's instructions (Macherey Nagel, Germany), and finally eluted with appropriate volumes of elution buffer containing imidazole. The purified proteins were verified by SDS-PAGE analysis.

#### 2.4.4 Electrophoretic Mobility Shift Assay (EMSA)

One of the core technologies to detect protein complexes with nucleic acids is gel electrophoresis mobility shift assay (EMSA) (Hellman and Fried, 2007). It has been applied to a wide range of interacting systems qualitatively and quantitatively. The classical way of EMSA is to combine proteins and nucleic acids in solutions, and then subject the resulting mixtures to electrophoresis under native conditions through polyacrylamide or agarose gel (Hellman and Fried, 2007). The principle of this detection is that proteinbound nucleic acids migrate slower than the free nucleic acids. Therefore, if protein-nucleic acid binding occurred, the distribution of different nucleic acid species could be detected after gel electrophoresis. The nucleic acid sizes used for EMSA can vary from short oligonucleotides to several thousand nt/bp (Fried and Daugherty, 1998; Rasimas *et al.*, 2007), and it is also compatible with different structure (Musso *et al.*, 2000; Tolstonog *et al.*, 2005). For electrophoretic mobility monitoring purpose, the nucleic acids in the classical EMSA assay are usually labeled (Hellman and Fried, 2007). It can be labeled with radioisotopes (Maxam *et al.*, 1977), covalent or non-covalent fluorophores (Rye *et al.*, 1993) or biotin (Kang *et al.*, 2005), followed by detection by autoradiography, fluorescence imaging, chemiluminescent imaging and/or chromophore deposition, respectively (Hellman and Fried, 2007).

Although the isotope-labeled DNA probe can provide highly sensitive result, its hazardous property requires special laboratory equipment, when high sensitivity is not needed, the other labeling options are preferable. The procedures of EMSA in this work are as follows:

- Probe generation

DNA fragments from annealed oligonucleotides were used as probes. Table 5 shows the oligonucleotides used.

Table 5. probe sequences for EMSA.

Name	Sequences and descriptions *
WTparSc-FAM-F	5' -TGTTTCCCGTGAAACATCAGGCGCC- 3', forward oligonucleotides containing the wild-type <i>parSc</i> sequence, 6-carboxyfluorescein (FAM) labeled
WTparSc-F	5'-TGTTTCCCGTGAAACATCAGGCGCC-3', forward oligonucleotides containing the wild-type <i>parSc</i> sequence, unlabeled
WTparSc-R	5'-GGCGCCTGATGTTTCACGGGAAACA-3', reverse oligonucleotides containing the wild-type <i>parSc</i> sequence, unlabeled
MuparSc-F	5'-cGTgcCcaGgGAGACcTCAGGCGCC-3', forward oligonucleotides containing the mutant <i>parSc</i> sequence, unlabeled
MuparSc-R	5'-GGCGCCTGAgGTcTCcCtgGgcACg-3', reverse oligonucleotides of containing the mutant <i>parSc</i> sequence, unlabeled

\*Lower cases indicate the mutation sites.

The probes were generated by annealing the complementary oligomers with an equal molecular concentration at 98 °C for 10 min and cooling down at RT for O/N. The prepared probes were stored at -20 °C before using.

- Protein-DNA reaction system

Confirmation of binding (only labeled probe was used)

10 x EMSA binding buffer (0.5 M KCl, 0.1 M Tris, 0.01 M EDTA, pH 7) 2.5 µl

0.1 M DTT 0.25 µl

50% glycerol 2 µl

Poly (dI-dC) (1 µg/µl, Thermo Scientific, St. Leon-Rot, Germany) 0.5 µl

Labeled wild type probe (5 pmol/µl) 3 µl

Protein x µl

dd H<sub>2</sub>O up to 25 µl

The reaction was incubated at 25 °C for 30 min before gel electrophoresis.

In order to verify the protein binding specificity, sophisticated competition experiments were performed. The principle is based on the visibility of protein-bound labeled DNA. If the protein-DNA interaction was a specific process, the addition of increasing amount of unlabeled wild-type probe to the reaction system containing fixed amount of protein should gradually lower the binding frequency between the protein and the labeled one, and with a speed much faster than the procedure performed with unlabeled mutant probe. When the binding between the protein and the labeled probe was completely competed by the unlabeled probe, there would be no shifted DNA species visible under detection.

Competition experiment (labeled and unlabeled probes were used)

10 x EMSA binding buffer (0.5 M KCl, 0.1 M Tris, 0.01 M EDTA, pH 7) 2.5  $\mu$ l

0.1 M DTT 0.25  $\mu$ l

50% glycerol 2  $\mu$ l

Poly (dI-dC) (1  $\mu$ g/ $\mu$ l, Thermo Scientific, St. Leon-Rot, Germany) 0.5  $\mu$ l

Labeled wild type probe (5 pmol/ $\mu$ l) 3  $\mu$ l

Unlabeled wild type probe/mutant probe x  $\mu$ l (a series of increasing volumes)

Protein 13  $\mu$ l

dd H<sub>2</sub>O up to 25  $\mu$ l

The reaction was incubated at 25 °C for 30 min before gel electrophoresis.

- Agarose gel electrophoresis separating bound and un-bound DNA

The agarose gel was used for detecting DNA mobility shift. It was prepared in 1 x TBE buffer with a concentration of 1% (w/v). After reaction, the 25  $\mu$ l protein-DNA mixtures was mixed with 5  $\mu$ l 6 x DNA loading buffer and directly loaded into the gel pocket. The gel was run in 1 x TBE buffer with a constant voltage of 100 volts, and last for 50 min at RT. The signals on the gels were documented by ImageQuant 400 (GE Healthcare Life Sciences, Freiburg, Germany).

5 x TBE stock solution

Tris-HCl 54 g

Boric acid 27.5 g

0.5 M EDTA (pH = 8.0) 20 ml

dd H<sub>2</sub>O up to 1000 ml

### 2.5 $\beta$ -glucosidase activity assay for *T. thermophilus*

The  $\beta$ -glucosidase activity assay for *T. thermophilus* was performed as described (Ohta *et al.*, 2006):

- Required solutions

#### Phosphate buffer (0.1 M)

Na<sub>2</sub>HPO<sub>4</sub> · 7H<sub>2</sub>O 16.1 g

NaH<sub>2</sub>PO<sub>4</sub> · H<sub>2</sub>O 5.5 g

Added 800 ml dd H<sub>2</sub>O, adjusted pH to 7.0

Added dd H<sub>2</sub>O up to 1000 ml

After autoclave (121 °C, 20 min), the phosphate buffer was stored at RT.

#### 4-nitrophenyl- $\beta$ -d-glucopyranoside (p-NP- $\beta$ -Glc) solution (10 mg/ml)

p-NP- $\beta$ -Glc 0.1 g dissolved with 10 ml 0.1 M phosphate buffer

#### Stopping solution (1 M)

Na<sub>2</sub>CO<sub>3</sub> 105.99 g

Added dd H<sub>2</sub>O up to 1000 ml

After autoclave (121 °C, 20 min), stored at RT.

- Preparation of cells

Exponentially growing cell cultures were used. The cell cultures were placed on ice for 20 min to stop growth. For each sample, at least 2 ml cell culture was pelleted by centrifugation at 4 °C for 10 min. After pouring off the supernatant, the cell pellet was resuspended with the same volume of chilled 0.1 M phosphate buffer, followed by measuring the OD<sub>600</sub> of the cell suspension. 1 ml of the resuspended cell sample was taken, added 10  $\mu$ l toluene and vortexed until the cell solution became clear. Mixed 0.5 ml of the permeabilized cell solution with 0.5 ml of the 0.1 M phosphate buffer. The reactions were started by addition of 50  $\mu$ l of p-NP- $\beta$ -Glc, and incubated at 80 °C for 30 min. After that, chilled the reactions on ice immediately, and stopped by addition of 200  $\mu$ l of 1 M Na<sub>2</sub>CO<sub>3</sub>, centrifugated at 4 °C for 5 min, and the

supernatants were subjected to OD measurements at wavelengths at 420 and 550 nm.

- Calculation of units of activity

Miller Units were used to define the  $\beta$ -glucosidase activity.

$$\text{Miller Units}^* = 1000 \times [(\text{OD}_{420} - 1.75 \times \text{OD}_{550})] / (\text{T} \times \text{V} \times \text{OD}_{600})$$

\*OD<sub>420</sub> and OD<sub>550</sub> are read from the reaction mixture. OD<sub>600</sub> reflects the cell density in the washed cell suspension; T = the time of the reaction in minutes (30 min in this case); V = volume of culture used in the assay in mls (0.5 ml in this case).

## 2.6 Microscopy

To visualize DNA and membrane of the bacterial cells, the fluorescent dyes 4',6-Diamidino-2-phenylindole-dihydrochloride (DAPI) and 6-carboxyfluorescein (CFS) were used. DAPI is a fluorescent dye that binds strongly to A-T rich region of DNA, and it can traverse an intact cell membrane, thus it has been used for both living and fixed cells. The maximum absorption wavelength of DAPI is 358 nm, and the maximum emission wavelength is 461 nm. CFS is a fluorescent dye with a maximum excitation/emission wavelength at 492/517 nm, respectively. Since it can be incorporated into liposomes, it has been used to label cell membranes, and track cell divisions.

The bacterial cultures used for fluorescent microscopy were grown in nutrient or synthetic medium at optimal temperatures with agitation. 1 ml of exponentially growing cells were collected and washed once with 1 x PBS, after resuspension in 0.5 ml 1 x PBS, staining was performed by addition of the fluorescent dyes with a final concentration of 0.2  $\mu\text{g/ml}$  for DAPI, and 10  $\mu\text{g/ml}$  for CFS followed by incubation at RT for 20 min. After staining, the residual dyes were washed off by 1 x PBS (three times, each time 1 ml 1 x PBS), and the cell pellet was finally resuspended in 0.5 ml 1 x PBS. For microscopy slide preparation, 5  $\mu\text{l}$  cell solution was spread evenly on glass slide (VWR, Darmstadt, Germany), and dried completely followed by immobilized with 0.8% warm agarose and covered with cover slice (VWR, Darmstadt, Germany).

Fluorescence microscopy was performed by Zeiss microscope (Zeiss Axio Imager M1, Carl Zeiss, Germany). The images were acquired by AxioCam MRm

## *2. Materials and methods*

---

camera and the corresponding software. The images were later analyzed by Image J (NIH, USA) and Axio vision rel. 4.8 (Carl Zeiss, Germany).

### 10 x PBS buffer

NaCl 80 g

KCl 2 g

Na<sub>2</sub>HPO<sub>4</sub> 14.4 g

KH<sub>2</sub>PO<sub>4</sub> 2.72 g

Added 800 ml dd H<sub>2</sub>O, adjusted pH to 7.4, filled up with H<sub>2</sub>O to 1000 ml.



### 3. Results

#### 3.1 A new genetic modification tool for *T. thermophilus*

*T. thermophilus* is now widely used as a model organism to study the molecular nature of a thermophilic lifestyle. This is partly due to the typically high growth rates, the ease of cultivation and the constitutively expressed natural competence system, which facilitate genetic manipulations. The most often used method for the isolation of directed knockout mutants in *T. thermophilus* is based on the insertion of antibiotic resistance markers, i. e. kanamycin (Lasa *et al.*, 1992; Mather and Fee, 1992), bleomycin (Brouns *et al.*, 2005) or hygromycin resistance genes (Nakamura *et al.*, 2005). The disadvantages of this approach are that the antibiotic resistance marker cannot be reused and that polar effects on downstream genes are possible. However, the alternative strategies based on counter-selection principle, which allows generation of marker-free deletion mutants are still limited. Thus, to uncover the properties of *T. thermophilus*, new genetic modification tools are requisite.

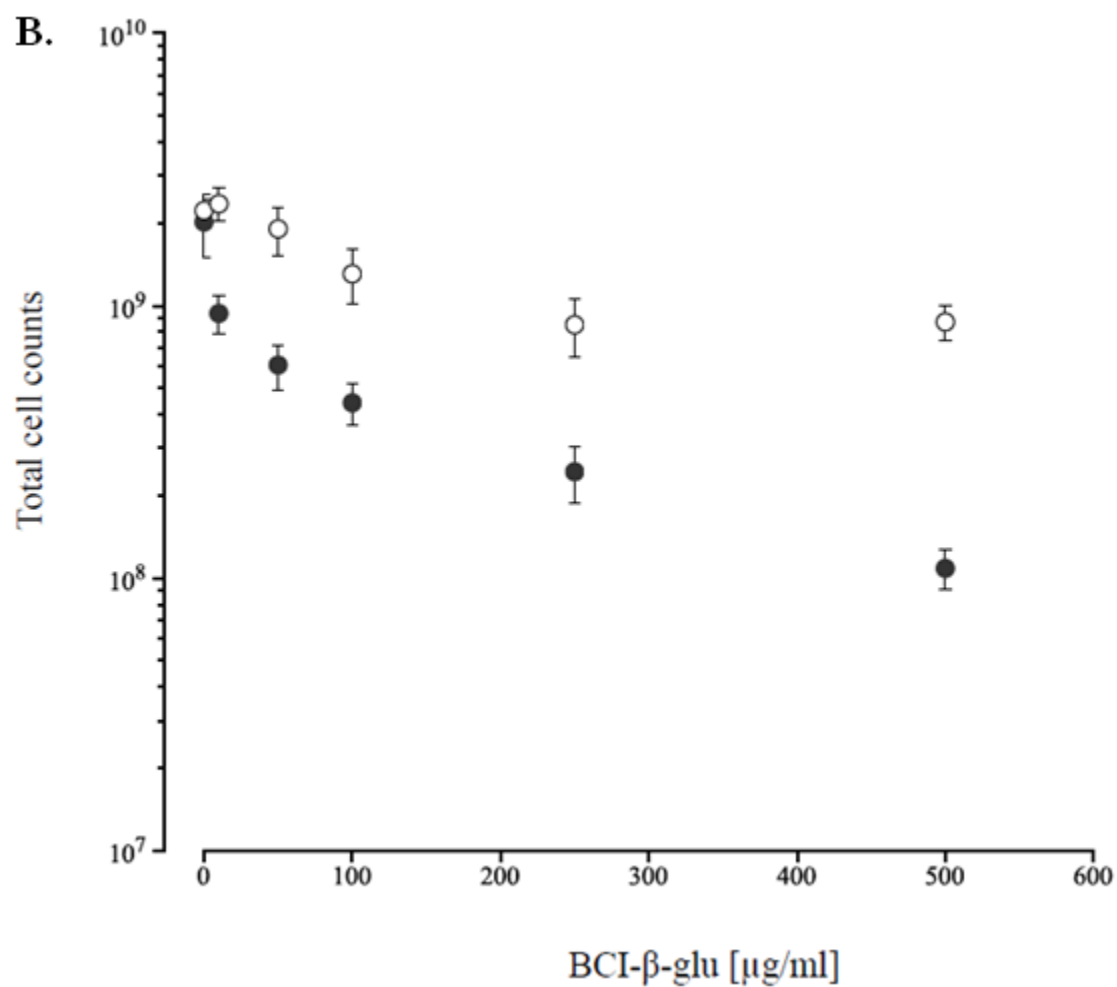
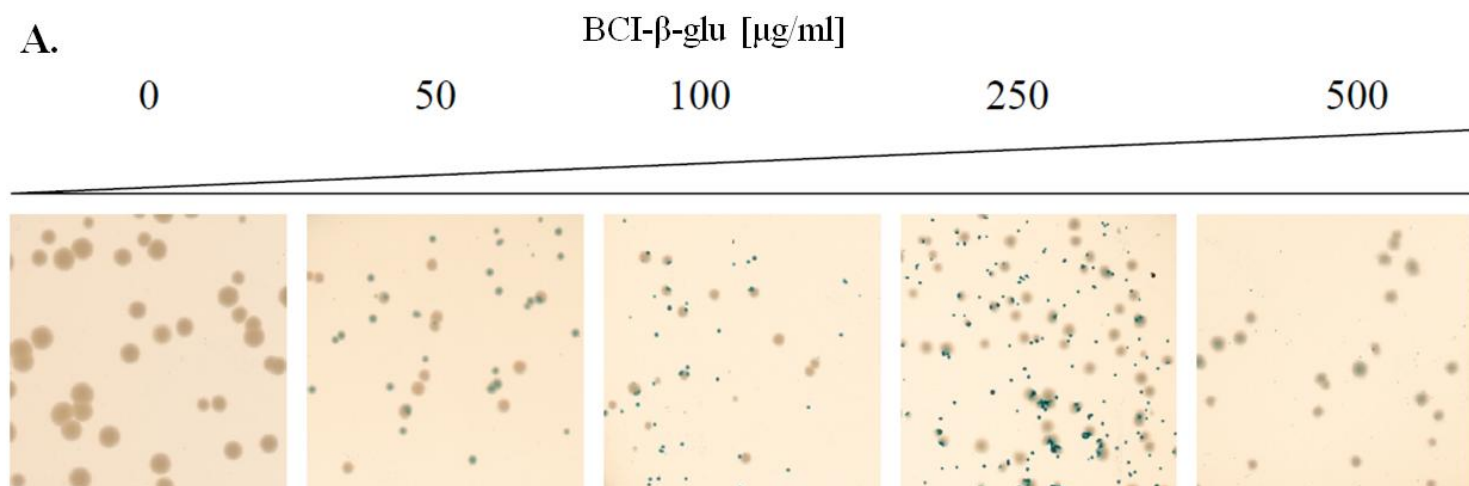
##### 3.1.1 Toxic effect of substituted indoxyl substrates and its use for counterselection in gene exchange experiments in *T. thermophilus*

It has been shown that wild-type *T. thermophilus* cells (HB27) can produce  $\beta$ -glucosidase (Bgl) and the main Bgl activity is caused by the megaplasmid-encoded *bgl* gene (TT\_P0042) (Ohta, 2006). Colonies containing Bgl activities (Bgl<sup>+</sup>) turn blue when grown on agar plates supplemented with the indicator substrate BCI- $\beta$ -glu (5-bromo-4-chloro-3-indolyl- $\beta$ -D-glucopyranoside). In this study, it was noticed that increasing the BCI- $\beta$ -glu concentration led to a considerable reduction in the size of the Bgl<sup>+</sup> colonies. In order to confirm that the observed toxic effect was caused by and was dependent on the *bgl* gene, a marker-free *bgl* deletion strain ( $\Delta bgl$ ) was constructed by transforming the wild-type cells with a suicide vector pT- $\Delta 42$  which carries the megaplasmid regions upstream and downstream of the *bgl* gene but devoid of the *bgl* ORF. Several candidate  $\Delta bgl$  colonies were identified by screening on TB

agar plates supplemented with BCI- $\beta$ -glu at 100  $\mu$ g/ml and their genotype was confirmed by PCR and Southern blot (data not shown). When 1:1 mixtures of wild-type and  $\Delta bgl$  cells were plated on TB BCI- $\beta$ -glu agar plates, the wild-type HB27 cells were not able to grow at BCI- $\beta$ -glu concentration above 500  $\mu$ g/ml, while  $\Delta bgl$  mutant cells were largely insensitive to the substrate at the tested concentrations (Fig. 2A). Growth of the wild-type cells was also strongly inhibited by BCI- $\beta$ -glu in liquid medium, as indicated by determining the cell counts after 15 hours of growth in the presence of the substrate (Fig. 2B). These observations indicated that, in combination with BCI- $\beta$ -glu, the *bgl* gene could be used as a counterselection marker in a “pop-in, pop-out” strategy to generate unmarked mutations in the genome of *T. thermophilus*.

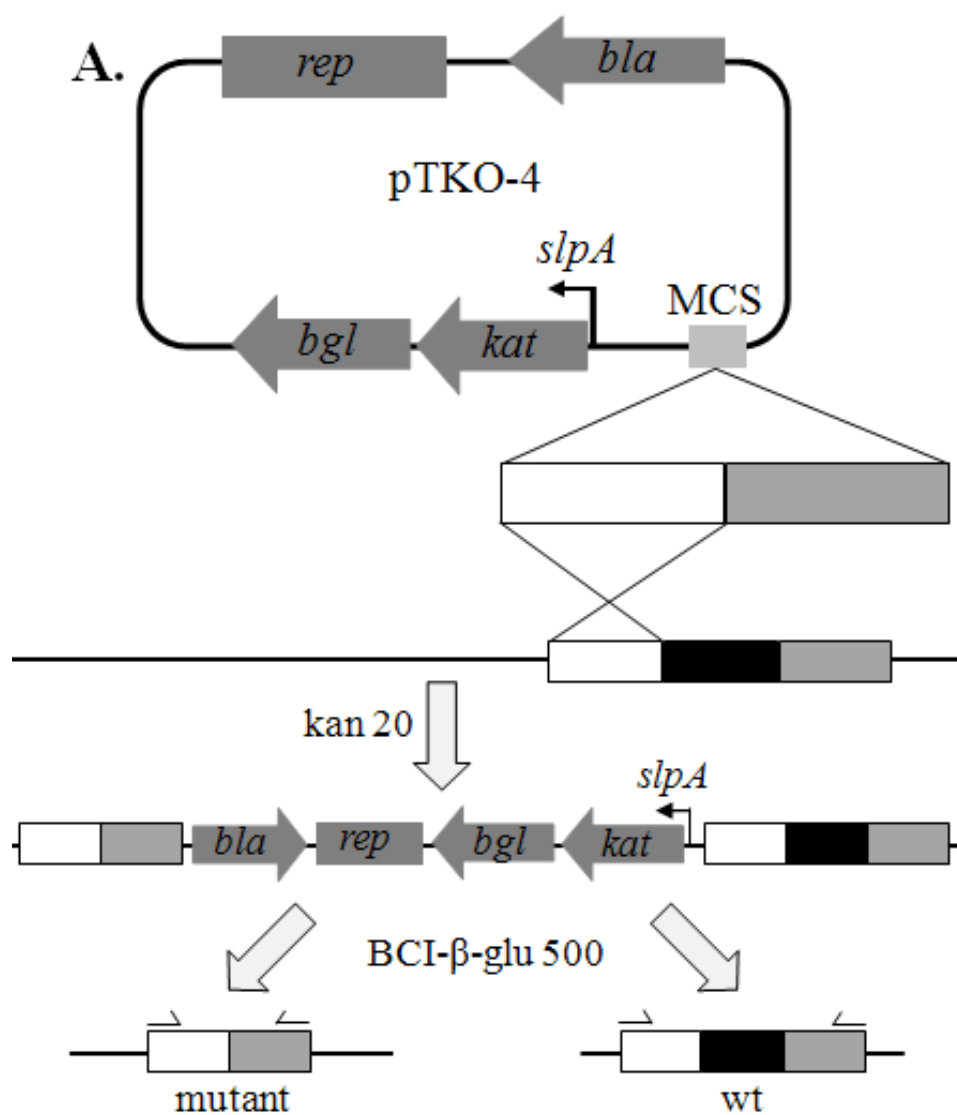
In order to be able to perform allelic exchange experiments, a non-replicative *T. thermophilus* vector (pTKO-4) was constructed (Fig. 3A), which carries the *bgl* gene transcriptionally fused to a thermostable kanamycin resistance marker (*kat*) under transcriptional control of the *T. thermophilus* *slpA* promoter. This constitutive *T. thermophilus* promoter (Lasa *et al.*, 1992) ensures strong expression not only of the *kat* gene but also of the *bgl* gene (Fig. 3A). To test the utility of the new counterselection strategy with pTKO-4 as the vector for markerless deletion in *T. thermophilus*, a chromosomal locus containing ORFs TT\_C0340-0341 (referred to hereafter as *340*) was targeted. Sequences upstream and downstream of this locus were cloned in the multiple cloning site of pTKO-4 yielding pTKO- $\Delta 340$ . After transformation of the  $\Delta bgl$  strain with pTKO- $\Delta 340$ , kanamycin resistant colonies resulting from the recombinatorial chromosomal integration of pTKO- $\Delta 340$  were isolated. The kanamycin resistant clones were grown for 4 hours in antibiotic-free medium and streaked on TB agar plates supplemented with BCI- $\beta$ -glu at 500  $\mu$ g/ml. Under these conditions, it is expected that only cells that have lost the *bgl* marker are able to grow (Fig. 2). The observed average frequency of colonies that grew on TB BCI- $\beta$ -glu after this step was  $1.7 \times 10^{-6}$  (measured by determining the total colony-forming units on TB and TB BCI- $\beta$ -glu). Next, the genotype of several colonies that grew on the TB BCI- $\beta$ -glu plates were verified by PCR and Southern blot. As expected, approximately half of the colonies were found to carry the knockout allele, evident from the observed 3327 bp SacII fragment instead of the

4807 bp wild-type band in the Southern blot (Fig. 3B). Using this pTKO-4-vector based gene deletion approach, we further obtained some other marker-free gene deletion mutants at targeted loci in *T. thermophilus* (data not shown). Taken together, these results indicated that the *bgl* gene can be used as a counterselection marker.



### 3. Results

Fig.2. (A) Growth-inhibiting effect of high concentrations of BCI- $\beta$ -glu on *T. thermophilus* HB27 expressing the *bgl* gene as a counterselection marker. Equal amounts of cell suspensions of the wild type and the  $\Delta bgl$  strains were mixed and dilutions were plated on TB agar plates supplemented with increasing concentrations of BCI- $\beta$ -glu and grown overnight at 70 °C. (B) Growth-inhibiting effect of BCI- $\beta$ -glu on *T. thermophilus* wild type (black circles) and  $\Delta bgl$  (white circles) in liquid medium. The respective strains were inoculated (108 CFU/ml) in TB medium supplemented with the indicated amount of BCI- $\beta$ -glu and were grown for 15 h at 70 °C. The total cells counts in each sample were determined with a Thoma chamber; the average and standard deviation of three experiments is shown.



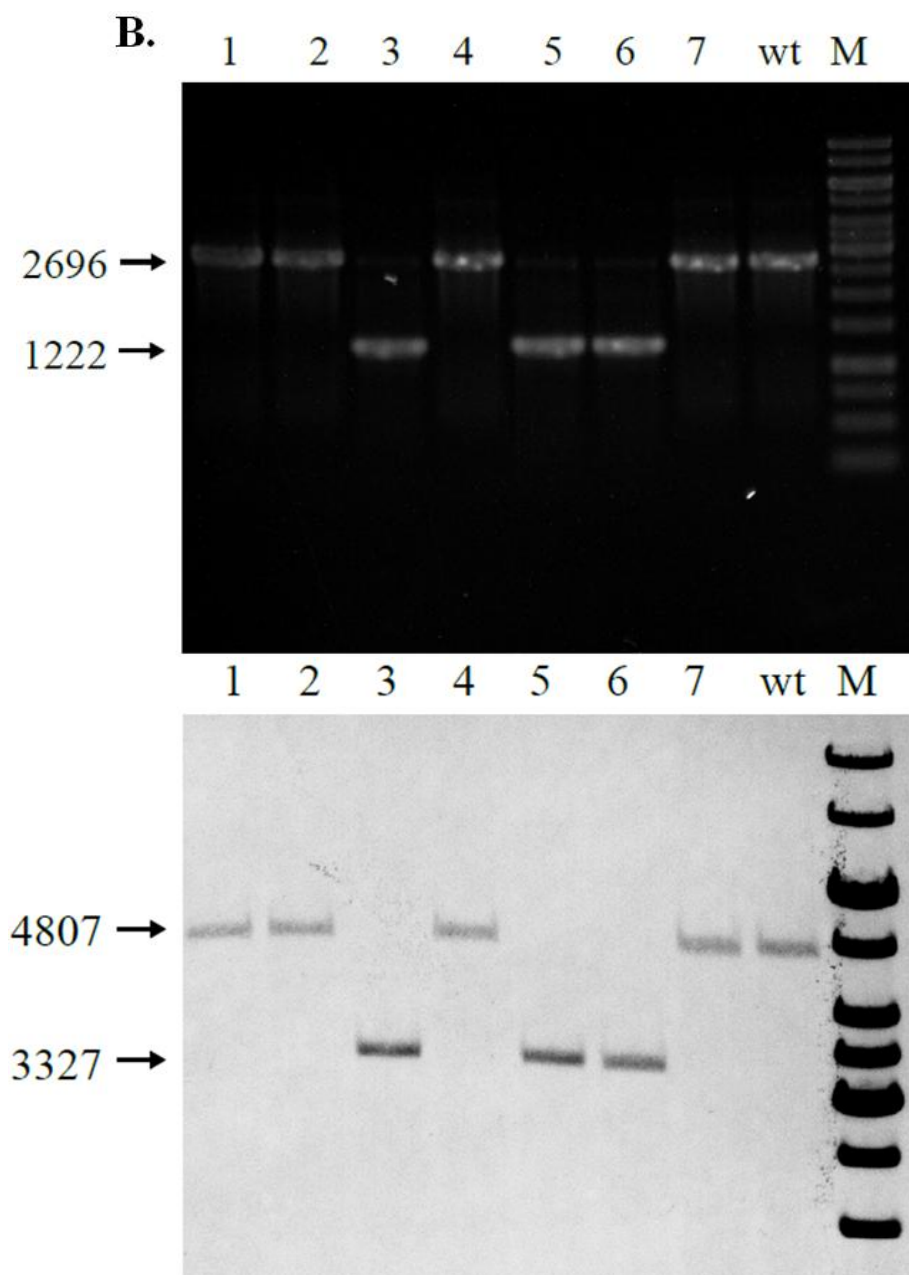


Fig. 3. (A) Scheme of the pTKO-4 vector and the steps involved in generating the markerless deletions in *T. thermophilus*. (B) PCR and Southern blot genotype analysis of several randomly picked colonies after selection on BCI- $\beta$ -glu plates in the *T. thermophilus* locus 340 allelic exchange experiment. The theoretically calculated sizes of the wild type and the knockout alleles are indicated with arrows. M -molecular weight marker. For the Southern blot, total genomic DNA isolated from the colonies was digested with SacII; the probes used were generated by PCR with primers listed in Appendix Table and labeled using the Biotin DecaLabel DNA Labeling Kit (Fermentas, St. Leon-Rot, Germany).

### 3.1.2 Possible mechanisms of toxicity of substituted indoxyl substrates

Apparently, the toxic effect observed when Bgl<sup>+</sup> cells were incubated with the BCI- $\beta$ -glu substrate was caused in some way by the substituted indoxyl moiety which is released upon cleavage by the  $\beta$ -glucosidase. The toxic effect becomes particularly evident at high concentrations of the chromogenic BCI substrate (see Fig. 2). In the presence of molecular oxygen or other oxidizing agents, pairs of the diffusible 5-bromo-4-chloro hydroxyindole form an insoluble, blue indigoid dye, 5,5'-dibromo-4,4'-dichloro-indigo (Kiernan, 2007). It was not clear which of the two molecules, the monomer or the dimer, exerted the toxic effect. It was also not clear whether the toxicity was an intra- or extra- cellular effect. Although Bgl is an intracellular enzyme and therefore the cleavage of the substrate should take place after it has been transported into the cell, it cannot be excluded that some enzyme is released by lysed cells in a colony during growth on agar plates and the released hydroxyindole could act extracellularly. To clarify the latter question, the toxic effect of an indigo dye (unmodified indoxyl dimer) for the Bgl<sup>+</sup> cells was examined. No toxic effect could be observed in this experiment, as judged by the comparison of the colony sizes of *T. thermophilus* HB27 grown on TB agar plates supplemented with the indigo dye at the concentration range of 50-500  $\mu$ g/ml (data not shown). Supporting this observation, differential interference contrast (DIC) microscopy of *T. thermophilus* cells grown in the presence of BCI- $\beta$ -glu showed the presence of small, cell-associated blue indigoid dye precipitates, which most probably accumulated in or near the cytoplasmic membrane (Fig. 4).

In order to further uncover the mechanisms leading to resistance or sensitivity to the cleavage of BCI substrates, a library of approximately 8000 transposon insertion mutants of *T. thermophilus* HB27 (our group, unpublished data) was screened to detect colonies with a BCI- $\beta$ -glu resistant phenotype. Three BCI- $\beta$ -glu resistant mutants (termed Tn-1, 5 and 8) were identified and their transposon insertion sites were mapped by vectorette PCR (Arnold and Hodgson, 1991). All of them had transposon insertions in gene clusters related to sugar utilization (encoding probable sugar transporters (TT\_C0611-0613 in Tn-1, TT\_P0223 in Tn-8 and TT\_P0039-0041 in Tn-5)). These results further support the hypothesis that the toxic effect is exerted

only after the BCI substrate is transported in the cell, where it is cleaved and the insoluble, blue indigoid dye accumulates.

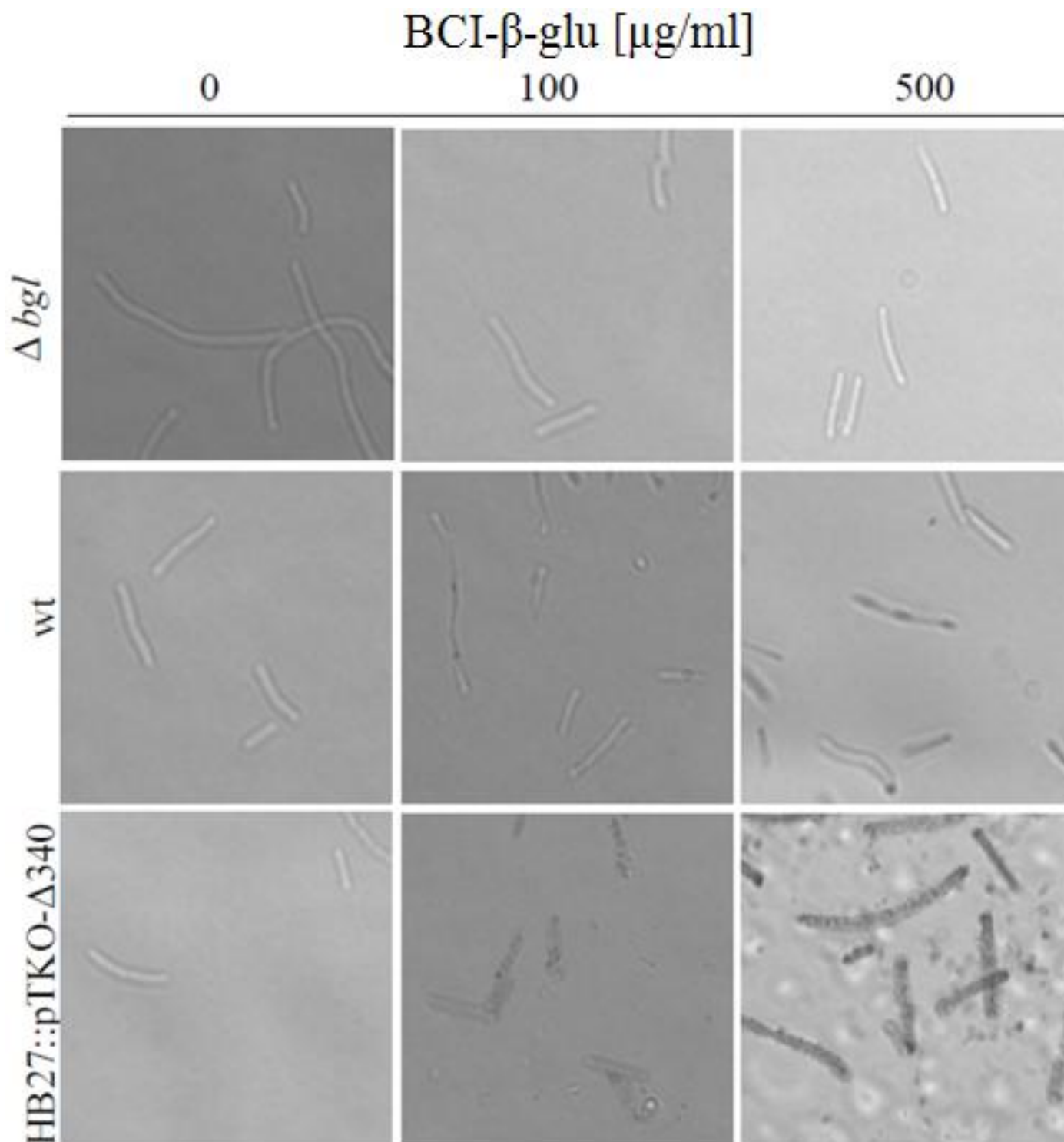


Fig. 4. Differential interference contrast (DIC) microscopy of *T. thermophilus*  $\Delta bgl$ , wild type and the vector integration strain HB27::pTKO- $\Delta$ 340. The strains were grown in TB medium at 60°C in the presence of the indicated amounts of BCI- $\beta$ -glu.

### 3.1.3 Toxicity test of substituted indoxyl substrates in other bacteria

Further, we investigated if similar sensitivity to the products of the cleavage of BCI substrates can be observed in other microorganisms. For this, we tested several representative Gram-positive as well as Gram-negative bacteria which expressed enough  $\beta$ -glucosidase,  $\beta$ -galactosidase,  $\alpha$ -glucosidase, or phosphatase activity to produce blue-stained colonies on the respective substrate plates (Table 6). The sensitivity to BCI substrates of the different bacteria was tested by plating dilutions of cell solutions on the agar plates supplemented with respective BCI substrates at 0, 100 and 500  $\mu\text{g/ml}$ . In order to exclude toxic effects of the solvent used for BCI- $\beta$ -glu and BCI- $\beta$ -gal, controls were included consisting of plates supplemented only with the solvent DMF (N, N-dimethyl formamid). Although in each case the expression level of the enzyme used was different, by comparing the colony sizes on plates with and without BCI substrate it could be clearly determined if a toxic effect existed or not. As can be seen from Table 6, the substituted hydroxyindole-mediated toxicity could be measured in both Gram-positive and Gram-negative bacteria, and no direct correlation between overall cell wall structure and the presence of toxicity could be made. In several cases, no reduction in the colony size could be detected although the colonies appeared blue on the respective substrate plates (e. g. *E. coli* and *P. putida*). It seems that in these cases the lack of toxicity can be attributed to the inability to transport the respective BCI substrate into the cell. The blue color can be explained by extracellular cleavage of the substrate, resulting from cell lysis in the colony.



Table 6. Sensitivity to 5-bromo-4-chloro-hydroxyindole substrates in different bacterial species\*.

Species	Strain	Substrate <sup>b</sup>	Toxicity	Medium <sup>a</sup> and growth temperature
<i>Francisella novicida</i> <sup>c</sup>	U112	BCIP	yes	LB, 37 °C
<i>E. coli</i>	MG1655	BCI-β-gal	no	LB, 37 °C
<i>Vibrio harveyi</i>	NCIMB 1280 <sup>T</sup>	BCI-β-glu	no	BHI/NaCl, 30 °C
<i>P. putida</i>	DSM 291 <sup>T</sup>	BCIP	no	HD, 30 °C
<i>Klebsiella planticola</i>	DSM 3069	BCIP	no	HD, 37 °C
<i>Paracoccus denitrificans</i>	DSM 413 <sup>T</sup>	BCIP	yes	HD, 30 °C
<i>Xanthomonas campestris</i>	DSM 1350 <sup>T</sup>	BCIP	yes	HD, 30 °C
<i>B. subtilis</i>	W23	BCI-β-glu	yes	LB, 37 °C
<i>Bacillus licheniformis</i>	DSM 13 <sup>T</sup>	BCI-β-glu	yes	LB, 37 °C
<i>Staphylococcus aureus</i>	DSM 20235	BCIP	yes	HD, 37 °C
<i>Corynebacterium glutamicum</i> <sup>d</sup>	DSM 20300 <sup>T</sup>	BCI-β-gal	yes	LB, 30 °C
<i>Micrococcus luteus</i>	ATCC 27141	BCI-α-glu	yes	LB, 30 °C
<i>Rhodococcus rhodochrous</i>	DSM 43241	BCI-β-glu	yes	HD, 30 °C

\*The sensitivity assays were performed by observing the BCI substrate-dependent reduction in colony size. The substrates used were 5-bromo-4-chloro-3-indolyl-β-D-glucopyranoside (BCI-β-glu), 5-bromo-4-chloro-3-indolyl-β-D-galactopyranoside (BCI-β-gal), 5-bromo-4-chloro-3-indolyl-α-D-glucopyranoside (BCI-α-glu), and 5-bromo-4-chloro-indolyl phosphate (BCIP). Only bacteria forming blue-colored colonies on the respective substrate plates are listed. <sup>a</sup>Media components are introduced in Chapter 2.1.2. <sup>b</sup>The substrates BCI-β-glu, BCI-β-gal, BCI-α-glu and BCIP were supplemented at 0, 100 and 500 µg/ml. <sup>c</sup>Indication of toxicity from Baron and Nano (1998). <sup>d</sup>The β-galactosidase activity of this strain is due to the expression of the *E. coli lacZ* gene on the pECL3x plasmid (Brabetz *et al.*, 1991).

## 3.2 Chromosomal and megaplasmid partitioning (*par*) loci in *T. thermophilus*

### 3.2.1 Locations, components and genetic structures of *parABc* and *parABm*

Partitioning genes (*par*) were initially identified on low-copy-number plasmids, and they are required for faithful plasmid segregation at cell division. More recently, they were also found on bacterial chromosomes. Nearly all known plasmid encoded *par* loci contain three components: a *cis*-acting centromere-like site (*parS*) and two *trans*-acting proteins (ParA and ParB). The three components of the plasmid Par system have been characterized to a great extent, by contrast, less is understood about the chromosome-encoded Par system. One of the best studied chromosomal partitioning systems is the *B. subtilis* *par* operon (referred as *soj* (*parA*), *spo0J* (*parB*), and *parS*). The first chromosomal *parS* was identified in *B. subtilis*, and since then, the 16-bp pseudopalindromic sequence 5'-TGTTNCACGTGAAACA-3' was identified in many bacterial species.

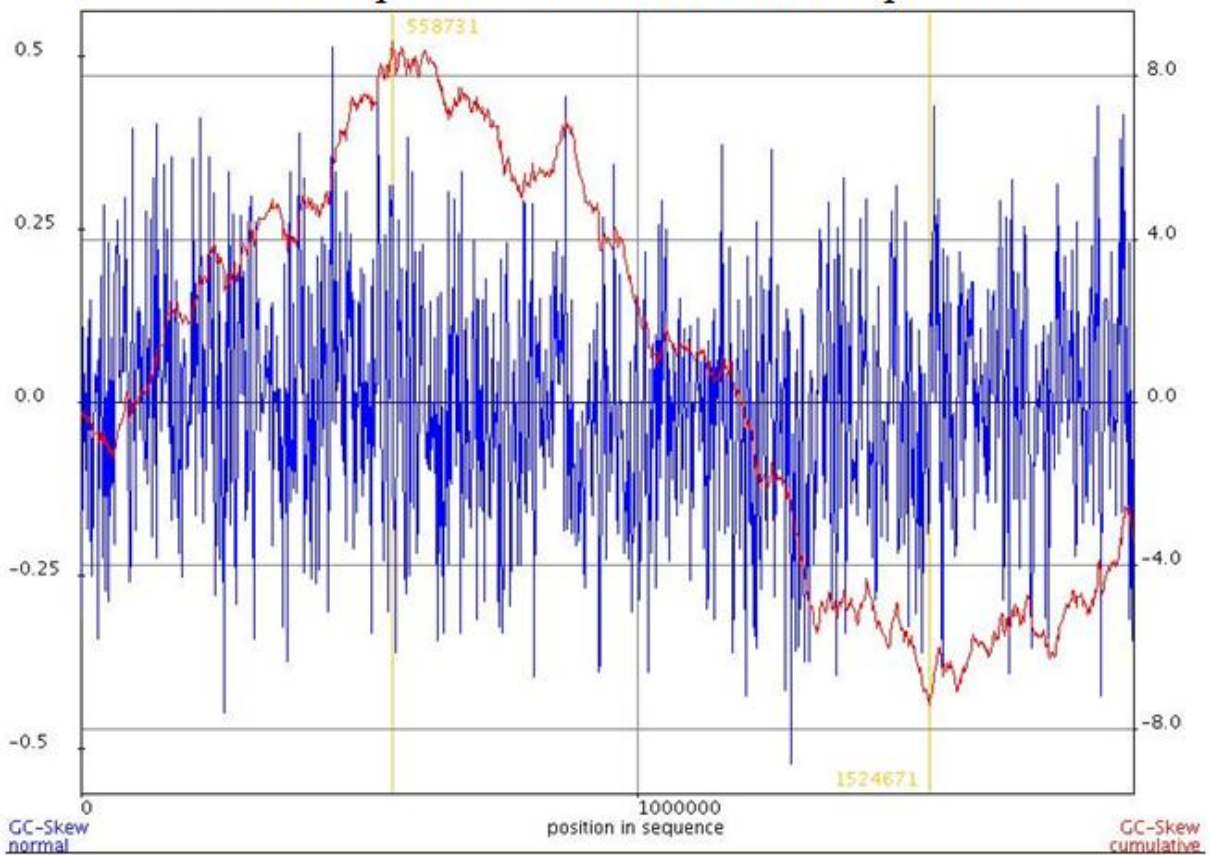
In this study, it was found that both the chromosome and megaplasmid of *T. thermophilus* contain *par* loci (*parABc* and *parABm*, respectively). Through BlastP analysis using ParAc, ParBc, ParAm and ParBm as the respective probes, only one homologue of each gene was identified. The chromosome encoded *par* loci were found to consist of *parAc* (TT\_C1605), *parBc* (TT\_C1604), and *parSc*. Like the situation in other bacterial chromosomes, *parAc* and *parBc* were organized as one operon. According to the report (Nardmann and Messer, 2000) and our own GC skew analysis (Fig. 5A), the chromosome replication origin (*oriC*) is positioned right downstream of *dnaA* (TT\_C1608), thus, the *parABc* loci are origin-proximally located (~ 6 kbp from *oriC*) (Fig. 5C). The *parSc* site was identified using the 16-bp consensus sequence allowing one base pair mismatching, after searching through the whole genome, only one site was found (this study; Livny *et al.*, 2007). When two or three mismatches were allowed, no other sequences were found. The sequence of *parSc* is 5'-TGTTTCCCGTGAAACA-3', which is located in a gene encoding 16S rRNA methyltransferase (GidB) immediately upstream of *parAc* (Fig. 5C).

Based on GC skew analysis, the cumulative minimum indicating the

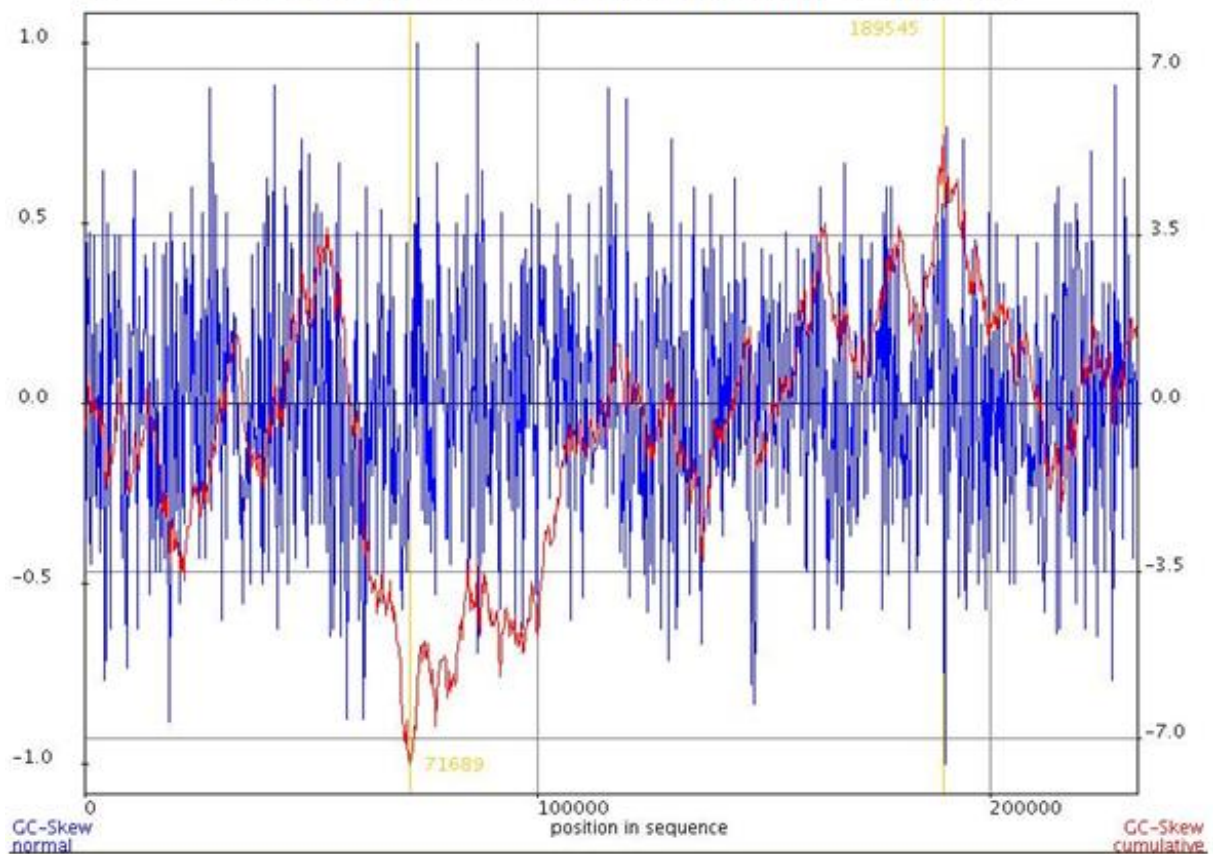
megaplasmid replication origin position was observed around the open reading frame of TT\_P0079 (Fig. 5B, C). Thus, the megaplasmid *parAB* genes (TT\_P0084 and TT\_P0083) are also in the vicinity of the corresponding *oriC* (Fig. 5C). Several inverted repeats were found in the upstream and downstream of *parABm* (data not shown), it would be possible that they serve as the megaplasmid *parS* sites.

The genetic structure of the *T. thermophilus* chromosomal *par* loci is in high consistence with other bacterial chromosomal *par* systems (Nardmann and Messer, 2000). The situation of the *parABm* operon, on the other hand, is close to that of low-copy-number plasmids. The *parABm* genes are adjacent to the *repA* gene for a plasmid-like replication initiator, and also have a number of direct repeats resembling iterons clustered around (data not shown). Therefore, we asked whether the chromosomal and megaplasmid Par proteins also possess different features. The *parAm* and *parBm* genes encode much larger products (322 and 297 amino acid residues, respectively) than *parAc* and *parBc* (249 and 269 amino acid residues respectively). Through protein conserved motif searching (BlastP) and protein alignments, it was found that ParAc and ParAm are both Walker-type ATPases containing conserved P-loop ATP binding motifs (Fig. 5D). In contrast to ParAc, ParAm contains a predicted Helix-Turn-Helix motif (HTH) at its N-terminus, a feature that normally appears in plasmid ParAs but not in chromosomal ones (Gerdes *et al.*, 2000) (Fig. 5D). Taken together, it seems the *T. thermophilus* chromosomal *par* resembles a typical chromosomal *par* loci, whereas the megaplasmid *par* genes are more related to those from low-copy-number plasmids.

A. GC-skew plot for the chromosomal sequences



B. GC-skew plot for the megaplasmid sequences





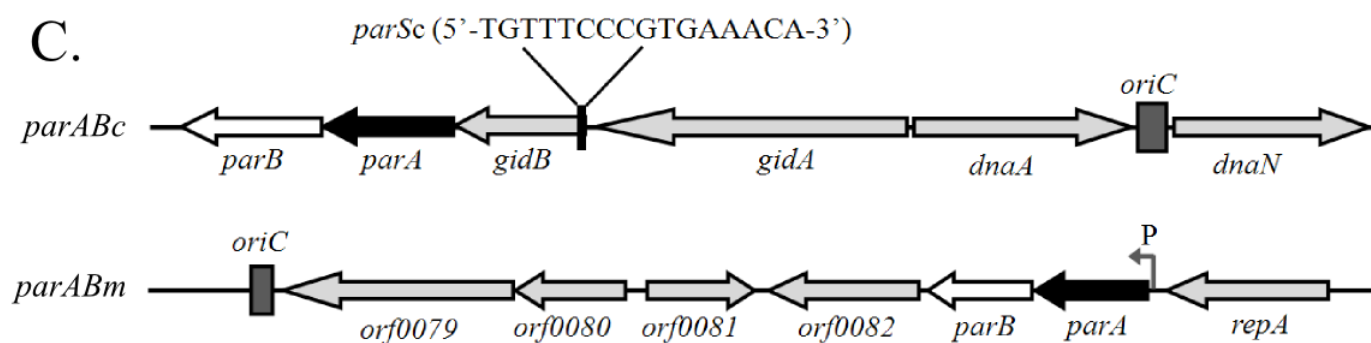


Fig. 5. Locations of the chromosomal and megaplasmid *par* loci (*parABc* and *parABm*), and features of the corresponding ParA proteins. (A, B) The online GenSkew software was used to compute the normal and cumulative GC skew for the chromosome and megaplasmid sequences (<http://genskew.csb.univie.ac.at/>). The setting window size and step size for the chromosome sequences were both 1000 bp, and those for the megaplasmid sequences were both 100 bp. The cumulative GC-skew minimum indicating the chromosome origin region is at position 1, 524, 671 (A), and that indicating the megaplasmid origin region is at position 71, 689 (B). (C) Schematic gene organizations of the *parABc* and *parABm* regions. Arrows show the genes, arrow directions indicate the gene transcription directions. Genes encoding proteins with unknown functions are marked with ORF numbers. The predicted replication origins in the chromosome and megaplasmid are indicated with dark-gray bars. The chromosomal *parS* site is represented with a short black bar. (D) Parts of alignment among ParAc, ParAm and other ParAs. Strain abbreviations: Bs, *B. subtilis*; Vc, *V. cholerae*; Cg, *C. glutamicum*; Tth, *T. thermophilus*; P1, *E. coli* P1 phage. Numbers above show distances, double hatch marks indicate not shown sequences. Completely conserved amino acids are shown in blue. The conserved motifs are shown: Walker box A (nucleotide binding), A' (catalytic), B motif (Mg binding). Black frames indicate the predicted Helix-Turn-Helix motifs in P1 ParA, and Tth ParAm.

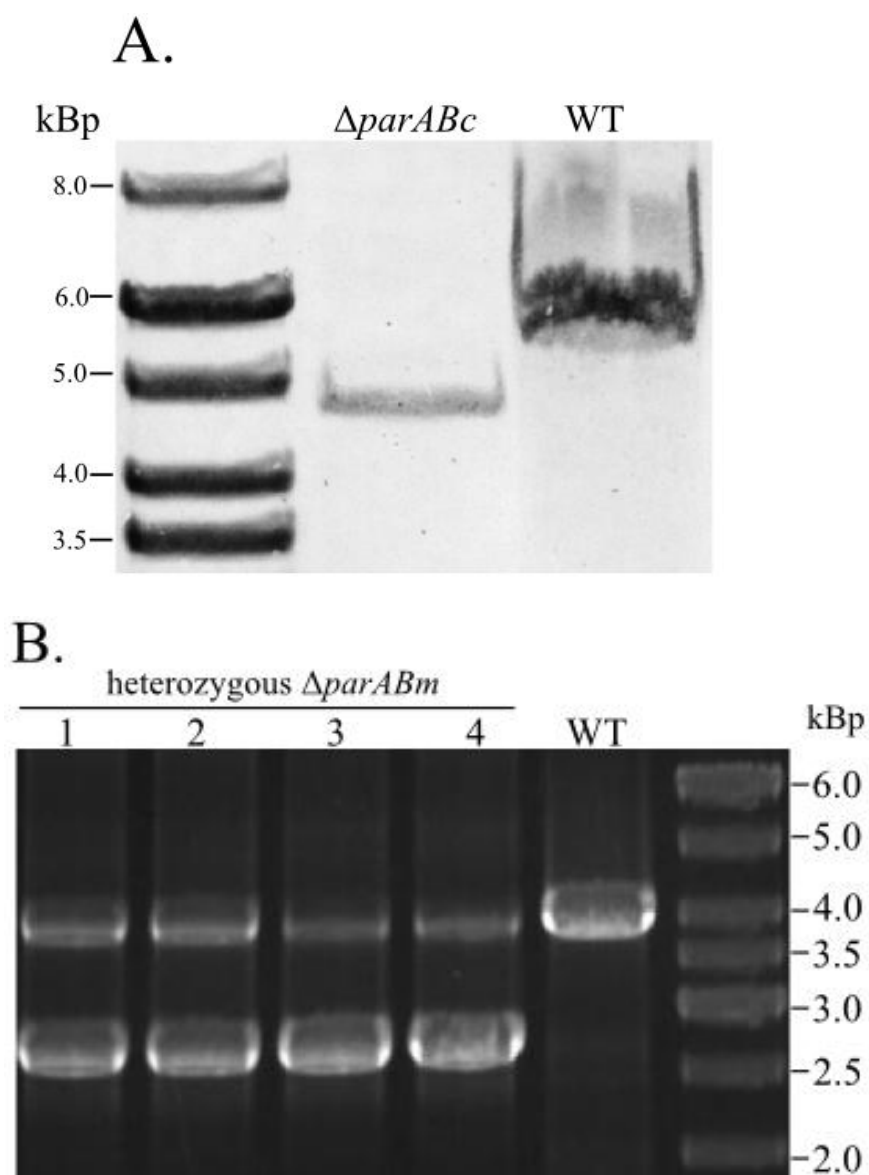
### 3.2.2 Complete deletion of *parABc* is possible, whereas *parBm* is essential

Given the important roles of the *par* loci in certain bacterial species, evaluation of the functions of these loci in *T. thermophilus* was initiated. First, gene deletion mutants were attempted to be generated. The coding regions of the chromosomal *parAB* genes (amino acid positions 4-249 in *parAc*, 1-243 in *parBc*) were replaced by a thermostable kanamycin gene cassette (*kat*) in opposite orientation relative to *parABc* transcription (for detailed plasmid constructions, see Chapter 2.1.1). The mutant  $\Delta$ *parABc* was then verified by Southern blot which showed complete deletion of the *parABc* operon (Fig. 6A). In the same way, initially, the whole *parAB* operon

in the megaplasmid was attempted to be replaced with a thermostable bleomycin resistance gene (*blm*). However, obtaining a homozygous mutant was impossible, all the resulting transformants were found to be heterozygotes containing both wild-type and mutant alleles (Fig. 6B) (*T. thermophilus* is polyploid, therefore a heterozygous state is possible (Ohtani *et al.*, 2010)). Thus, *parABm* is probably not deletable. Then, we tried to knockdown the *parABm* operon to test whether an adequate amount of ParABm is truly critical for the cellular process, and also delete the two genes separately to pinpoint which gene is essential. To this end, the *blm* marker was used to replace the N-terminus-encoding region (amino acids 1-40) of *parAm* in a direction opposing the promoter region of *parABm*. As the *blm* gene is expressed under a strong promoter (Lasa *et al.*, 1992), this replacement would on one hand probably impede the transcription of the *parABm* operon, and in addition, it would inform whether *parAm* is deletable ( $\Delta parAmN-1$ , Fig. 6C). Further, to illustrate whether the resulting effect of the  $\Delta parAmN-1$  mutant is provoked by deletion of the N-terminus-encoding region of *parAm* or down-regulated levels of the truncated ParAm and ParBm, the same *parAm* region (amino acids 1-40) was also replaced by *blm* in a direction co-linear with the *parABm* transcription ( $\Delta parAmN-2$ , Fig. 6C). The residual part of *parAm* with the corresponding amino acid positions 42-322 was designed to be functional; in this case, the resultant effect would be probably caused by the *parAmN* deletion or even considerably higher expressions of the truncated ParAm and ParBm, due to the strong promoter of *blm* (Lasa *et al.*, 1992). The *parBm* gene was also attempted to be exchanged by *blm* in opposite direction relative to *parABm* transcription. Complete exchange of *parBm* was impossible (Fig. 6E), while the N-terminus-encoding sequences of *parAm* could be successfully replaced by *blm* in both directions (Fig. 6D). Thus, it seems the megaplasmid *parB* is an essential gene, while *parAm* is not. Further, the transcription levels of the truncated *parAm* and *parBm* genes in  $\Delta parAmN-1$  and  $\Delta parAmN-2$  were determined by RT-qPCR (see Chapters 2.2.4.3 and 2.3.2). A chromosomally located constitutively expressed gene (TT\_C1610) was chosen as an endogenous reference, and expressions were quantified by a relative quantification method ( $2^{-\Delta\Delta Ct}$ ) based on Livak *et al.* (2001). As expected, in  $\Delta parAmN-1$ , the transcription levels of the truncated *parAm*, *parBm*

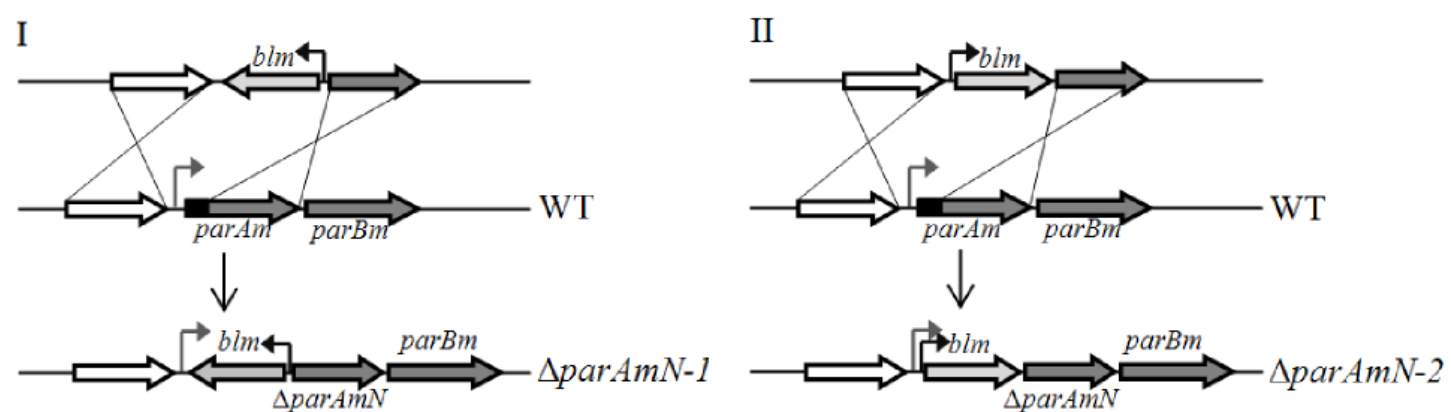
### 3. Results

genes were decreased, the relative expressions of the two genes to the wild-type strain were  $0.13 \pm 0.01$ ,  $0.21 \pm 0.04$ , respectively; by contrast, in  $\Delta parAmN-2$ , increased levels of the *parABm* expression were detected, the relative changes of the two genes to wild type were  $4.00 \pm 0.27$ ,  $2.02 \pm 0.33$ , respectively (Fig. 6F). These experiments showed that *parABc* is not essential, while a deletion mutant of *parABm* appears to be lethal.

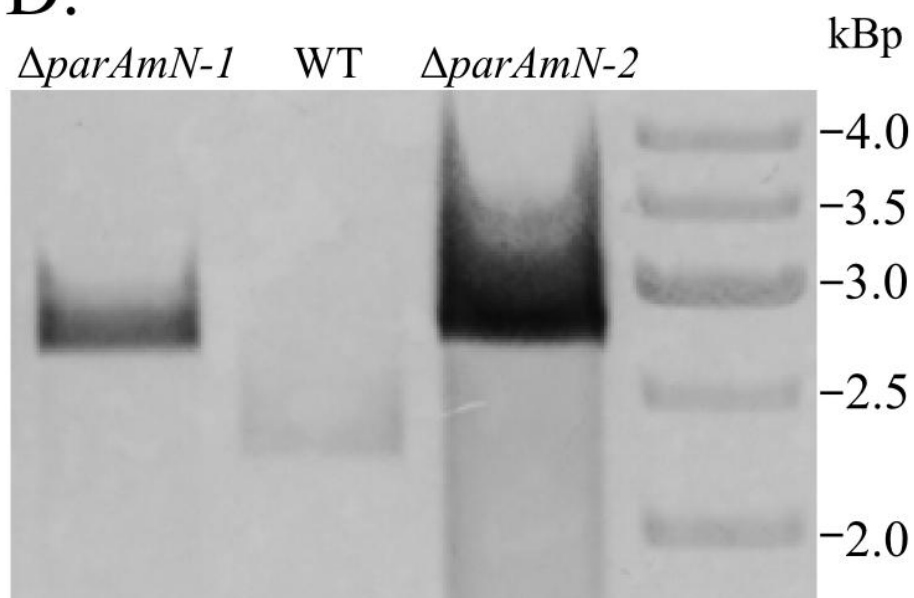




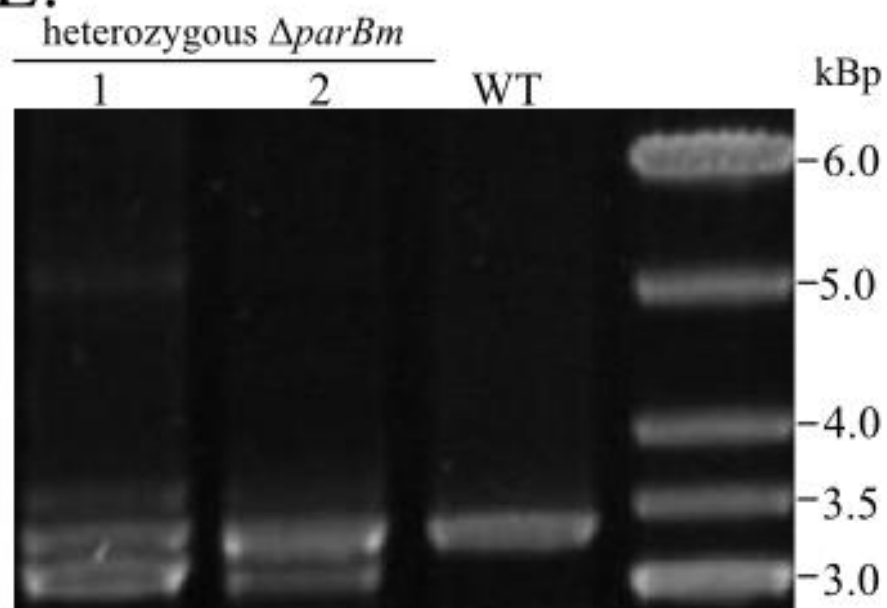
C.



D.



E.



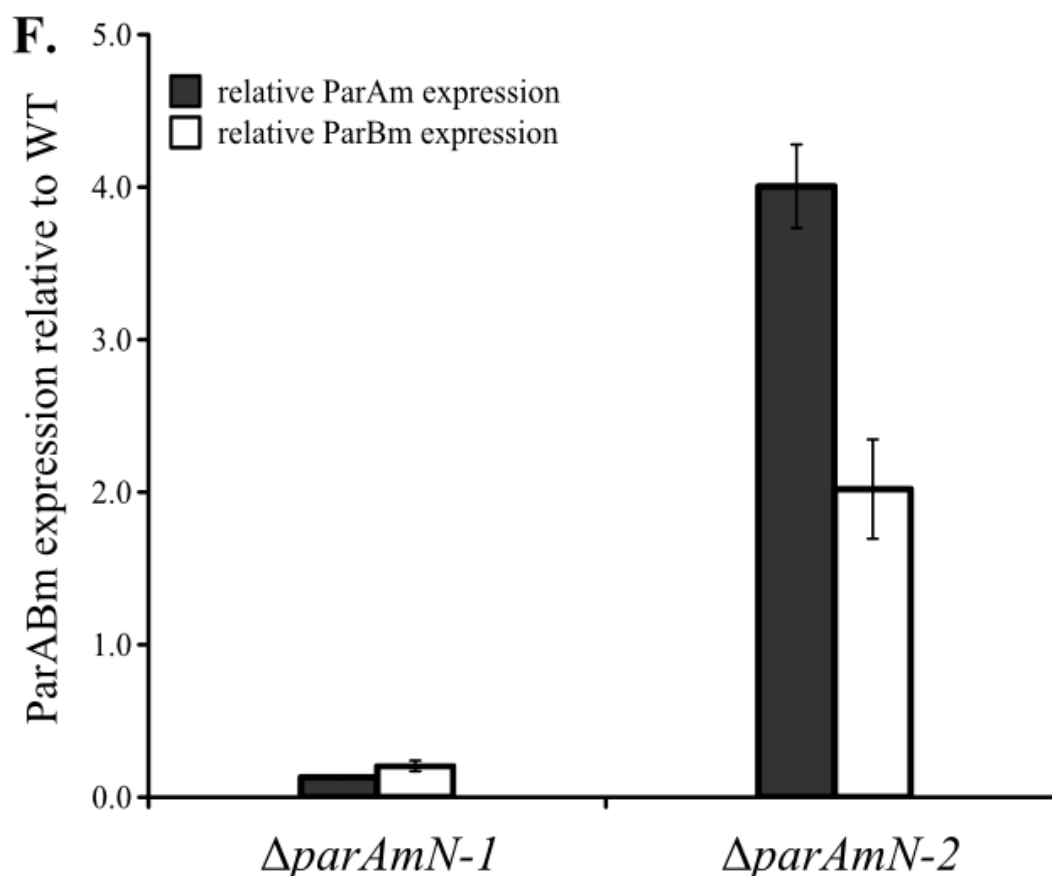
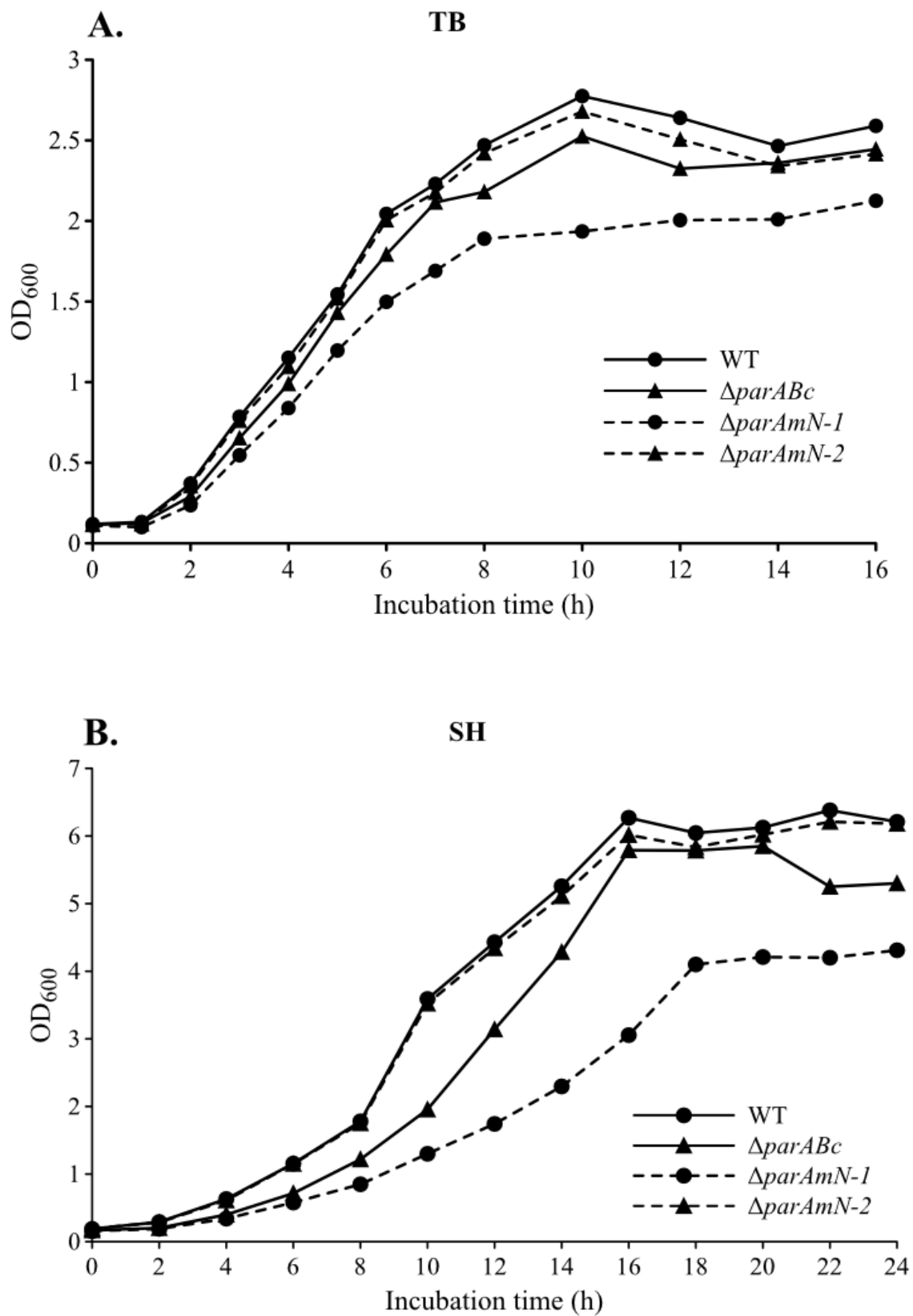


Fig. 6. Generations and genotype confirmations of the chromosomal and megaplasmid *par* mutants. (A) Genotype confirmation of the  $\Delta parABc$  mutant by Southern blot. The genomic DNA was digested with BamHI. For Southern hybridization, a 991-bp biotin-labeled DNA fragment was used as a probe. The predicted sizes are 5.21 kbp for wild type, 4.86 kbp for  $\Delta parABc$ , respectively. (B) The *parABm* operon was replaced by *blm*, four colonies were checked by PCR (predicted sizes: 3.99 kbp for the wild-type allele, and 2.91 kbp for the  $\Delta parABm$  allele) (C) Schematic diagrams showing exchange of the N-terminus encoding region of *parAm* (corresponding amino acids 1-40) with *blm*. Panel I, panel II indicate the *blm* cassette was integrated in the opposite ( $\Delta parAmN-1$ ) and co-linear directions ( $\Delta parAmN-2$ ) relative to the *parABm* transcription, respectively. Gray arrowhead, promoter region of *parABm*; black arrowhead, promoter of *blm*. (D) Genotype confirmation of the  $\Delta parAmN-1$  and  $\Delta parAmN-2$  mutants by Southern blot. The genomic DNA was digested with PstI, the predicted sizes are 2.26 kbp for wild type, 2.72 kbp for  $\Delta parAmN-1$  and  $\Delta parAmN-2$ , respectively. (E) The PCR results showed that the *parBm* mutant replaced by *blm* had a heterozygous genotype (wild-type band, 3.38 kbp;  $\Delta parBm$  band, 3.13 kbp). (F) Expression levels of the truncated *parAm*, *parBm* genes relative to wild type in the  $\Delta parAmN-1$  and  $\Delta parAmN-2$  mutants were determined by RT-qPCR, respectively. The means and SDs shown are from three experiments. Gray bar represents the relative expression of the truncated *parAm*, white bar represents that of *parBm*.

### 3.2.3 *parABm* is required for wild-type cell growth, while *parABc* is not

The growth phenotypes of the obtained *par* mutants were initially analyzed using nutrient (TB) and minimal (SH) media. In both media,  $\Delta parABc$  did not display an appreciable growth defect. On the other hand, the growth rate of  $\Delta parAmN-1$  was drastically affected, and this effect did not appear in  $\Delta parAmN-2$  (Fig. 7A, B), thus an inadequate amount of ParABm provoked impaired cell growth. Next, we undertook microscopy experiments to observe the cell morphology, DNA segregation, and cell division of the  $\Delta parABc$ ,  $\Delta parAmN-1$  and  $\Delta parAmN-2$  mutants. When grown in TB medium, no cell morphology or cell division defects occurred in either  $\Delta parABc$ ,  $\Delta parAmN-1$  or  $\Delta parAmN-2$  (Fig. 7C). The frequencies of anucleate cells were also not increased in these mutants (data not shown). However, quite a number of cells containing a smaller amount of stainable nucleic acid (DNA-less cells) were observed in  $\Delta parAmN-1$  but not in  $\Delta parAmN-2$  or  $\Delta parABc$  (Fig. 7C). Statistically ( $n \sim 300$ ), the frequencies of DNA-less cells of  $\Delta parABc$  grown in TB and SH medium were both indistinguishable from the frequencies observed in wild type (Table 7; data not shown). In combination with the growth phenotype (Fig. 7A, B), these data suggested that deletion of *parABc* did not provoke appreciable genome loss, i.e., no apparent genome replication and segregation defects had occurred. In the case of  $\Delta parAmN-2$ , the frequency of DNA-less cells was also not increased (Table 7), by contrast, in  $\Delta parAmN-1$ , 33.02% of cells were found to contain a smaller amount of stainable nucleic acid when grown in TB medium (Fig. 7C; Table 7). Thus, it seems that an inadequate amount of the megaplasmid ParAB protein may lead to loss of genome content in  $\Delta parAmN-1$ . Whether the chromosome or the megaplasmid has been affected is still unknown.



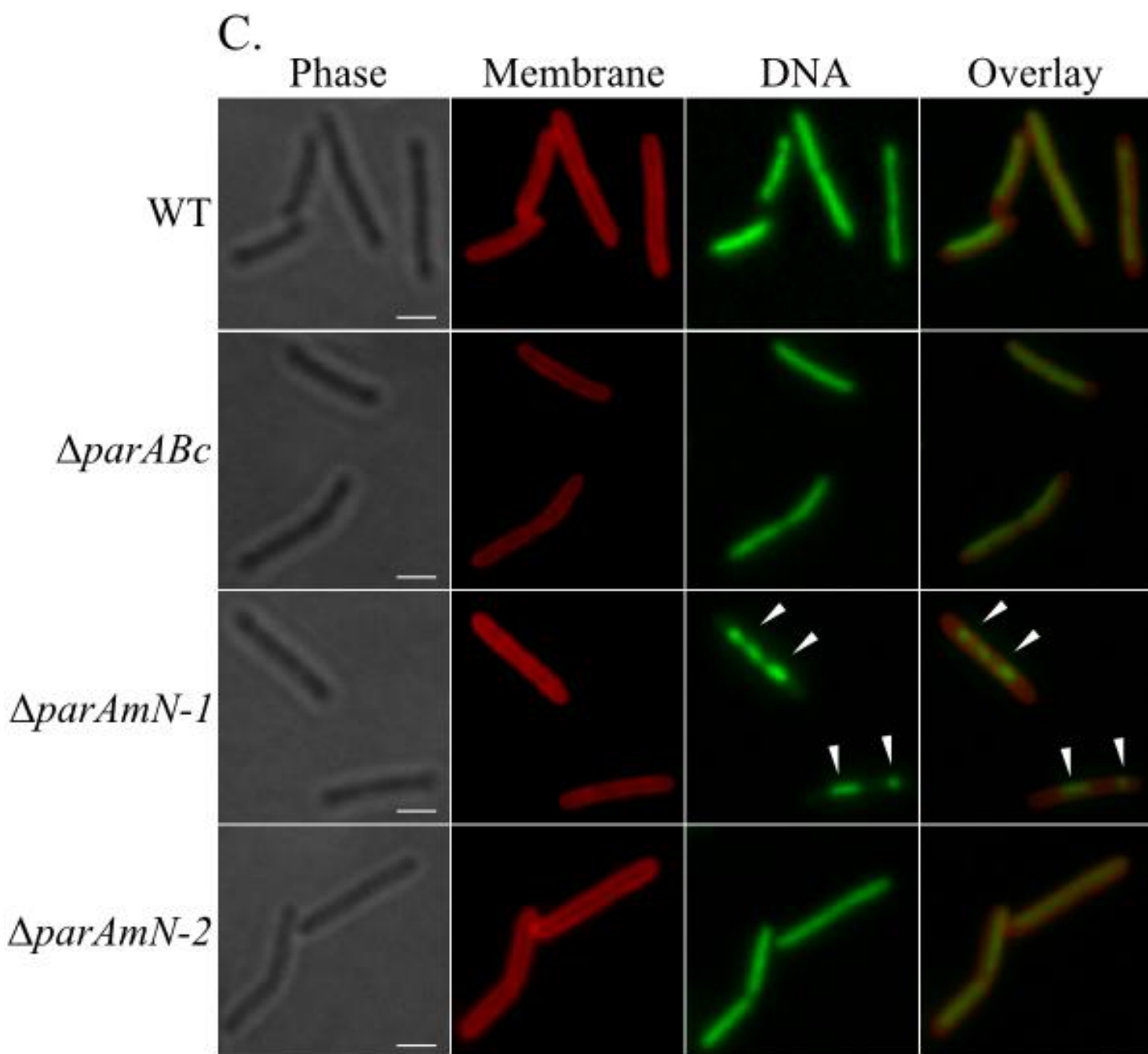


Fig. 7. Growth phenotypes, cell shape, cell division, and DNA morphology observations of the  $\Delta parABC$ ,  $\Delta parAmN-1$  and  $\Delta parAmN-2$  strains. (A, B) The cultures were grown in antibiotic-free TB medium (A) and SH medium (B). One represent of three independent experiments is shown, wild type -solid line with circles,  $\Delta parABC$ -solid line with triangles,  $\Delta parAmN-1$ -dashed line with circles,  $\Delta parAmN-2$ -dashed line with triangles. (C) Microscopic analyses of the cell shape, cell division and DNA morphology of  $\Delta parABC$ ,  $\Delta parAmN-1$  and  $\Delta parAmN-2$  grown in TB medium. Shown are phase-contrast cells (Phase), CFS stained cell membranes (Membrane), DAPI stained DNA (DNA), and a merge between Membrane and DNA (Overlay). White arrowheads, DNA-less cells. Scale bars, 2  $\mu\text{m}$ .

### 3.2.4 *parABm* is required for maintaining the megaplasmid but not the chromosome, while *parABc* is not important for maintenance of the both replicons

The severe growth retardation and high frequency of DNA-less cells in the  $\Delta parAmN-1$  mutant raised a possibility that the genome replication and segregation had been impeded. To understand this, the phenotypes of the *par* mutants in the aspect of genome content were analyzed. Interestingly, the  $\Delta parAmN-1$  colonies were additionally found to show white colour in growing medium. The megaplasmid of *T. thermophilus* carries the genes (e.g. TT\_P0057) necessary for the final steps of carotenoid synthesis, wild-type colonies display orange-yellow colour. Thus, the white colour of  $\Delta parAmN-1$  indicated reduction or absent of carotenoid synthesis. We then tested the expressions of the  $\beta$ -glucosidase (TT\_P0042, *bgl*) and  $\beta$ -galactosidase genes (TT\_P0022, *bgal*) located on the megaplasmid in these mutants, based on the principle that both gene products can cleave 5-bromo-4-chloro-3-indolyl (BCI) substrates resulting in blue colour precipitations. After streaking on TB and TB supplemented with XGlc (50  $\mu$ g/ml) and XGal (50  $\mu$ g/ml), the colonies of  $\Delta parAmN-1$  remained completely white on both types of plates, while those of wild type,  $\Delta parABc$ , and  $\Delta parAmN-2$  were orange-yellow on TB plate and blue on the TB plate with the chromogenic substrates (Fig. 8A). Further,  $\beta$ -glucosidase (Bgl) activities in the mutants were measured using p-NP- $\beta$ -Glc as a substrate, with a clean deletion strain lacking Bgl activity as a negative control ( $\Delta bgl$ ). Compared with wild type,  $\Delta parAmN-2$  and  $\Delta parABc$ ,  $\Delta parAmN-1$  showed nearly undetectable enzyme activity (wild type,  $28.29 \pm 0.14$  units/OD<sub>600</sub>;  $\Delta parAmN-1$ ,  $0.09 \pm 0.02$  units/OD<sub>600</sub>;  $\Delta parAmN-2$ ,  $30.07 \pm 1.28$  units/OD<sub>600</sub>;  $\Delta parABc$ ,  $27.02 \pm 0.78$  units/OD<sub>600</sub>), with a value even lower than that of the  $\Delta bgl$  strain ( $3.98 \pm 0.20$  units/OD<sub>600</sub>) (Fig. 8B). The residual low activity in the strain devoid of the *bgl* gene is probably due to unspecific cleavage of the substrate by family 2 glycoside hydrolases encoded by ORFs TT\_P0220-0222. No unspecific cleavage of the substrate was observed in  $\Delta parAmN-1$ , indicating that apart from the lack of the  $\beta$ -glucosidase, the family 2 glycoside hydrolases were also lacking. Thus, it is highly possible that in  $\Delta parAmN-1$ , the copy numbers of the loci encoding these proteins are extremely reduced, or even the loci

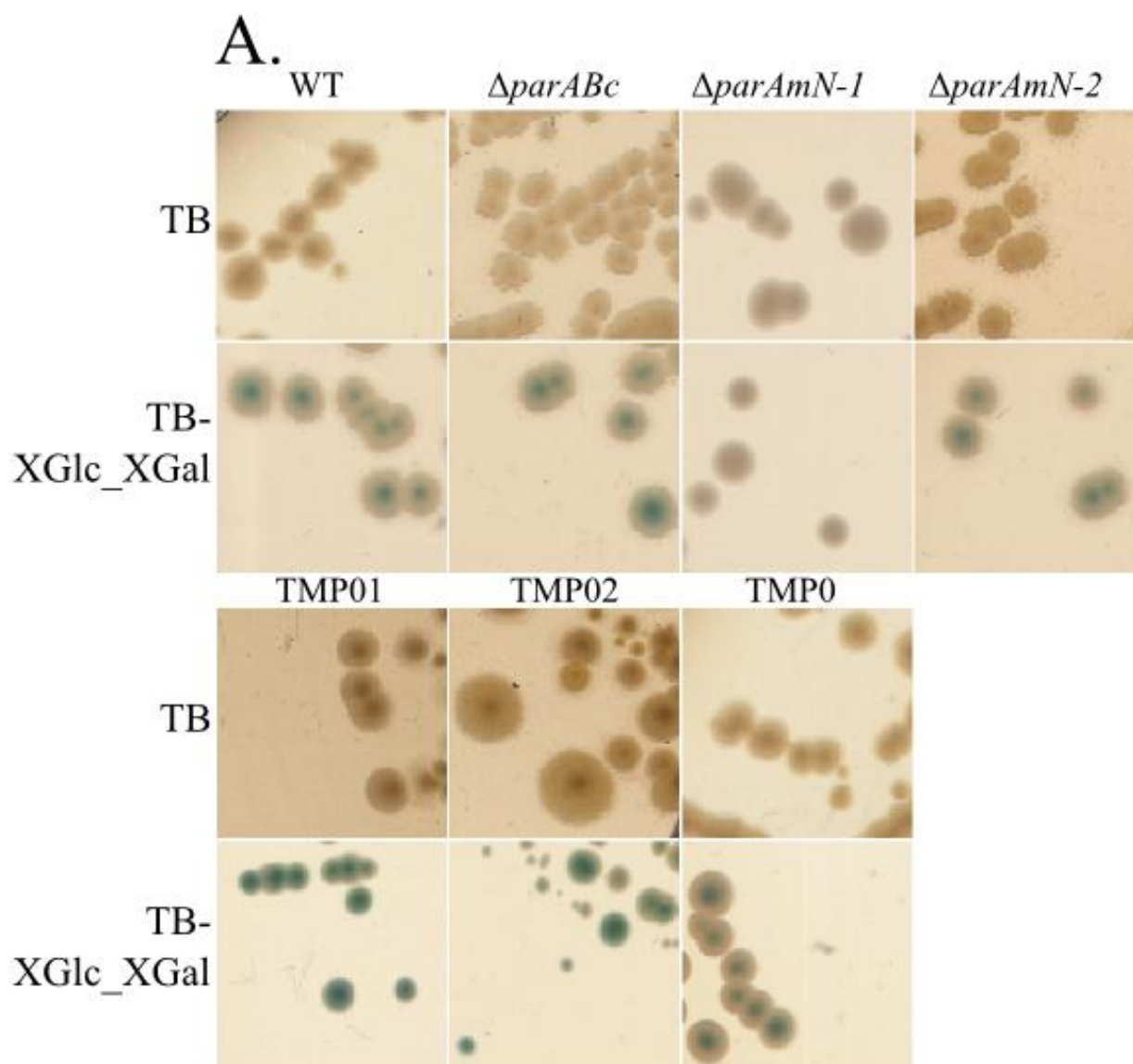
are completely lost in the megaplasmid, while this effect did not appear in  $\Delta parAmN-2$  or  $\Delta parABc$ .

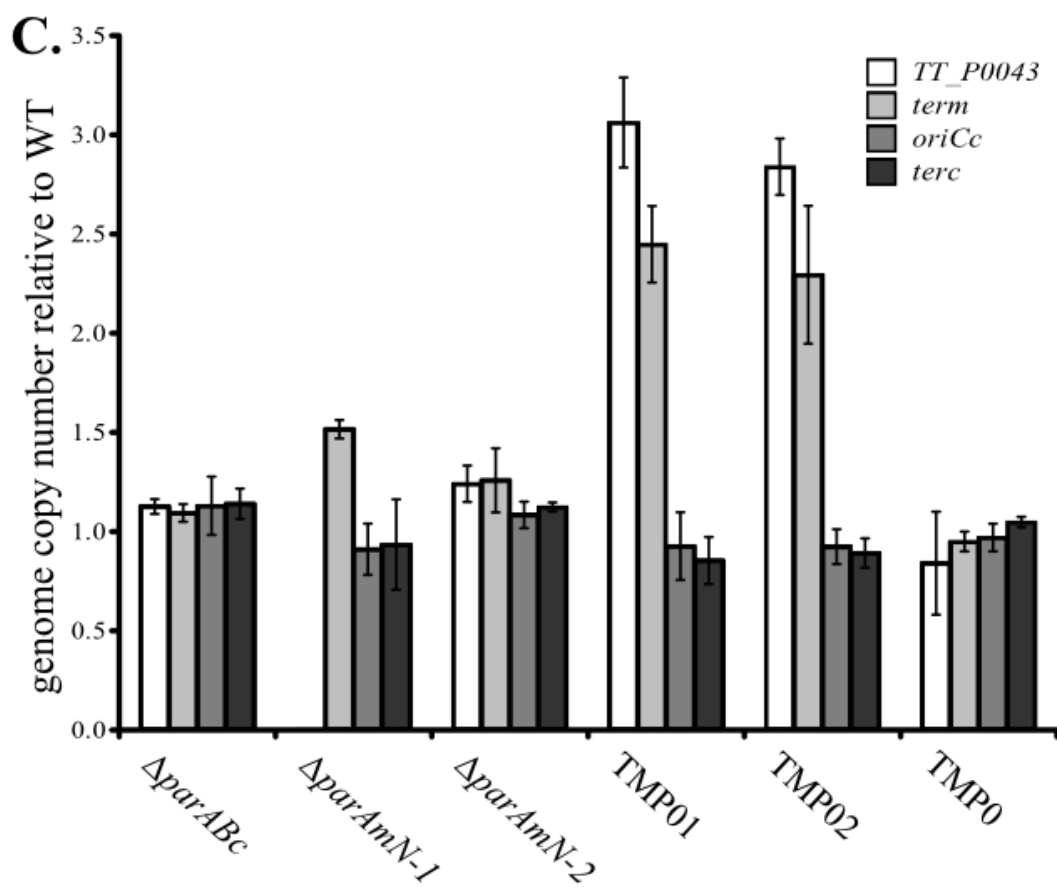
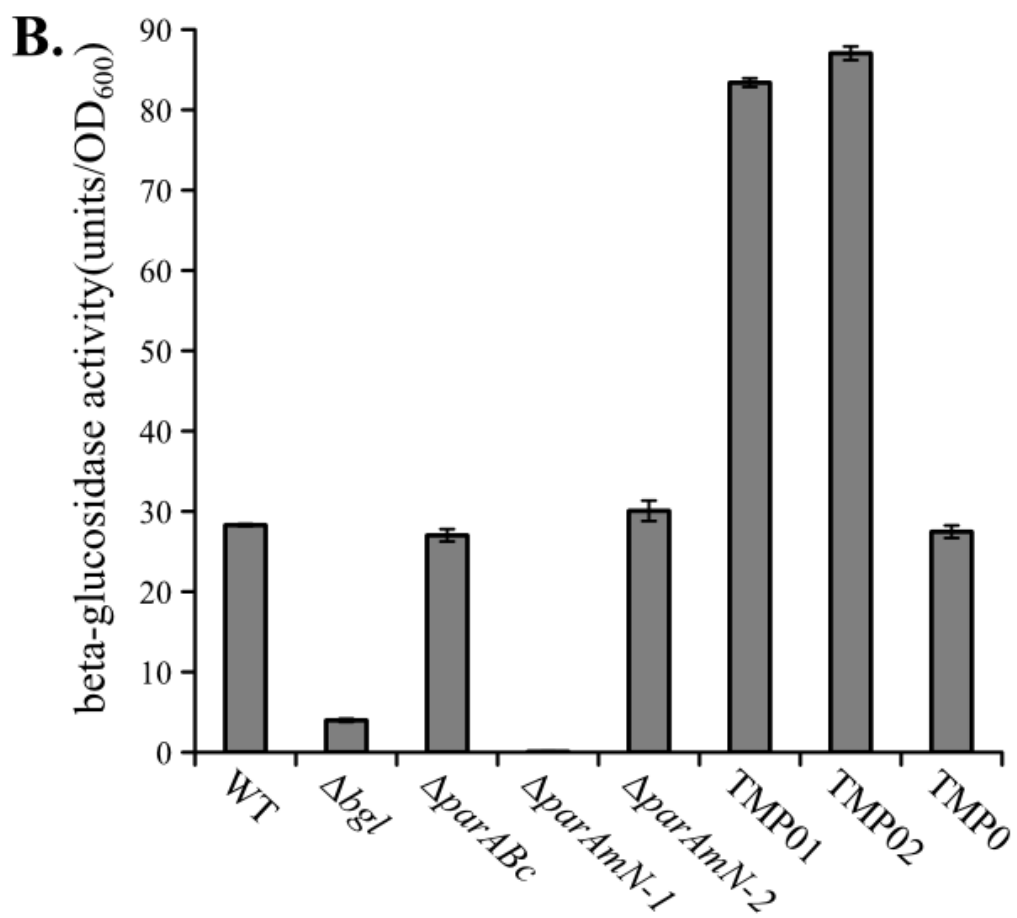
To reveal the truth, real-time qPCR was used to measure the genome copies relative to wild type at multiple genome sites in  $\Delta parABc$ ,  $\Delta parAmN-1$  and  $\Delta parAmN-2$ . For qPCR, two megaplasmid loci were chosen, TT\_P0043 and TT\_P0195, which are located at about 32.0 kbp from *oriCm*, and 3.0 kbp from *term*, respectively; the chromosomal sites chosen were located at approximately 2.5 kbp from *oriCc* and 1.5 kbp from *terc*, respectively. Consistent with the phenotypes observed, the chromosome and megaplasmid copy numbers of  $\Delta parABc$  were not altered compared with the wild-type strain in which the values were set as 1 (Fig. 8C; Table 7), indicating that *parABc* is not involved in either the chromosome or megaplasmid bulk DNA replication. In  $\Delta parAmN-2$ , the relative copy numbers of the chromosomal sites were also not changed, while the values of the megaplasmid sites were mildly increased (Fig. 8C; Table 7). In  $\Delta parAmN-1$ , the copy numbers of the chromosomal sites were also not changed compared with wild type (Fig. 8C; Table 7). By contrast, no signal was detectable at the locus TT\_P0043 (the  $C_t$  value was near with that from the qPCR reaction without template), suggesting this locus was completely lost but not its copy number was reduced; surprisingly, the value of the other locus TT\_P0195 which is near *term* was even slightly higher than that of wild type (Fig. 8C; Table 7). This result suggested that not the entire megaplasmid was lost in  $\Delta parAmN-1$ . Instead, it was probable that only certain portions were eliminated, these portions might be non-essential regions. To confirm this hypothesis, pulsed field gel electrophoresis was performed to visualize the chromosome and megaplasmid in  $\Delta parAmN-1$  and  $\Delta parAmN-2$ . In  $\Delta parAmN-2$ , the chromosome and megaplasmid were intact by comparison with the wild type (Fig. 8D). As expected, in  $\Delta parAmN-1$ , a portion of the megaplasmid sequence had been eliminated, the size of the resultant megaplasmid was only approximately 125-130 kbp (WT, 232.6 kbp) (Fig. 8D). Interestingly, it seems this smaller megaplasmid also could not be partitioned properly after replication, since duplicated, triplicated, and even quadruplicated megaplasmid sizes could be observed (Fig. 8D). In order to estimate which portion of the megaplasmid was lost, PCR amplifications of 10 loci distributed over the

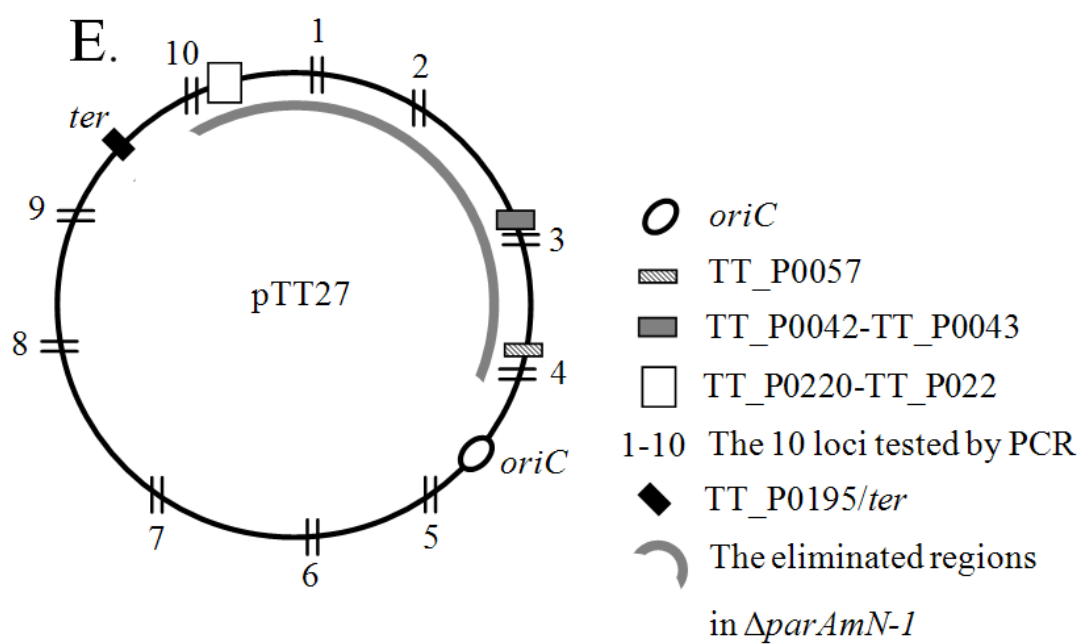
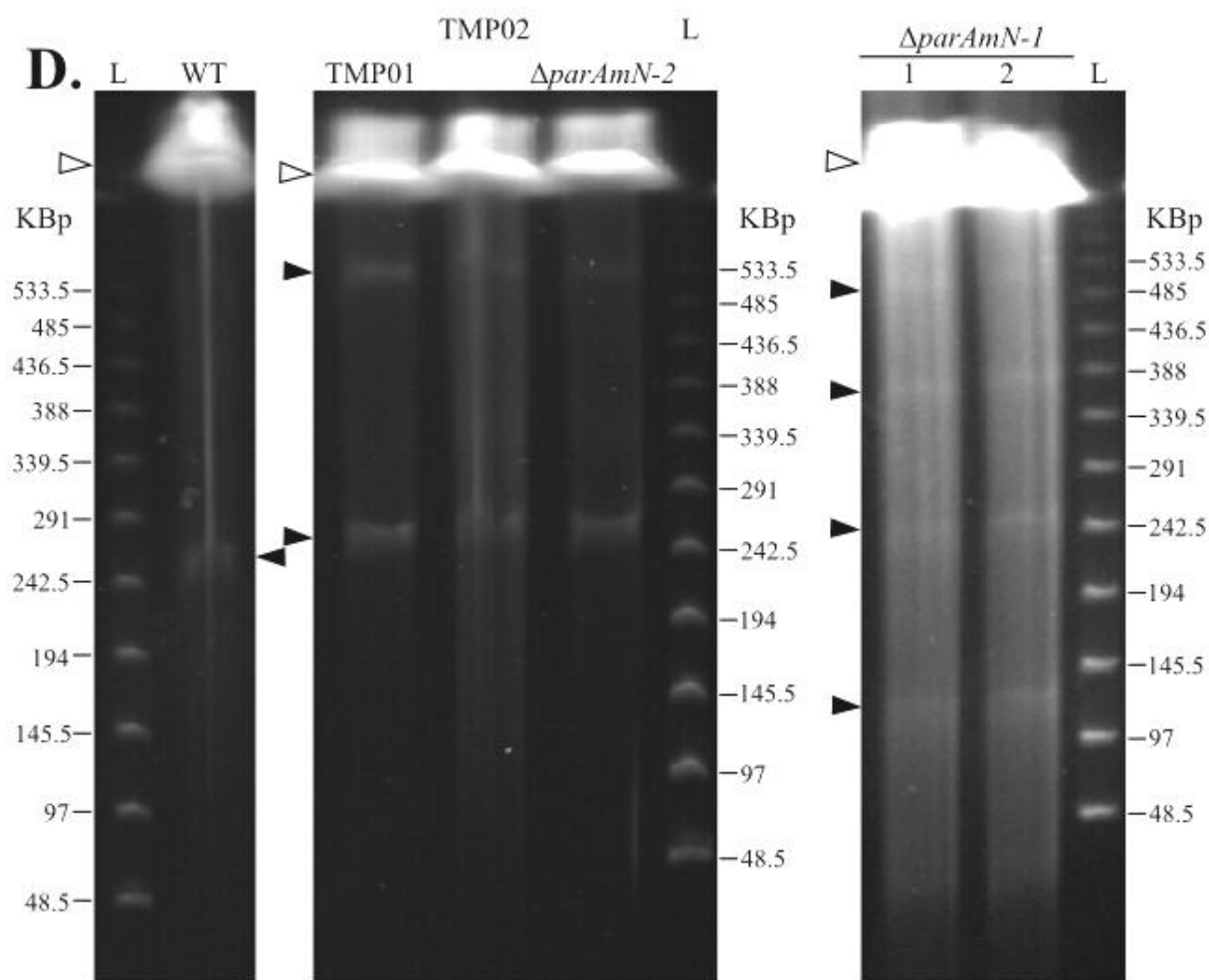
megaplasmid were performed (Fig. 8E). No PCR amplicons were detected in the regions between approximately 11 kbp and 102 kbp distance from one side of the megaplasmid replication origin, suggesting these regions were lost; on the contrary, the regions located on the opposite site of the replication origin were still present since amplicons were detectable (Fig. 8E, F). The PCR result was in a good agreement with the above data that the loci TT\_P0042-TT\_P0043, TT\_P0057 and TT\_P0220-TT\_P0222 were absent, while the locus TT\_P0195 (*term*) was still present in  $\Delta parAmN-1$  (Fig. 8), and it also accounted for the slightly higher copy numbers of the *term* region, as after excision of the deleted regions, *term* was supposed to be closer to *oriCm* (Fig. 8C, E).

Mild increase of the megaplasmid copy number was observed in  $\Delta parAmN-2$  that has higher expression levels of the N-terminus truncated ParAm and ParBm compared with wild type (Fig. 8C; Table 7), indicating the megaplasmid copies are related to the ParABm protein amount. Thus, two strains allowing overexpression of ParAm or ParBm from plasmids were constructed, respectively. The phenotypical consequences in the two strains, TMP01 (pMK-*parAm*) and TMP02 (pMK-*parBm*) were also analyzed. In both strains, the cell growth, cell morphology, cell division, or DNA segregation were not apparently influenced (data not shown). However, the colonies of TMP01 and TMP02 were found to be more yellowish and bluish on TB plates and TB plates supplemented with XGlc and XGal plates, respectively (Fig. 8A). A Bgl activity assay also showed that compared with wild type, TMP01 and TMP02 had increased Bgl activities ( $83.39 \pm 0.55$  and  $87.05 \pm 0.87$  units/OD<sub>600</sub>, respectively; Fig. 8B). Further, qPCR experiments demonstrated that the both strains had 2.5-3.5 fold more megaplasmid copies compared with wild type and TMP0 carrying empty vector (pMK18) (Fig. 8C; Table 7). Moreover, untangled megaplasmid after duplications could be observed in PFGE analysis of TMP01 and TMP02, indicating megaplasmid replication speed had probably exceeded DNA separation and cell division speeds (Fig. 8D). Taken together, it seems that *parABm* is critical for megaplasmid maintenance, probably through mediating its replication and segregation. The above data also implied that *parABm* does not play a role in maintaining the chromosome.









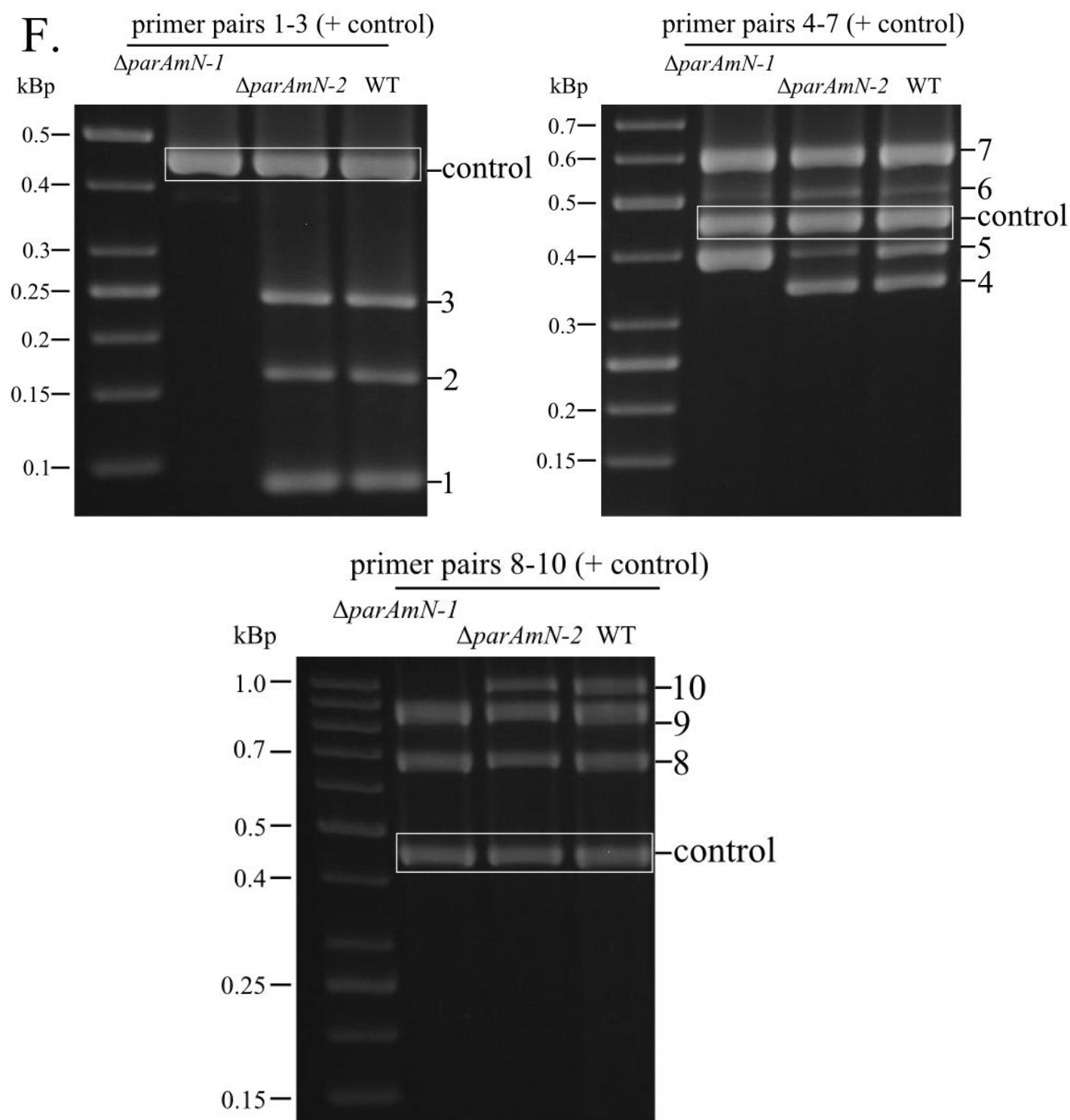


Fig. 8. Characterization of genome features of the chromosomal and megaplasmid *par* mutants ( $\Delta parABC$ ,  $\Delta parAmN-1$ ,  $\Delta parAmN-2$ , TMP01, and TMP02). (A) Phenotypes of the mutants on TB and TB-XGlc\_XGal plate. (B) Intracellular  $\beta$ -glucosidase activity measurements of the mutants. The means and the SDs of three independent experiments are shown. (C) Chromosome and megaplasmid copy number relative to wild type of the individual mutant was determined by qPCR. The means and SDs

were from three experiments. White bar, TT\_P0043; light-gray bar, TT\_P0195 (locus near the megaplas mid terminus (*term*)); mid-gray bar, locus near the chromosomal origin (*oriCc*); dark-gray bar, locus near the chromosomal terminus (*terc*). (D) Pulsed field gel electrophoresis visualizing chromosome and megaplas mid. “L”, lambda ladder; “1, 2” indicates two independent colonies of  $\Delta parAmN-1$ ; the positions of the chromosome and megaplas mid are indicated with white and black arrowheads, respectively. (E) Schematic drawing of the megaplas mid pTT27. The positions and names of the primer pairs used for detecting megaplas mid sequence loss in  $\Delta parAmN-1$  are indicated with short black lines and numbers from 1 to 10, respectively. The loci on the megaplas mid that have been investigated are indicated with different bars, and their names are on the right panel of the figure. (F) PCR amplification results of the 10 loci indicated in (E) from wild type,  $\Delta parAmN-1$  and  $\Delta parAmN-2$ . The primer pairs 1 to 3, 4 to 7, 8 to 10 were respectively mixed into three pools, and in each reaction, amplification of a chromosomal gene locus (*pyrF*) was used as a control. The predicted sizes of the products 1 to 10 are 87, 164, 247, 346, 400, 498, 610, 812, 898, 1014 bp respectively. The size of the control amplicon is 460 bp (white frame). The bands of the 10 PCR products are indicated with numbers 1-10 on the right side of the corresponding figure. The gray arc in (E) indicates the eliminated megaplas mid regions in  $\Delta parAmN-1$  estimated from the results of enzyme assay, qPCR, PFGE, and PCR.

Table 7. DNA-less cell frequencies and relative genome copies to wild type in the *par* mutants\*.

Strain	DNA-less cells (%)	Relative TT_P0043 copies	Relative <i>term</i> copies	Relative <i>oriCc</i> copies	Relative <i>terc</i> copies
WT	1.24	1	1	1	1
$\Delta parABc$	3.05	1.13 ± 0.04	1.09 ± 0.05	1.13 ± 0.15	1.14 ± 0.08
$\Delta parAmN-1$	33.02	/	1.52 ± 0.05	0.91 ± 0.13	0.93 ± 0.23
$\Delta parAmN-2$	2.28	1.24 ± 0.09	1.26 ± 0.16	1.08 ± 0.07	1.12 ± 0.02
TMP01 <sup>a</sup>	1.26	3.06 ± 0.23	2.45 ± 0.19	0.93 ± 0.17	0.85 ± 0.12
TMP02 <sup>b</sup>	2.12	2.84 ± 0.14	2.29 ± 0.35	0.92 ± 0.09	0.89 ± 0.07
TMP0 <sup>c</sup>	1.15	0.84 ± 0.26	0.95 ± 0.05	0.97 ± 0.07	1.05 ± 0.03

\* DNA-less cell frequencies were measured from the cells grown in TB medium. The cells used for qPCR measurements were grown under a same condition (TB medium, 60 °C). Relative genome copies are shown with mean ± SD from three independent experiments. <sup>a</sup> TMP01 is a HB27 derivative permitting overexpression of ParAm from a replicative vector pMK-*parAm*. <sup>b</sup> TMP02 is a HB27 derivative permitting overexpression of ParBm from a replicative vector pMK-*parBm*. <sup>c</sup> TMP0 is a HB27 derivative carrying pMK18 vector. “/” indicates no signal was detectable in the qPCR reaction.

#### 3.2.5 *In vitro*, ParBc binds specifically to *parSc*, while *ParBm* does not

Analysis of the potential functions of *parABc* and *parABm* showed that the two systems play different roles. Thus, we were inspired to understand whether the two different ParBs bind to the same site or if they behave as a replicon-specific manner. To this end, *in vitro* binding of ParB to the chromosomal *parS* site was performed by electrophoretic mobility shift assays (EMSA). The probe-designing principle was based on Lin *et al.* (1998) (see Chapter 2.4.4), and recombinant His-tagged ParB proteins were used for the assays (Fig. 9). In the case of ParBc, it was clear that the binding affinity (the distance between bound DNA and free DNA species, or the intensities of the bound species) was dependent on the protein concentration, indicating specific bindings (Fig. 10A). Superficially, ParBm also bound to the *parSc* probe, however, no step-wise affinity was observed, suggesting the bindings were probably unspecific (Fig. 10B). Almost all DNA-binding proteins contain more than one nucleic acid binding sites, and during *in vitro* DNA binding assays, they tend to bind any non-specific DNA (Hellman and Fried, 2007). Thus, to test whether ParBm can truly bind *parSc*, binding specificity assays are requisite. Competition experiments were performed to test the binding specificities by using a fixed amount of labeled wild-type probe and a series of increasing amounts of unlabeled wild-type or mutant probe (see Chapter 2.4.4). In the competition experiment of ParBc binding to the *parSc* probe, the band intensities of the bound DNA species competed with the unlabeled wild-type probe were apparently weaker than those competed by the unlabeled mutant probe at the same concentration (200-600 pmol) (Fig. 10C). And when the concentration of the unlabeled probes reached a value of 750 pmol, the binding of ParBc to the labeled *parSc* completely vanished, whereas the binding still occurred in the presence of the mutant *parSc* (Fig. 10C). By contrast, the competing situation of ParBm binding to *parSc* was processed as an opposite direction. It appeared as that the mutant probe competed even better than the wild-type probe; with the addition of 400 pmol mutant probe, the band showing bound labeled probe was almost gone, while the binding still occurred in the presence of the unlabeled wild-type *parSc* (Fig. 10D). These observations showed that ParBc binds specifically to the *parSc* site, whereas the binding between ParBm and *parSc* was unspecific, i.e.

ParBm does not bind *parSc*. Thus, the *parS* sites of the two Par systems are replicon-specific.

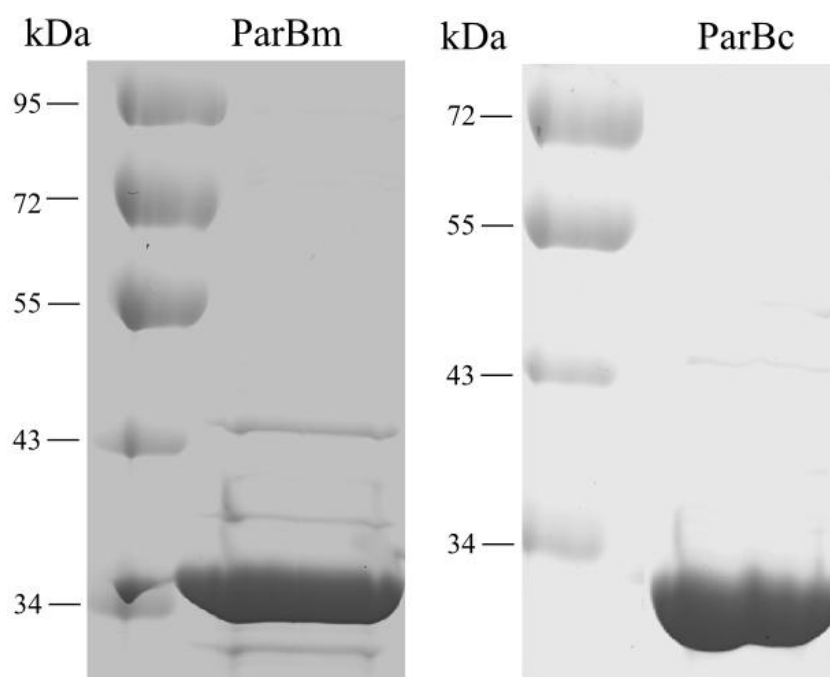
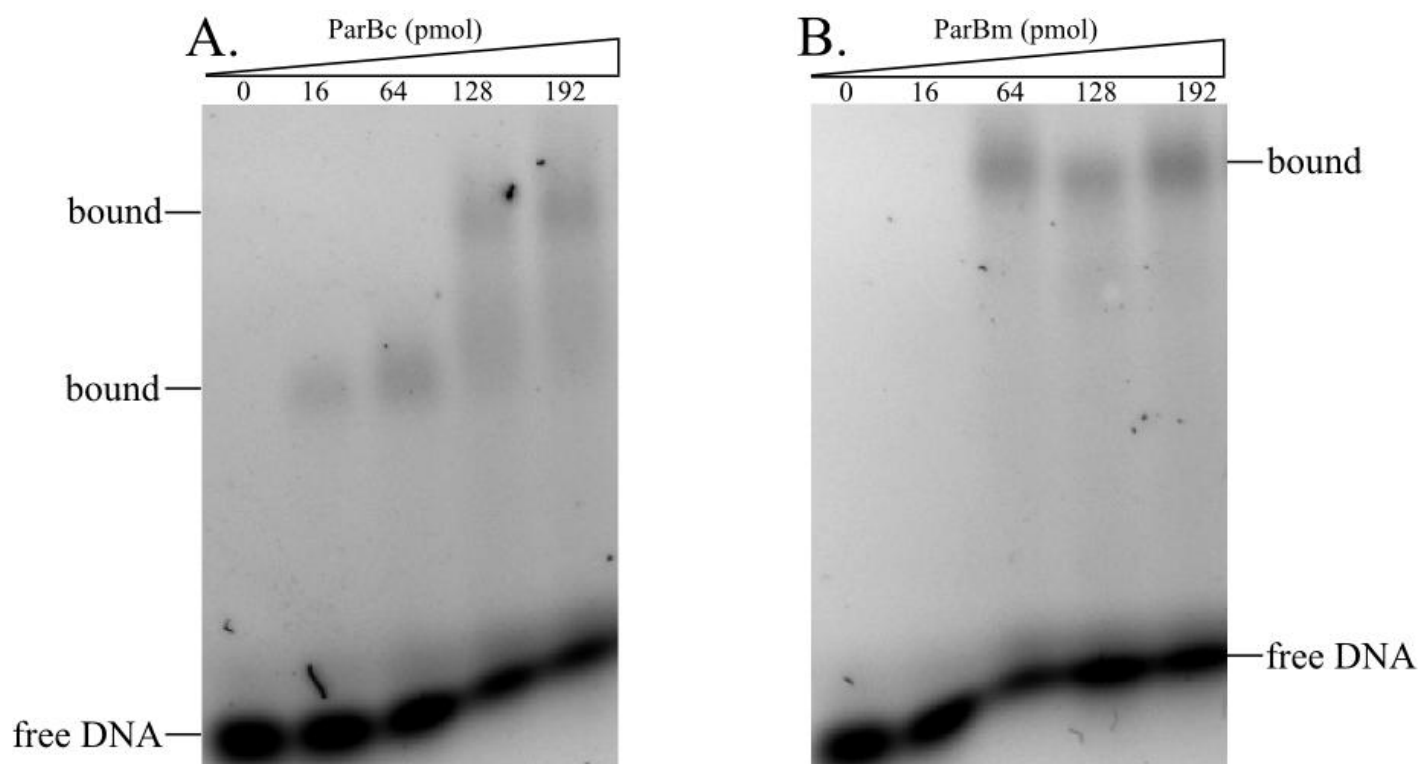
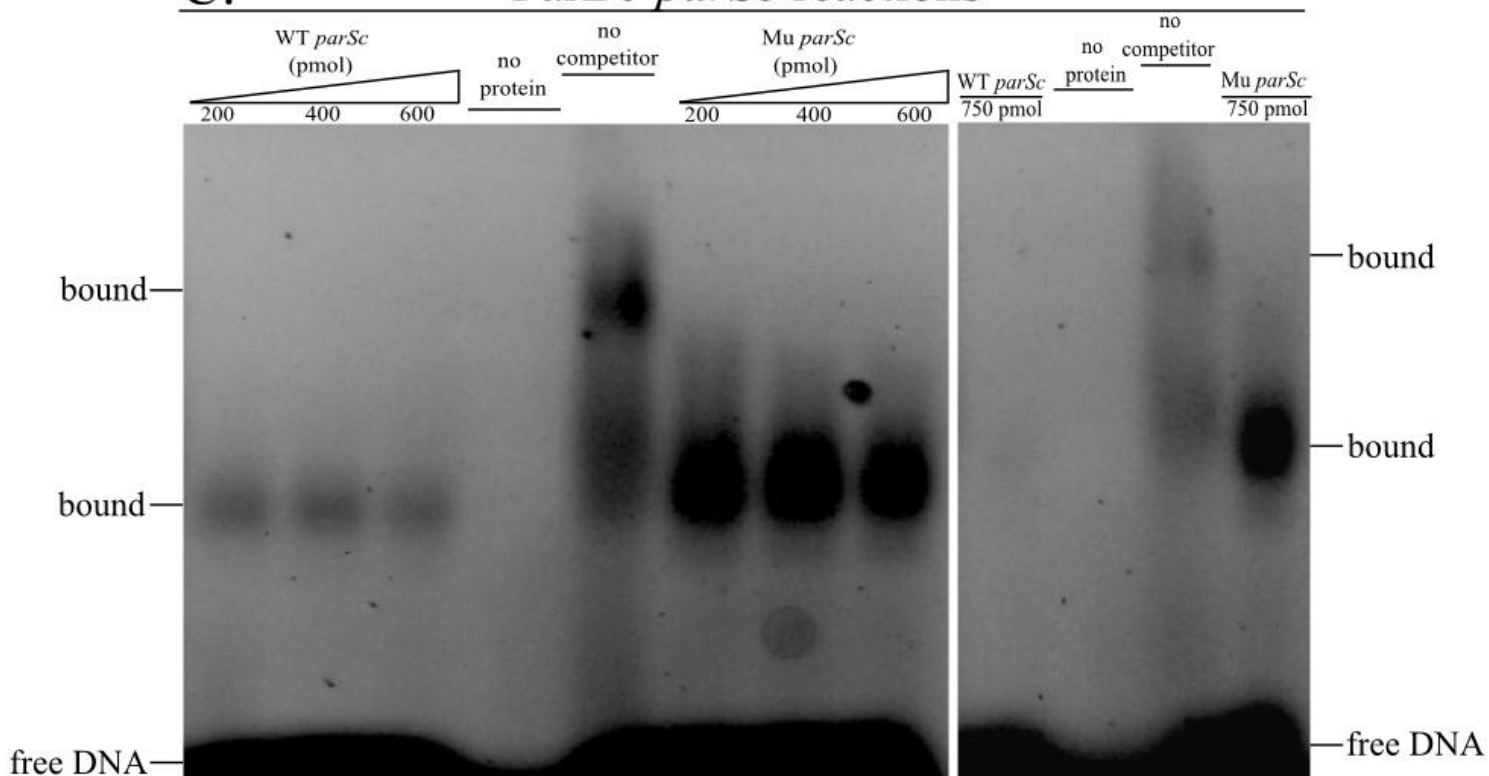


Fig 9. Purified His-tagged ParBc and ParBm proteins on SDS-PAGE gel. The protein concentrations were determined by Bradford assays, 10  $\mu$ g of each protein was applied. The predicted size of ParBc is 30.8 kDa, of ParBm is 34.4 kDa.



**C. ParBc-*parSc* reactions**



**D. ParBm-*parSc* reactions**

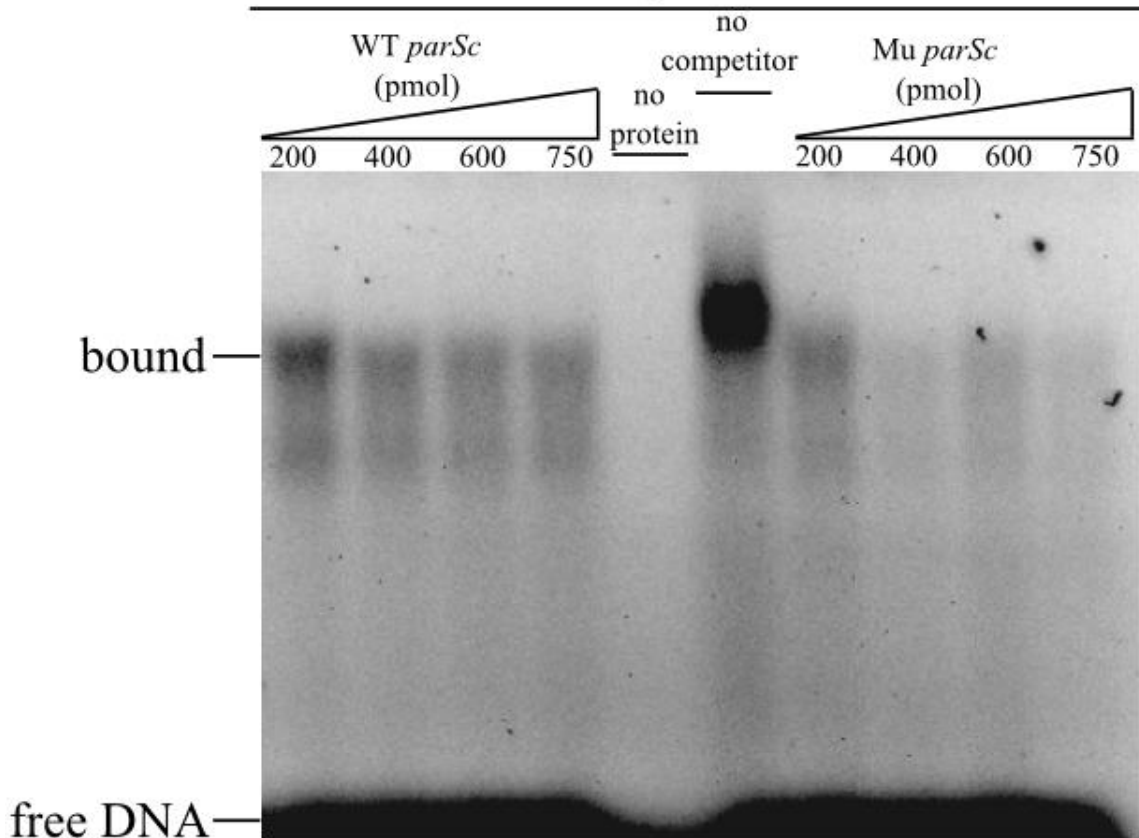




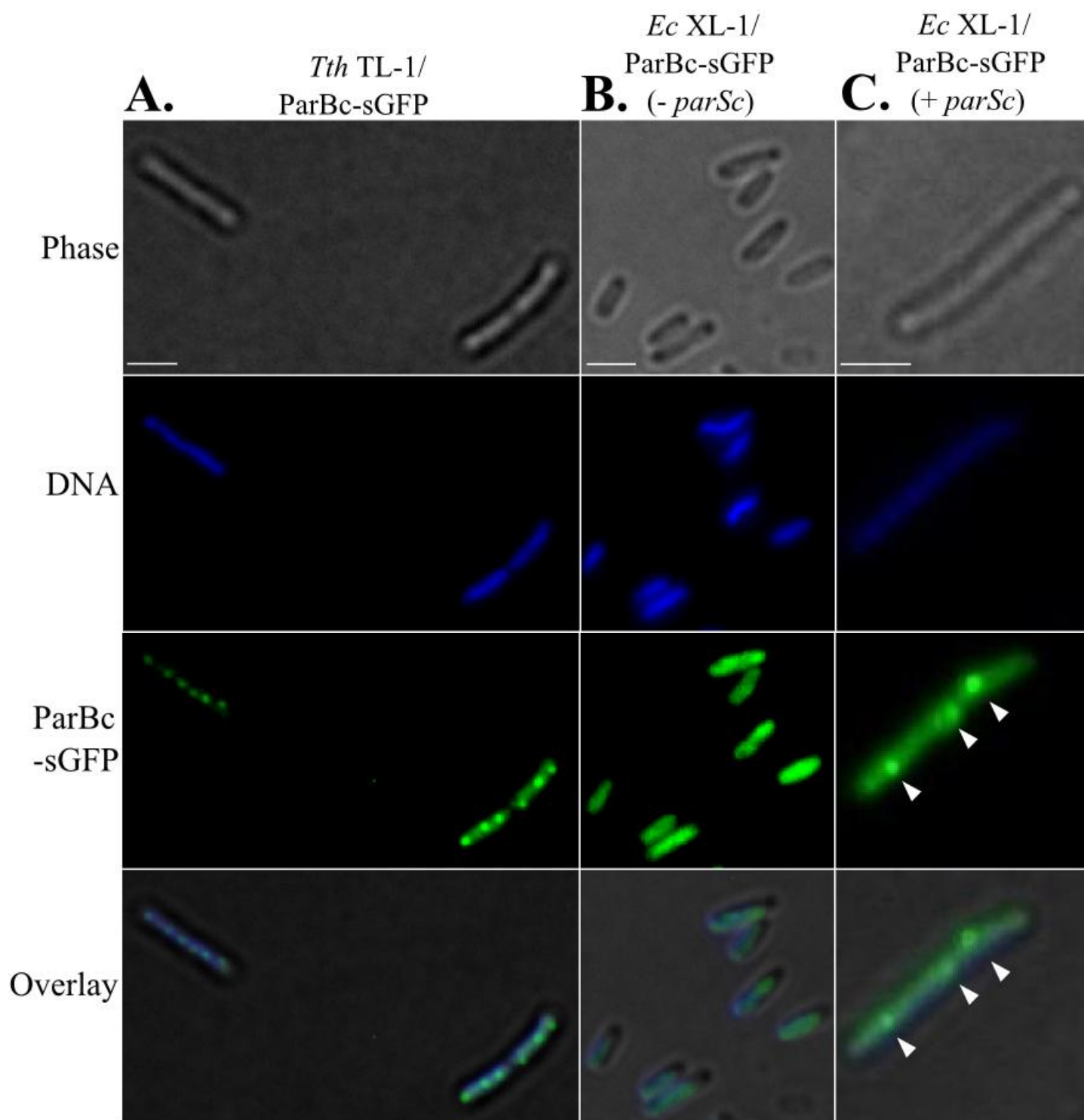
Fig. 10. *In vitro* DNA binding assays of the ParB proteins to the *parSc* sequence. Gel mobility shift assays were performed. In all cases, a FAM-labeled 25-bp DNA fragment containing the 16-bp *parSc* sequence was used as a probe, and all the reactions were performed under the same condition (Chapter Chapter 2.4.4). Shifted DNA species are marked as “bound”, free DNA species are marked as “free DNA”. (A, B) Gel shift assays were performed with 15 pmol FAM-labeled *parSc* probe and various concentrations of ParBc (A) and ParBm (B) (from left to right: no protein, 16, 64, 128, and 192 pmol, respectively). (C, D) Competition experiments with unlabeled wild-type and mutant *parSc* sequences (indicated with WT *parSc*, Mu *parSc*, respectively; C, ParBc-*parSc* reactions; D, ParBm-*parSc* reactions). Each reaction contained 15 pmol FAM-labeled wild-type *parSc*, and ParB proteins were added with a concentration of either 0 (no protein) or 200 pmol. Competition assays were performed with increasing amount of either unlabeled wild-type or mutants *parSc* probes (a series of 200, 400, 600, and 750 pmol ).

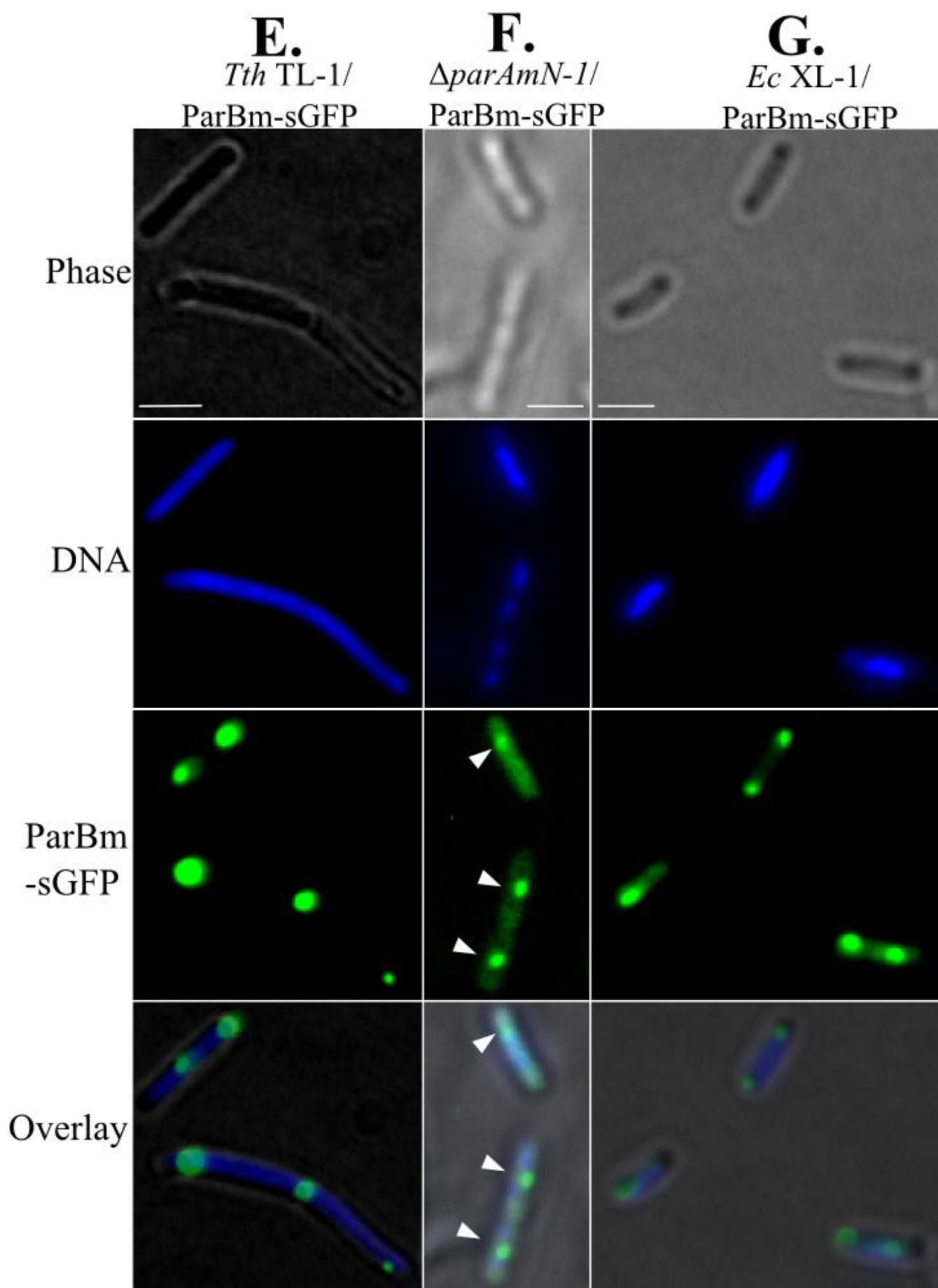
### 3.2.6. Polar localizations of ParBc-sGFP and ParBm-sGFP in wild-type *T. thermophilus* cells

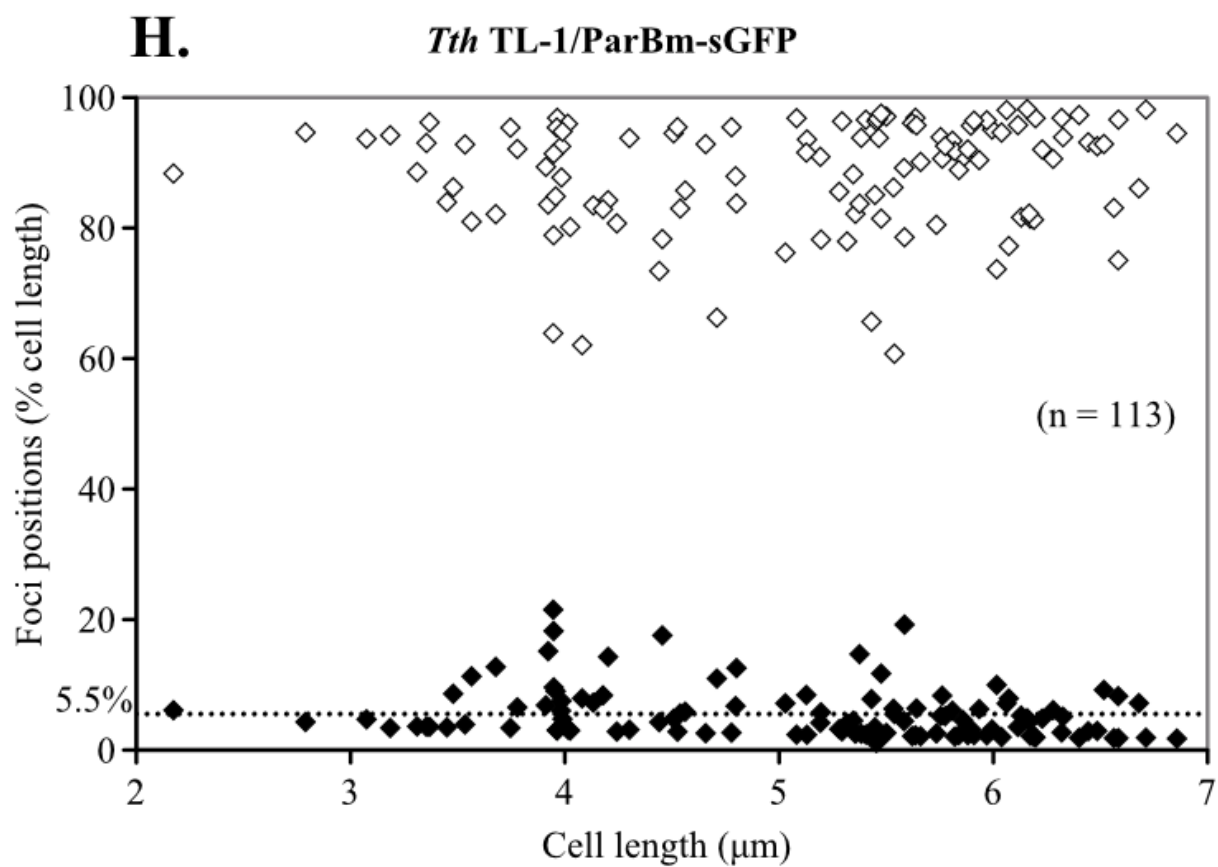
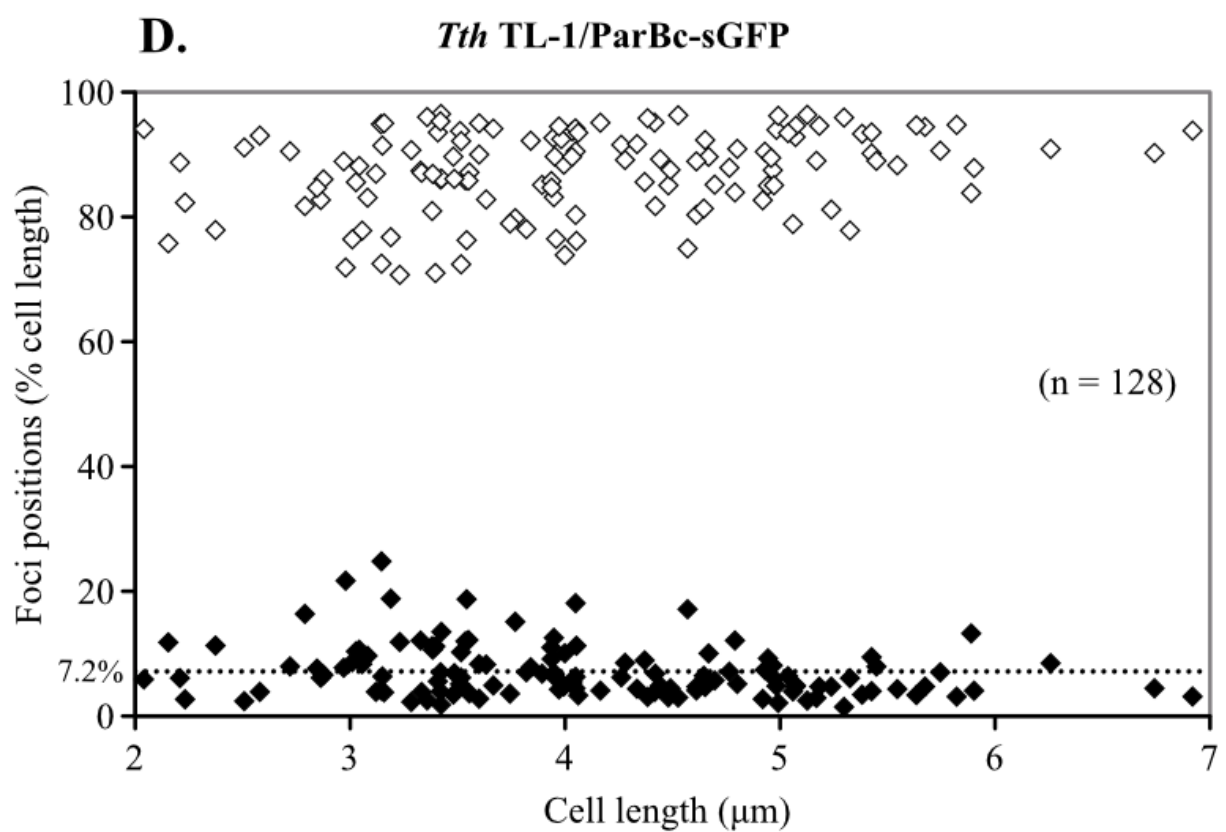
Studies of ParB localization patterns in other bacteria showed that fusions of fluorescent proteins to ParB proteins form punctate fluorescent foci representing ParB-*parS* nucleoprotein complexes in the cells (Li and Austin 2002; Fogel and Waldor, 2006; Yamaichi *et al.*, 2007). To further reveal the characteristics and functions of *parABc* and *parABm*, *in vivo* localizations of the ParB proteins were also investigated. Fusions of sGFP to the C-terminal of ParBc and ParBm were constructed, respectively (for detailed plasmid constructions, see Chapter 2.1.1). When expressed in *T. thermophilus* TL-1 (carotenoid synthesis deficient, otherwise wild-type strain), ParBc-sGFP formed well-defined fluorescent foci, providing *in vivo* proof that ParBc can bind *parSc* (Fig. 11A). Results from approximately 150 cells containing well-defined fluorescent foci (grown in rich medium TB), showed that almost all of these cells contained at least one focus positioned at the cell pole (95%). The majority of cells contained 2-6 foci, and in these cases, two were localized at cell poles (“old” poles), and the others were localized at positions of ongoing septum formation (“new” poles). For better illustration, the positions of the two most pole-proximal foci were measured from the nearest poles and expressed as fraction proportions of the cell lengths. The result showed that the mean position of the pole-nearest focus was at 7.2% fraction of the cell length (Fig. 11D), indicating ParBc-*parSc* is localized to cell

poles.

In the case of ParBm localization, when ParBm-sGFP was expressed in *T. thermophilus* strain TL-1, the fluorescent signals were also found to form discrete foci, suggesting that there were indeed ParBm binding sites in *T. thermophilus* (Fig. 11E). Statistically (n ~ 150), in cells containing fluorescent foci, at least one focus was localized at the cell poles (90%). When grown in TB medium, 82% of cells contained 2-3 foci, with 2 positioned at the cell poles (“old” poles), and the other was localized near to the cell centers (“new” poles) (Fig. 11E). The subcellular positions of the two most pole-proximal foci in 113 foci-containing cells were also measured from the nearest poles and expressed as fraction proportions of the cell lengths. It was found that the mean position of the nearest-to-pole focus was 5.5% of the cell fraction (Fig. 11H). These results suggested that similar to the situation of ParBc-*parSc*, ParBm-*parSm* was also polar localized. Moreover, as also observed in the ParBc localizations (Fig. 11A), the foci could be detected at the cell centers or septum formation positions indicated that ParB-*parS* nucleoprotein complexes may travel from cell poles to cell division positions, thus their localizations are dynamic processes.







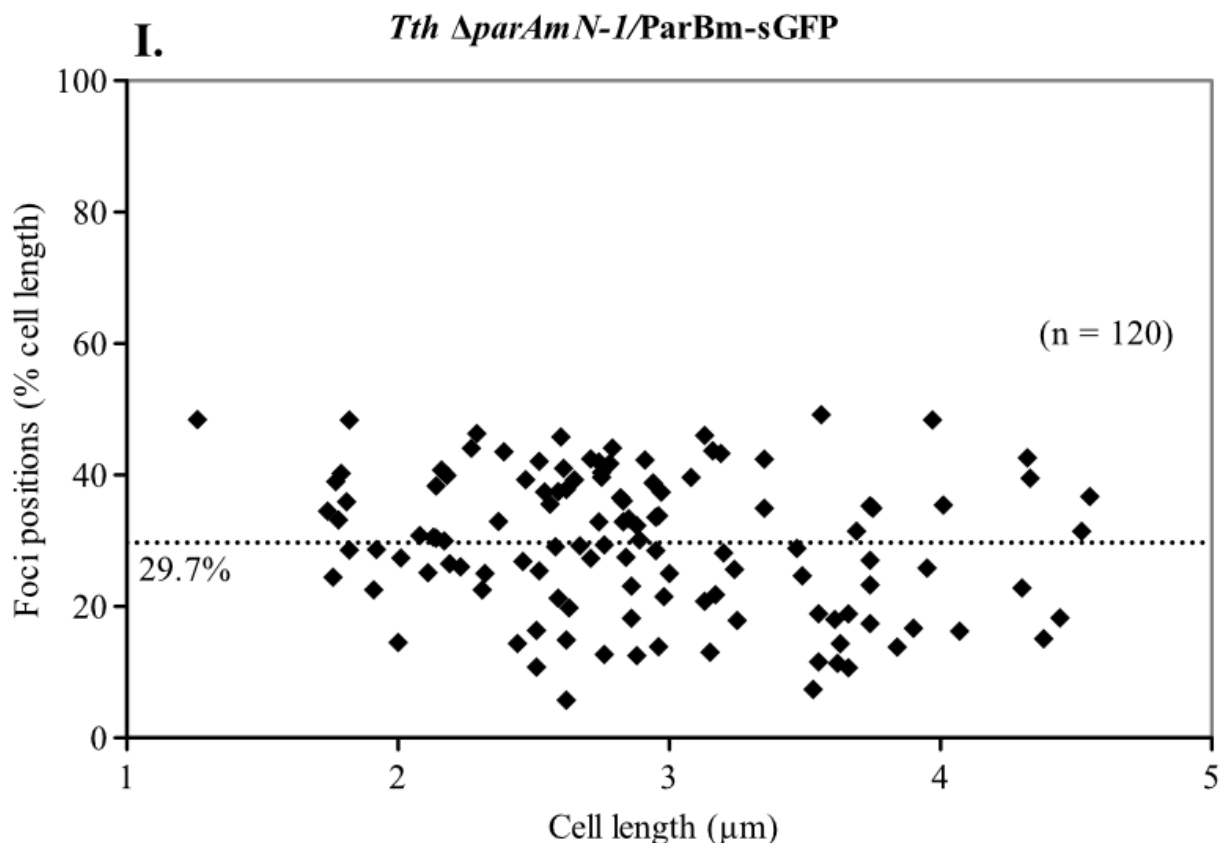


Fig. 11. Subcellular localizations of ParBc-s GFP and ParBm-s GFP in *T. thermophilus* or *E. coli* cells. Representative cells are shown with a gallery view of phase-contrast, DNA, ParBc-s GFP or ParBm-s GFP, and merged images (Overlay). Bars, 2  $\mu\text{m}$ . (A, E) ParBc-s GFP, ParBm-s GFP were expressed from the corresponding replicative vectors (pMK $paBc-sgfp$  and pMK $parBm-sgfp$ , respectively, Chapter 2.1.1) in the *T. thermophilus* TL-1 strain (lacking carotenoid synthesis, otherwise is considered as wild type), and the cells were grown in TB medium, respectively. (B, C, G) ParBc-s GFP, ParBm-s GFP were expressed in the *E. coli* XL-1 strain, respectively. Without the *parSc* site, ParBc-s GFP was found as patches (B); when the *parSc* sites were provided from a plasmid, ParBc-s GFP was localized as discrete foci (C); ParBm-s GFP was localized as discrete foci (G). (F) ParBm-s GFP was expressed in the  $\Delta parAmN-1$  strain, mislocalized foci were detected. (D, H) The two most pole-proximal foci positions of ParBc-s GFP (E) and ParBm-s GFP (H) expressed in *T. thermophilus* TL-1, respectively. Foci positions were measured from the pole from which the nearest focus was closer than the nearest focus of the opposite pole (Axio vision rel. 4.8, Carl Zeiss, Germany). Black-filled diamonds represent the nearest-to-pole foci positions, white diamonds represent the foci positions that are farthest from these poles. The mean position of the nearest-to-pole foci is shown with a dotted line. (I) The foci positions of 120  $\Delta parAmN-1/ParBm-sGFP$  cells containing one focus respectively. The mean position is 29.7% of the cell length (dotted line).

### 3.2.7 Distinct localization patterns of ParBc-sGFP and ParBm-sGFP in *E. coli* cells

To investigate the factors that may influence the ParBs localization patterns, their localizations in *E. coli* cells were also investigated. When ParBc-sGFP was expressed in *E. coli* that does not encode homologues of the chromosomal *parABS* system, no discrete fluorescent foci were observed, instead, they formed patches and spread over the nucleoid (Fig. 11B). This means the ParBc subcellular localization is dependent on the specific chromosomal *parS* sites. Indeed, when the *E. coli* strain expressed ParBc-sGFP in the presence of the *parSc* site (from a plasmid pUC- $\Delta$ *parABC::kat*), discrete fluorescent foci could be observed (Fig. 11C), and this effect was not observed in the empty vector control (data not shown). Surprisingly, it was found that ParBm-sGFP could form foci when expressed in *E. coli* cells, which was in marked contrast with the situation of ParBc-sGFP, suggesting there were ParBm binding sites in this system (Fig. 11G). ParBm might have bound to the *E. coli* genome, or the *parBm* gene itself as the case found in *B. subtilis spoOj* (*parB*) gene. Nevertheless, the distinct localization patterns of the chromosomal and megaplasmid ParB in *E. coli* cells further confirmed that the two ParBs bind different *parS* sites, i.e., the two Par systems act replicon specifically.

### 3.2.8 *parABm* is necessary for accurate subcellular localization of the megaplasmid origin region

As described (Fig. 6F; Fig. 7; Fig. 8), in  $\Delta$ *parAmN-1* lacking adequate amounts of ParABm proteins, the megaplasmid replication and segregation were probably disrupted. Then we wondered whether the subcellular localization of ParBm was also altered in this strain. To test this, ParBm-sGFP was expressed in  $\Delta$ *parAmN-1*. The ParBm-sGFP fusions were also found to form discrete foci in this background. Statistically (n ~ 150), in foci-containing cells, 16% of the cells contained two foci, while 75% of the cells contained only one focus. In both cases, the foci were mostly (72%) dissociated from the cell poles. Instead, they were inclined to be positioned near the cell center or cell quarter (Fig. 11F). The average pole-proximal focus

position in 120 cells that respectively contained one focus increased to 29.7% of the cell length (measured from the nearest poles) (Fig. 11I), compared with 5.5% in the wild-type cells (Fig. 11H). These results indicated the foci could not be separated properly (reduced foci number) and positioned at the right locations (detached from the cell poles). The ParBm locations are actually reflecting those of the megaplasmid *parS* sites (i.e., the megaplasmid origin regions). Thus, the above findings suggested that by lack of ParABm, the megaplasmid origin regions will not be positioned or segregated appropriately in the daughter cells, which is highly supportive of the proposal that *parABm* is important for the megaplasmid segregation.



### 3.3 The role of MreB in *T. thermophilus*

Another proposed bacterial cytoskeleton element that might be involved in chromosome segregation is the MreB system. Nearly all rod-shaped bacteria encode MreB, which is an actin-like protein. The role of MreB required for cell morphology maintenance is well-studied. In rod-shaped bacteria, disruption of *mreB* causes a dramatic change in cell morphology from the normal shape to a spherical form. Except for its role in the cell shape determination, recently, results from some groups have linked MreB to a function in the chromosome segregation (e.g., *B. subtilis*, *E. coli* and *C. crescentus*). In *E. coli*, it has been suggested that MreB is required for both origin and chromosome bulk nucleoid segregation (Kruse *et al.*, 2005). Consistently, depletion of *mreB* in *B. subtilis* and *C. crescentus* leads to a rapid defect in chromosome segregation, where replication origins fail to localize in a regular bipolar fashion (Soufo and Graumann, 2003; Gitai *et al.*, 2004). The MreB homolog was also identified in the *T. thermophilus* chromosome, given the suggestion of the important role of MreB in some other bacteria, its function in *T. thermophilus* was analyzed.

#### 3.3.1 *mreB* is deletable in *T. thermophilus*

*T. thermophilus* has only one *mreB* homolog encoded by the chromosome, and the *mreB* gene is not transcribed in an operon with *mreC* and *mreD*, which are also suggested to encode proteins for cell shape determination in *E. coli* and *B. subtilis* (Levin *et al.*, 1992; Formstone and Errington, 2005). In order to investigate the role of MreB in *T. thermophilus*, the *mreB* gene was replaced with the kanamycin resistance gene cassette (*kat*), followed by phenotypic characterization. Fig. 12 presents the Southern blot result showing that the mutant strain  $\Delta mreB::kat$  has a correct insertion of the kanamycin gene cassette, indicating that similar to the *parABc* operon (Fig. 6A), the *mreB* gene is also deletable.

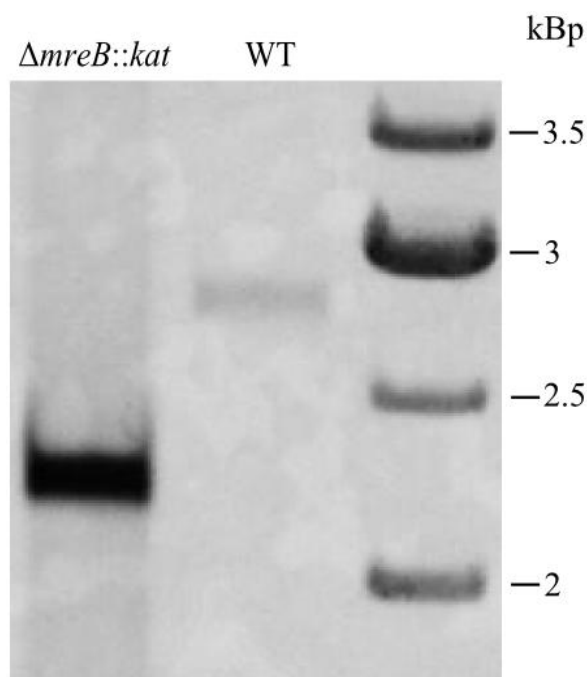
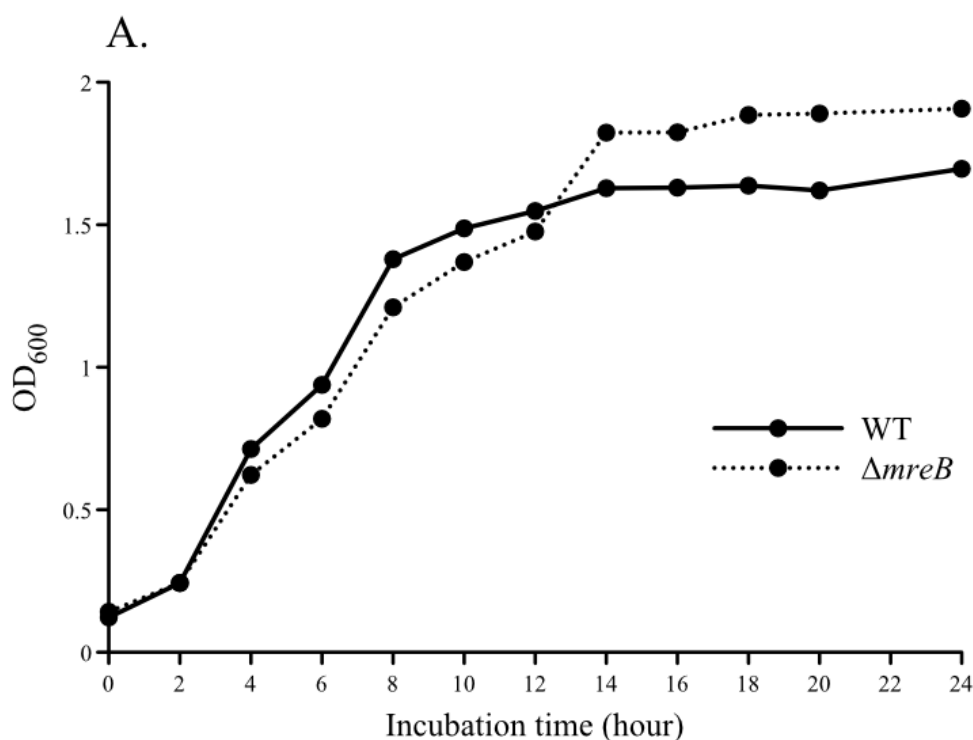


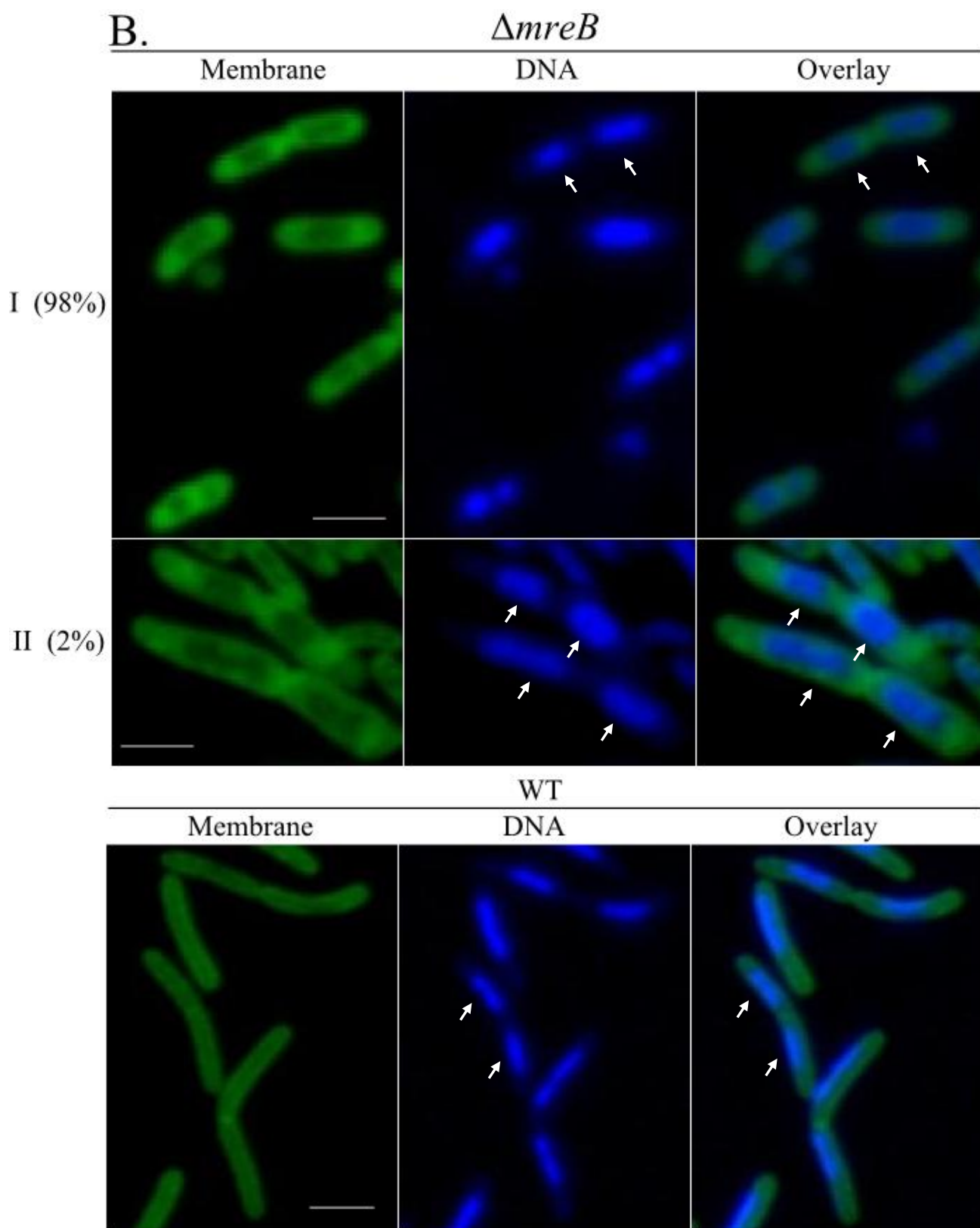
Fig. 12. Genotype confirmation of the *mreB* mutant by Southern blot. Southern blot was performed using a 912-bp biotin-labeled fragment (upstream region of *mreB*) as the probe for hybridization. The *in silico* predicted sizes are 2.75 kbp for wide type, and 2.19 kbp for  $\Delta mreB::kat$ , respectively.

### 3.3.2 *mreB* is involved in cell shape maintenance, but not in chromosome segregation in *T. thermophilus*

The growth curves of  $\Delta mreB$  and wild type in antibiotic-free TB medium indicated indistinguishable growth rates (Fig. 13A). To investigate the potential cell morphology and chromosome segregation defects, exponentially growing cells of the  $\Delta mreB$  and wild-type strains (in antibiotic-free TB) were collected and stained with DAPI and CFS followed by microscopic analyses. Two types of cell shapes were detected in the *mreB* mutant (Fig. 13B, panel I and II) which were fairly distinct from the shape of the wild-type cells (the bottom panel of Fig. 13B). Consistent with the suggested role of MreB in cell shape maintenance in other rod-shaped bacteria, the *T. thermophilus mreB* mutant cells were also much shorter, thicker and more spherical-looking (average ratio of cell length/diameter  $4.24 \pm 0.21$ ) compared with wild-type cells (average ratio of cell length/diameter  $8.71 \pm 0.86$ ). Approximately 98% of cells had a morphology shaped like the example shown in the panel I of Fig. 13B, the cells were still somehow rod-shaped. This might be due to the functions conveyed by other

cell shape determinants, such as MreC and MreD (Levin *et al.*, 1992; Formstone and Errington, 2005); 2% of the cells were found to be even more abnormal, as shown in the panel II of Fig. 13B. Nevertheless, in the *mreB* mutant, the replicated DNA could segregate normally into the daughter cells and even occurred in the extremely disordered cells (Fig. 13B). Furthermore, the frequency of DNA-less cells was also not increased (data not shown), suggesting that no chromosome bulk nucleoid segregation defect had occurred. To better analyze the relative DNA contents in dividing cells, 200 pairs of daughter cells were observed by DAPI signal intensity measurements, and the distributions were plotted. The distributions of the relative DNA contents in the daughter cells of  $\Delta mreB$  scattered from 0.67 to 0.99 with a mean of 0.89 and a SD of 0.07, which were nearly indistinguishable from those of the wild type with a mean of 0.86 and a SD of 0.10 (Fig. 13C). Taken together, these results implied that in *T. thermophilus*, MreB plays a role in maintaining the cell shape, but does not actively participate in the chromosome segregation process, unlike the situations in *E. coli*, *B. subtilis* and *C. crescentus*. A similar discovery was also made in the cyanobacterium *Anabaena* sp. PCC 7120 which is also polyploid (Hu *et al.*, 2007).





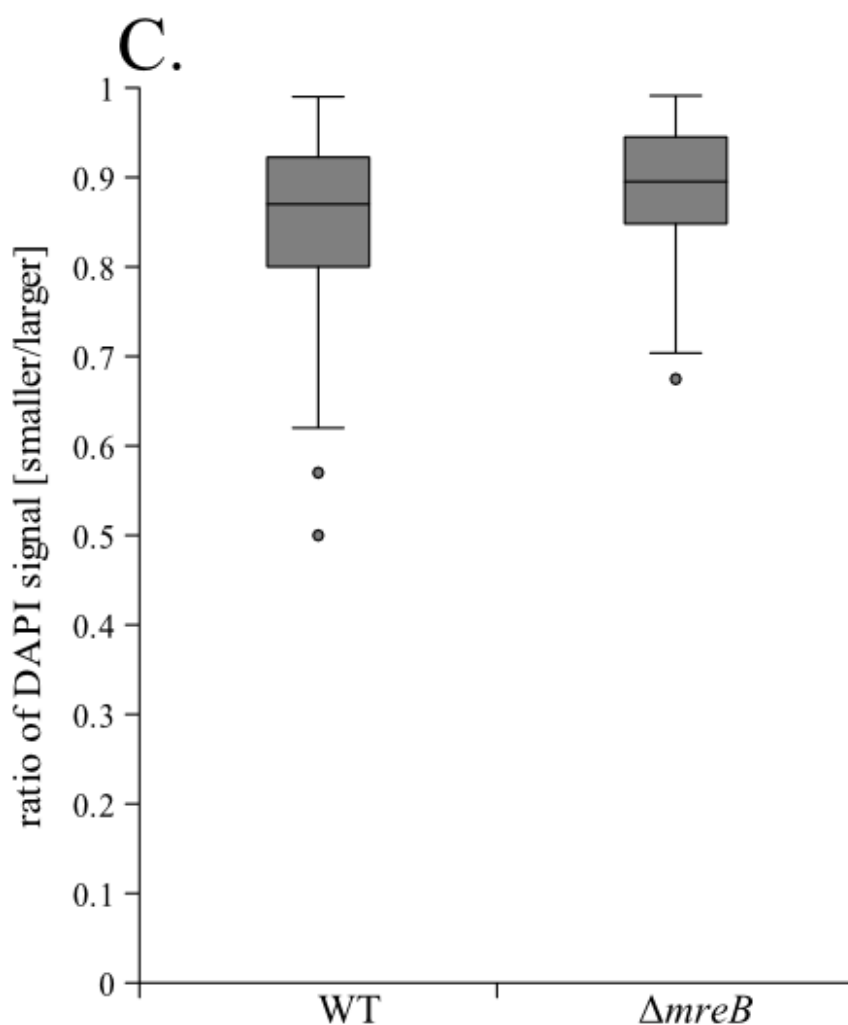


Fig. 13. Phenotypic characterization of the *mreB* mutant. (A) Growth curves of the  $\Delta mreB$  mutant and the wild type. Both strains were grown in antibiotic-free TB medium, solid line-wild type, dashed line- $\Delta mreB$ . (B) The  $\Delta mreB$  and wild-type cells were harvested at  $OD_{600} = 0.8$ , DNA and membrane were stained with DAPI and CFS, respectively, followed by microscopic analyses. Two types of cell shapes were observed in  $\Delta mreB$  (the panels I and II). Representative cells are shown in a gallery view with CFS stained membrane (Membrane), DAPI stained DNA (DNA), and merged images (Overlay). White arrows, the separated DNA. Bars, 2  $\mu m$ . (C) Box-plot of the relative DNA contents in the daughter cells of the *mreB* mutant and wild type were plotted as the smaller content divided by the larger one (200 pairs were analyzed, respectively). The ratios are represented by gray bars. In the *mreB* mutant, the ratios varied from 0.67 to 0.99 with a mean of 0.89 and a SD of 0.07; in wild type, the ratios scattered from 0.50 to 0.99 with a mean of 0.86 and a SD of 0.10.

### 3.4 Separation of two alleles located at one chromosomal gene locus

#### 3.4.1 Construction of a stable heterozygous strain in *T. thermophilus*

As introduced, the separation of two markers located at one chromosomal gene locus in *T. thermophilus* HB8 has been reported (Ohtani *et al.*, 2010), however, the potential mechanisms were not uncovered. In our former studies, the separation of two different alleles at one chromosomal gene locus in *T. thermophilus* HB27 was also noticed. For example, in the process of generation of non-essential gene deletion mutants, it was found that there were colonies carrying both the mutant allele and wild-type allele in one locus, and these colonies were unstable, since after growing and restreaking, colonies that were either homozygotes for the mutant allele or the wide-type allele were obtained. In order to investigate the potential mechanism driving the allele segregation, a stable heterozygous strain which carries two different selection markers simultaneously at the same chromosomal locus (*pyrE* gene) was generated, an experimental setup similar to the one recently used to prove polyploidy in *T. thermophilus* HB8 (Ohtani *et al.*, 2010). Primarily, the two homozygous strains  $\Delta pyrE::kat$  and  $\Delta pyrE::blm$  were generated by transforming linearized pCT3FK and pJ- $\Delta pyrE::blm$  to HB27 cells respectively (for detailed plasmid constructions, see Chapter 2.1.1). The complete replacement of the *pyrE* gene in both strains was confirmed by PCR and Southern blot (Fig. 14A, B). Afterwards, the  $\Delta pyrE::kat$  strain was transformed with linearized pJ- $\Delta pyrE::blm$ , resulting in the heterozygous strain HL01 by selecting on TB agar plates supplemented with both kanamycin and bleomycin. The genotype of the heterozygous strain (HL01) was also verified by PCR and Southern blot analysis, which showed the kanamycin and bleomycin resistance markers were both introduced into the *pyrE* locus (Fig. 14A, B). The heterozygous state of this strain (HL01) could be stably maintained in TB medium supplemented with both antibiotics.

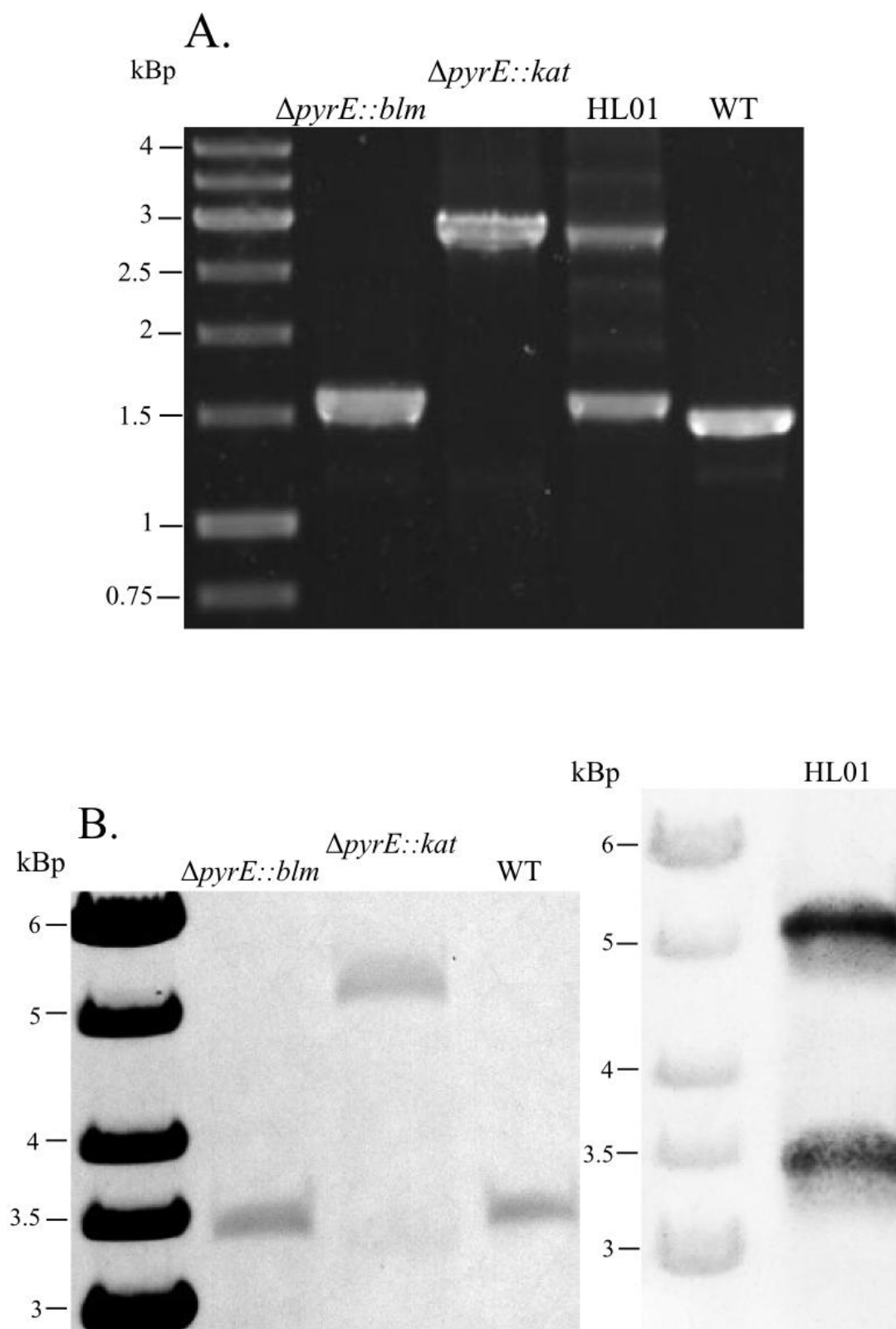


Fig. 14. Genotype confirmations of the  $\Delta pyrE::kat$ ,  $\Delta pyrE::blm$  and HL01 strains by PCR and Southern blot. (A) PCRs were performed using genomic DNA as template and primers flanking the

*pyr* region. The predicted sizes of the PCR products are 1.48 kbp for the wild type, 2.99 kbp for  $\Delta pyrE::kat$ , 1.50 kbp for  $\Delta pyrE::blm$ , and 2.99 kbp + 1.50 kbp for HL01, respectively. (B) For Southern blot, A 450-bp biotin-labeled fragment of the *pyrF* gene was used as a probe. The *in silico* predicted sizes are 3.48 kbp for the wild type, 5.12 kbp, 3.44 kbp for  $\Delta pyrE::kat$  and  $\Delta pyrE::blm$ , respectively, and 5.12 kbp + 3.44 kbp for the heterozygous strain HL01, respectively.

#### 3.4.2 Allele separation kinetics of the heterozygous strain HL01

It was considered that gene conversion and random partitioning of chromosome copies into the daughter cells as two possible mechanisms that could lead to the observed allele separation. While both processes are expected to lead to a loss of the heterozygous state (change in genotype frequency), gene conversion is in addition expected to be accompanied by a change in the average fraction of each genome type (change in allele frequency). To follow these changes, HL01 was grown in a batch culture in the absence of selection pressure and samples were collected at different time points. These were used to determine: i) the drug resistance of 50 individual colonies per time point by spreading the samples on antibiotic-free plates and re-streaking on plates containing either kanamycin or bleomycin and ii) the relative frequency of the two alleles in the samples by Southern blot. The drug resistance reflects the genotype of the tested colony (homozygous for either the kanamycin or the bleomycin allele or heterozygous), while the data from the Southern blot indicate changes in the relative abundance of each allele in the whole population. As expected from former observations, during growth in the absence of selection pressure the fraction of heterozygous cells (by resistance phenotype) decreased and that of homozygous cells apparently increased (Fig. 15A). The Southern blot analysis showed that although the apparent genotype ratio between kanamycin homozygotes and bleomycin homozygotes varied, the relative amount of each allele in the whole population remained largely constant throughout the experiment manifesting as approximately 2 times more *blm* alleles (Fig. 15B). At the end of the incubation in the experiment in Fig. 15A, the fraction of cells resistant to bleomycin but not to kanamycin ( $Kat^S/Blm^R$ ) was much higher (20 fold) than that of cells with the opposite phenotype ( $Kat^R/Blm^S$ ), while the band intensities measured from the Southern blot sample for the same time point showed only approximately 2 times



more *blm* alleles. This could be due to the fact that the phenotypic trait that was determined, i.e. antibiotic resistance, does not necessarily mirror exactly the genotype. One resistance allele copy per cell may suffice to display the resistance against one of the antibiotics while a larger number of copies of the other allele may be needed for the other resistance phenotype, but at present it is unknown how many *kat* (or *blm*) alleles have to be present in a polyploid *T. thermophilus* cell to render the cell kanamycin (or bleomycin, respectively) resistant. As introduced, except for rendering a change in the genotype frequency, gene conversion is in addition accompanied by a change in the average fraction of each genome type in the whole population (Lange *et al.*, 2011). Taken together, random partitioning of the chromosome copies into daughter cells is the most probable mechanism that gave rise to allele separation in heterozygous cells of *T. thermophilus*. The random chromosome partitioning pattern has also been observed in certain polyploid cyanobacteria (Hu *et al.*, 2007; Schneider *et al.*, 2007) and is reminiscent of vegetative segregation (or “sorting-out”) in fungi and plants. Another point demonstrated by Fig. 15A is that the fraction of homozygous cells increased more rapidly in stationary phase than that in exponential phase, and although less obvious, this was also observed in the allele separation kinetics in HB8 (Ohtani *et al.*, 2010). This may be due to the fact that *T. thermophilus* HB27 is impressively natural competent in exponential phase. Although cell divisions proceed faster, DNA exchange among the cells or uptake of free DNA released by dead cells may also occur (César *et al.*, 2011; Alvarez *et al.*, 2011), which may affect the frequency of the apparent genotypes of the two alleles. Meanwhile, due to reductive cell divisions in late stationary phase (Kolter *et al.*, 1993; Navarro *et al.*, 2010), the genome copy number in one cell may also decrease, and this would favour the daughter cells to receive the same type of parental genome copies by random partitioning.

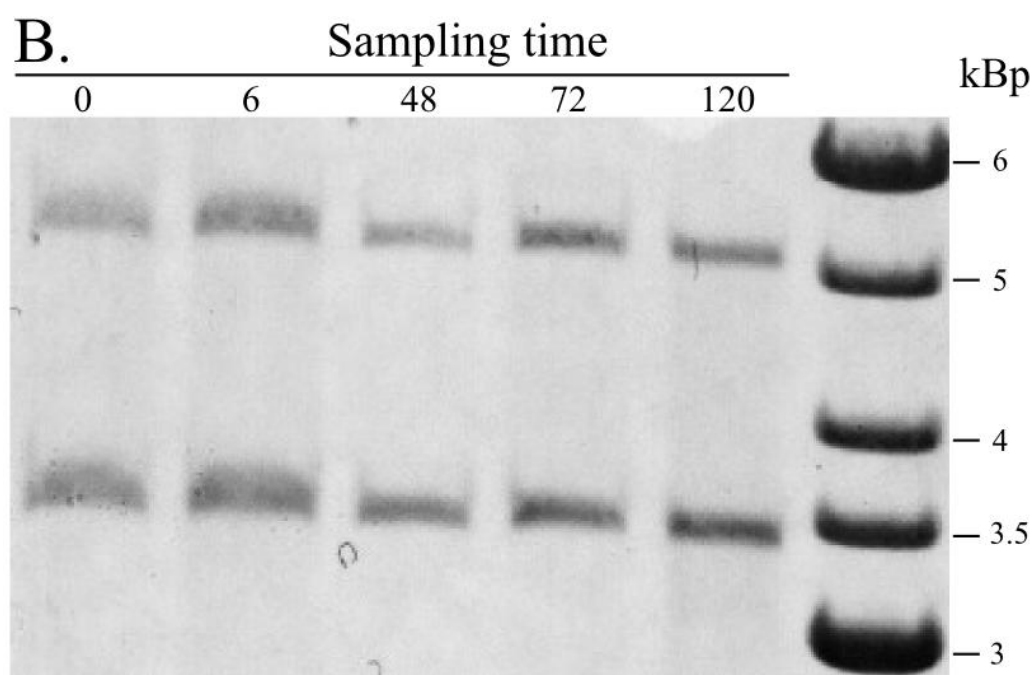
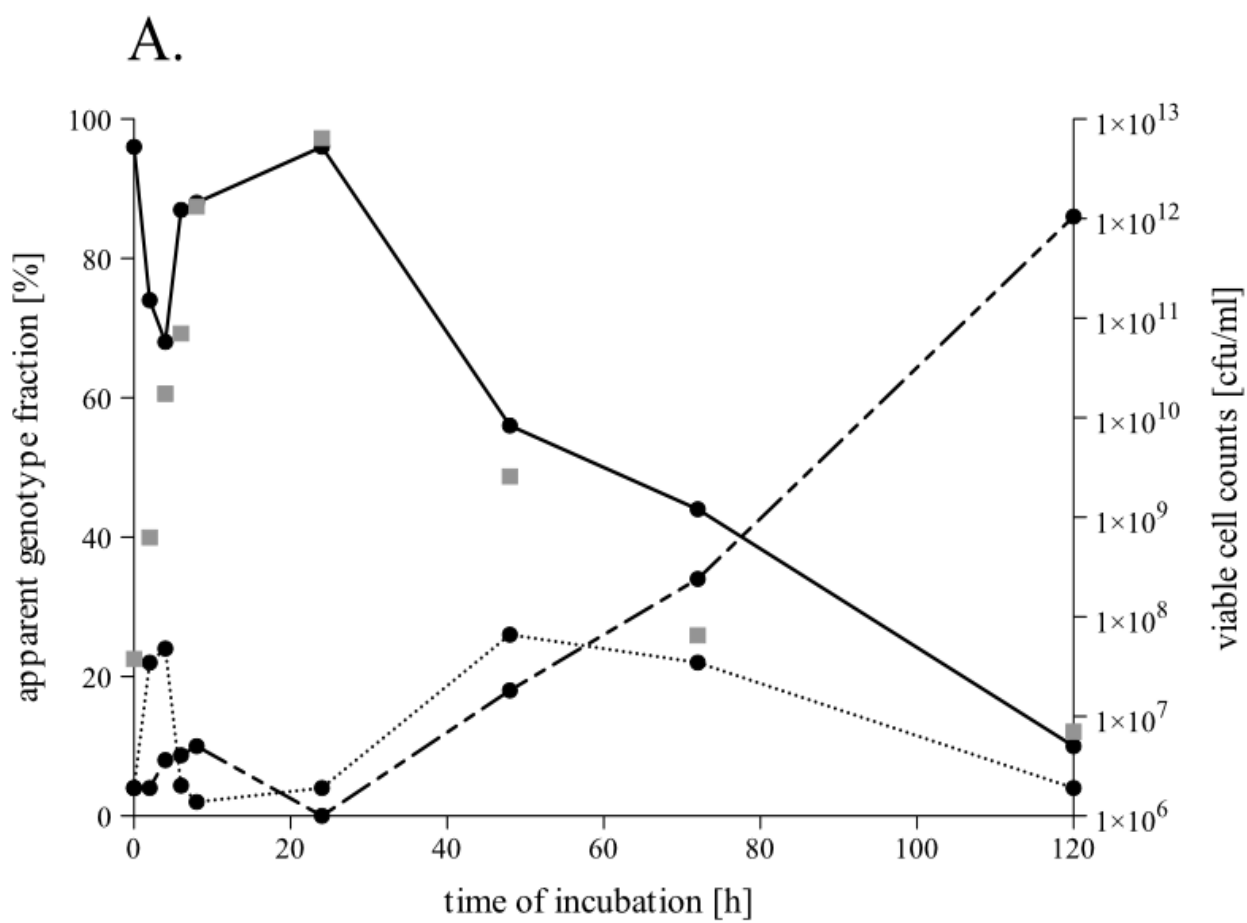
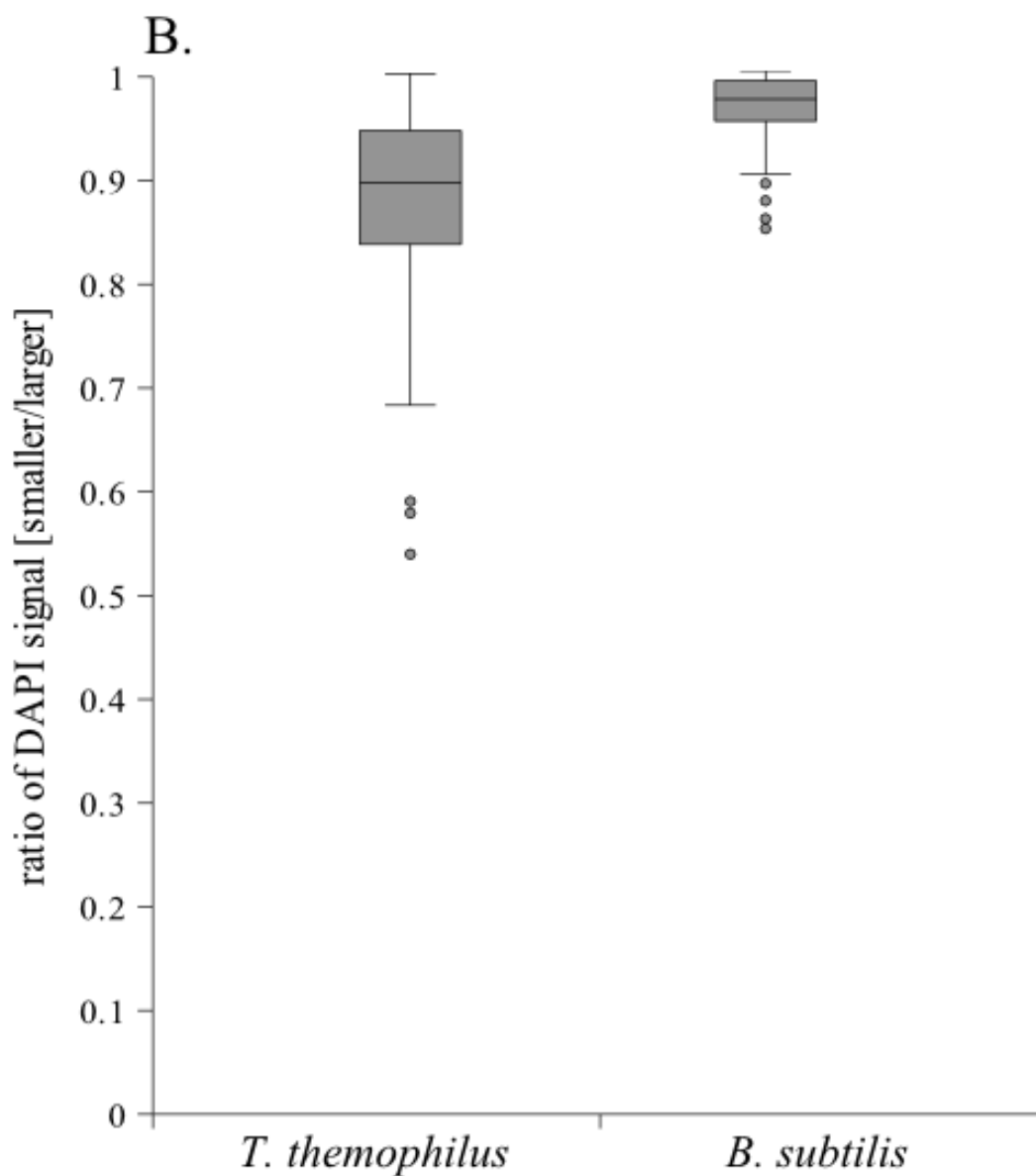


Fig. 15. Apparent genotype and allele frequency measurements of the heterozygous strain HL01 grown in the absence of selection. (A) One representative experiment of three performed is shown. The viable counts (gray squares) were determined from the antibiotic-free plates. The changes in the fraction of each phenotype in the population was followed by spreading the samples on antibiotic-free plates and restreaking 50 colonies for each time point on plates containing kanamycin or bleomycin ( $Kat^R/Blm^R$  - solid line,  $Kat^R/Blm^S$  - dotted line and  $Kat^S/Blm^R$  - dashed line). (B) The changes in the relative abundance of the two alleles (*kat* and *blm*) were acquired by measuring the intensities of the bands from Southern blot. The genomic DNA was prepared from the samples taken at the indicated time points and was digested with XbaI. The probe used was the same as that used to confirm the genotypes of the strains. The predicted sizes are 5.12 kbp, 3.44 kbp for the  $\Delta pyrE::kat$  and  $\Delta pyrE::blm$  allele, respectively.

### 3.4.3 Distributions of relative DNA contents of daughter cells in *T. thermophilus*

The allele separation observed in *T. thermophilus* heterozygous cells suggested the partitioning of chromosome copies into daughter cells may be a random event. However, here we were not informed whether different numbers of chromosomes were separated in daughter cells at cell division, since the situation in which daughter cells received any combinations of parental chromosomes but with equal numbers might also render the observed separation. For example, in a predividing *T. thermophilus* HL01 cell, there were in total 8 chromosome copies after DNA replication, 4 copies of them contained *kat* alleles, and the other 4 contained *blm* alleles. At cell division, if the daughter cells would receive a same number of the parental chromosome copies, but with random combination; there was a possibility that some daughter cells would receive 4 chromosome copies which all contained either the *kat* or *blm* alleles. To further investigate this, the relative DNA-content distribution patterns of daughter cells between *T. thermophilus* and *B. subtilis* were compared, using the method used previously (Chapter 3.3.2) for determining the phenotypes of the *mreB* mutant. *B. subtilis* was used as the control organism, as it contains only one chromosome copy during most of the cell cycle and is suggested to have active machineries to separate duplicated chromosomes (Defeu Soufo *et al.*, 2003). Compared with *B. subtilis* that contained almost equal nucleoid contents in two daughter cells, the sizes and fluorescence intensities of two separated nucleoids in certain proportion of *T. thermophilus* cells were strikingly differed (Fig. 16A).

The relative DNA contents in 200 pairs of daughter cells of *T. thermophilus* and *B. subtilis* were measured and plotted, respectively. In *B. subtilis* cells, the distributions varied from 0.82 to 1 with a mean of 0.96 and a standard deviation of 0.04, whereas in *T. thermophilus* cells, the values distributed from 0.45 to 1 with a mean of 0.85 and a standard deviation of 0.11, suggesting the DNA contents in *T. thermophilus* daughter cells varied to a much higher extent (Fig. 16B). Thus, it seems likely that the observed chromosome random partitioning is caused by segregation of different numbers of chromosome copies into daughter cells, resembling the situations observed in certain cyanobacterial species (Hu *et al.*, 2007; Schneider *et al.*, 2007).



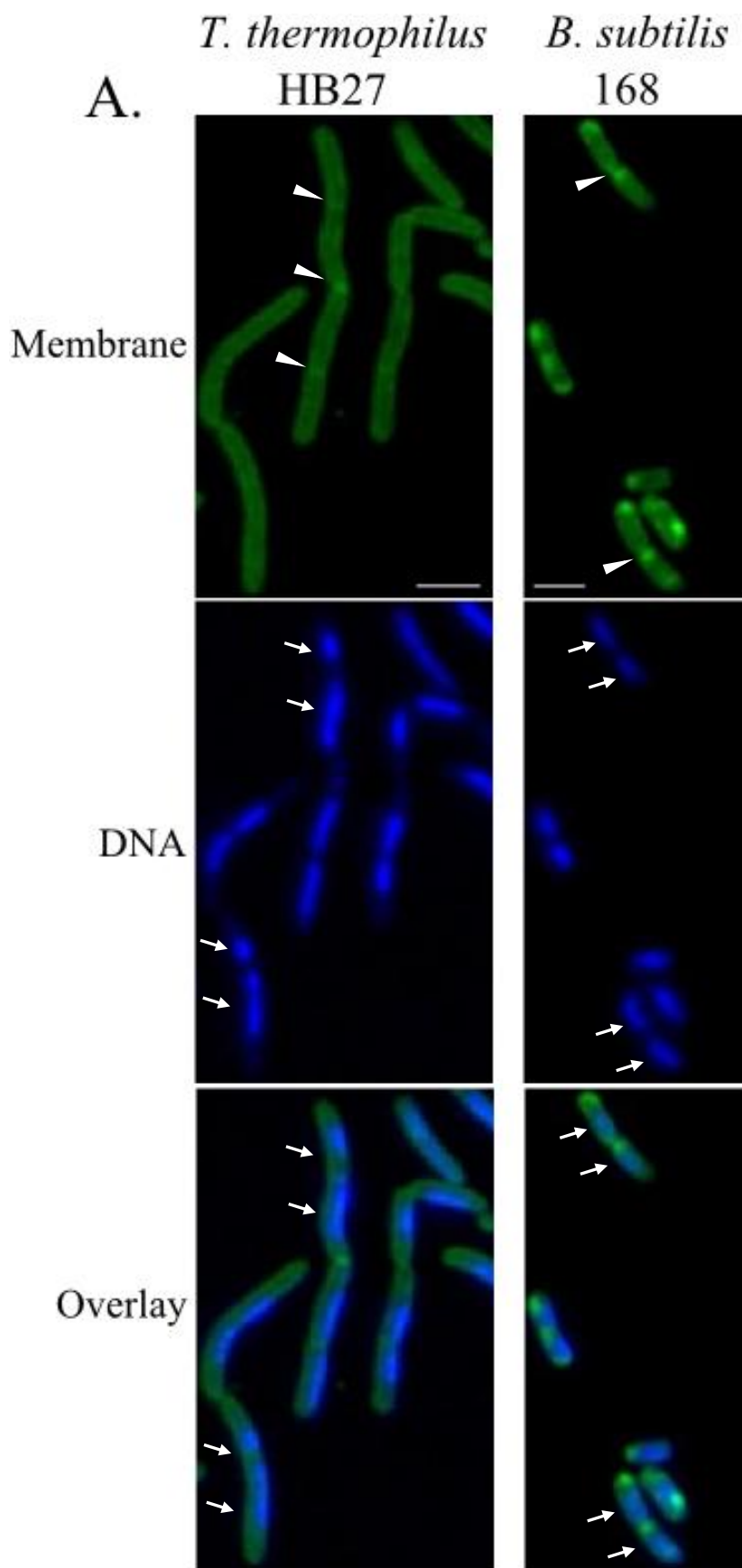


Fig. 16. Relative DNA contents in the daughter cells of *T. thermophilus* and *B. subtilis*. (A) The fluorescence signals of DNA (blue) and membrane (green) in *B. subtilis* and *T. thermophilus* cells.

### 3. Results

---

White arrows, separated DNA; white triangles, septum formation positions. (B) The distributions of the relative DNA contents determined by DAPI fluorescence intensities in the daughter cells of *T. thermophilus* and *B. subtilis*, 200 pairs were plotted. Of two daughter cells, the ratio was achieved by dividing the smaller content with the larger one, the ratio distributions are represented with gray bars. In *B. subtilis*, the ratios varied from 0.82 to 1 with a mean of 0.96 and a SD of 0.04, in *T. thermophilus*, the ratios scattered from 0.45 to 1 with a mean of 0.85 and a SD of 0.11.

## 4. Discussion

### 4.1 Genetic modification of *T. thermophilus*

For efficient genetic manipulation of the extreme thermophilic model organism *T. thermophilus*, the development of selection tools after transformation is indispensable. The method most often used for the isolation of directed knockout mutants in *T. thermophilus* is based on the insertion of antibiotic resistance markers (e.g., kanamycin, bleomycin or hygromycin resistance genes). This gene exchange approach has disadvantages, as the antibiotic resistance marker cannot be reused and polar effects of downstream genes are possible. To avoid these, alternative strategies based on counter-selection principle permitting generation of marker-free deletion mutants were developed. However, until now, only two counter-selection markers are applicable for *T. thermophilus* (*pyrE* and *rpsL1* allele based systems). Thus, to facilitate the genetic studies of *T. thermophilus*, a new counter-selection marker was developed in the present work.

#### 4.1.1 Toxic effect of substituted indoxyl substrates and its use for counterselection during introduction of gene deletions in *T. thermophilus*

*T. thermophilus* encodes a  $\beta$ -glucosidase (Bgl) on its megaplasmid. In this study, it was noticed that BCI- $\beta$ -glu substrate had a toxic effect for the *T. thermophilus* cells expressing Bgl, especially when the BCI- $\beta$ -glu substrate was at high concentration. The wild-type cells were incapable to grow when the BCI- $\beta$ -glu substrate concentration reached 500  $\mu$ g/ml (Fig. 2A). Thus, in combination with BCI- $\beta$ -glu as a media supplement, the *bgl* gene could be used as a counterselection marker in a “pop-in, pop-out” strategy to generate marker-free mutations in the genome of *T. thermophilus*. To test this, a vector (pTKO-4) was constructed, which carries the *bgl* gene transcriptionally fused to a *kat* marker under transcriptional control of the *T. thermophilus* *slpA* promoter (Fig. 3A). The utility of the pTKO-4 vector-based counterselection strategy was tested by deletion of the chromosomal locus *340* in the

HB27 $\Delta bgl$  background. As expected, after transformation with a pTKO-4-based gene deletion vector and the first selection on kanamycin plates selecting for vector integration events; and the subsequent counter-selection on BCI- $\beta$ -glu plates (500  $\mu$ g/ml) selecting for vector excision, colonies with the 340 locus deleted were detected with a frequency of approximately 50% (Fig. 4). Therefore, it is applicable to use this counterselection strategy in the *T. thermophilus*  $\Delta bgl$  strain.

The approach was also expected to be applicable in the wild-type genetic background, which would allow a more broad application of the counterselection strategy without being restricted to the  $\Delta bgl$  strain. The frequency of spontaneous Bgl<sup>I</sup> mutants, which like the  $\Delta bgl$  strain are insensitive to BCI- $\beta$ -glu at 500  $\mu$ g/ml and could pose a problem (false positives) in the counterselection step, was very low (below  $10^{-8}$ , data not shown). Because the *bgl* gene copy carried by the pTKO-4 vector is transcribed more strongly than the wild-type copy located on the *T. thermophilus* megaplasmid, it was anticipated that it should be possible to discriminate colonies which carry the integrated vector from those in which the vector has been lost. Indeed, when the locus 340 deletion procedure was repeated in the wild-type strain, two types of colonies (small and large) could be observed after plating on TB BCI- $\beta$ -glu 100  $\mu$ g/ml (data not shown). The small colonies were expected to represent pTKO- $\Delta 340$  integrants while the large ones were expected to have lost the integrative vector. In support, all of approximately 50 large colonies tested for kanamycin resistance were sensitive to the antibiotic, indicating loss of the vector-encoded resistance marker (data not shown). Determining the locus 340 genotype of the large colonies by PCR and Southern blot showed that approximately 1 out of 10 carried the knockout allele (data not shown). The lower frequency of observing the knockout allele when performing the allelic exchange in the wild-type background is most probably due to integration events of the vector not only at the locus targeted for deletion but also at the *bgl* locus. Nevertheless, despite the lower frequency of isolating the desired mutation, the above experiment showed that it is possible and feasible to use the selection scheme in wild-type *T. thermophilus* cells. In future, the undesired vector integration events at the genomic *bgl* locus could be avoided by replacing the *bgl* ORF in pTKO-4 with a different thermostable



$\beta$ -glucosidase ORF without high homology to *T. thermophilus bgl*.

#### 4.1.2 Possible mechanisms of toxicity and potential broad host range application of substituted indoxyl substrates

It was speculated that the toxic effect of the BCI- $\beta$ -glu substrate for Bgl<sup>+</sup> cells was caused by the substituted indoxyl moiety which was released upon cleavage by the  $\beta$ -glucosidase. The toxic effect becomes especially prominent at high concentrations of the chromogenic BCI substrate (Fig. 2). The presence of molecular oxygen or other oxidizing agents, pairs of the diffused 5-bromo-4-chloro hydroxyindole liberated by BCI substrate cleavage can form an insoluble, blue indigoid dye, 5,5'-dibromo-4,4'-dichloro-indigo (Kiernan, 2007). In our study, two possible reasons for the toxic effect were taken into account, i.e., the monomer or the dimer form of the 5-bromo-4-chloro hydroxyindole molecules. Further, although Bgl is an intracellular enzyme and thus the cleavage of the substrate should occur after it has been transported into the cell, it is also possible that some enzyme is released by lysed cells in a colony during growth on agar plates, and the released hydroxyindole could act extracellularly. To clarify these questions, first, the toxic effect of the indigo dye (unmodified indoxyl dimer) to *T. thermophilus* Bgl<sup>+</sup> cells were determined. The result showed that the indigo dye had no toxic effect for these cells (50-500  $\mu$ g/ml). Next, when differential interference contrast (DIC) microscopy was applied to the *T. thermophilus* cells exposed to BCI- $\beta$ -glu, small, cell-associated blue indigoid dye precipitates were detected, which apparently accumulated in or near the cytoplasmic membrane (Fig. 4). Further, through selecting a transposon insertion mutants library for BCI- $\beta$ -glu resistant colonies, it was found that all the three mutants that were resistant to BCI- $\beta$ -glu had transposon insertions in gene clusters encoding sugar transporters. Taken together, these observations suggest that the toxic effect is exerted only after the BCI substrate is transported into the cell, in which it is cleaved and the insoluble, blue indigoid dye accumulates. In contrast, extracellular substrate cleavage is not expected to lead to colony size reduction, despite the colonies also appear blue. This idea was further supported with the results of the BCI substrate toxicity test in some other bacterial species. For instance, when *E. coli* and *P. putida* cells were

exposed to the respective BCI substrate, no toxic effect (i.e., reduction in the colony size) could be detected although the colonies appeared blue on the respective plates (Table 6). Thus, it seems in these cases, the BCI substrates were not able to be transported into the cells. The blue color was probably attributed to the extracellular cleavage of the substrate, resulting from cell lysis in the colony.

To our knowledge, there is only one report available describing a growth retardation effect of substituted hydroxyindole substrates on bacteria, i. e. on *F. novicida*, where this phenotype (small blue colonies on plates supplemented with 5-bromo-4-chloro-indolyl phosphate) has been used in complementation experiments with a spontaneous phosphatase mutant forming large colonies on the same plates (Baron and Nanon, 1998). Given the commercial availability of a broad variety of substituted indoxyl substrates and the observed toxicity of their cleavage products (Table 6), it can be anticipated that the counterselection scheme developed here can be exploited in other bacterial species, also with genes encoding enzymes other than glycoside hydrolases, for example esterases, phosphatases etc. Some of the advantages of this approach are i) the possibility to use it in wild type bacterial strains, i.e. no prior genetic modifications are necessary; ii) the low frequency of obtaining spontaneous BCI-resistant colonies (in *T. thermophilus* this frequency was below  $10^{-8}$  which makes it suitable for the selection of vector elimination in bacteria with low recombination proficiency and iii) the flexibility to use different BCI substrate-enzyme combinations, depending on the presence or absence of native activity in the respective organism. Apart from its use in gene deletion and other genome engineering experiments, the toxic effect of the cleavage products of BCI substrates can be utilized in other cloning strategies, for example in the efficient generation of shotgun libraries by using a vector carrying a gene for a BCI substrate-cleaving enzyme which contains restriction sites for insertion of foreign DNA. Transfer of transformants to the appropriate BCI substrate-containing media leads to a strong selection for clones with recombinant insert-bearing plasmids (positive selection) and against clones with empty vector.

## 4.2 Chromosomal and megaplasmid partitioning (*par*) systems in *T. thermophilus*

There are multiple copies of the chromosome and megaplasmid in *T. thermophilus* (Ohtani *et al.*, 2010), but whether the segregation of the copies of these two replicons are stringently regulated is not clear. *T. thermophilus* contains chromosomal and megaplasmid encoded *par* loci. In this study, we set out to investigate the characteristics and functions of the two *par* loci and to obtain a fundamental understanding of the genome partitioning in *T. thermophilus*.

### 4.2.1 Characteristics and functions of the chromosomal *par* system

#### 4.2.1.1 Genetic structures and components of the chromosomal *par* loci

The genetic arrangement of the *T. thermophilus* chromosomal *par* loci is highly consistent with other chromosomal encoded *par* systems, in which the three components (*parAc*, *parBc* and *parSc*) are located proximal to the replication origin, and approaching *gidAB*, *dnaA*, *dnaN*, all characteristics of chromosomal origins (Fig. 5C). Through protein conserved motif searching and protein alignments, it was found that the chromosome encoded *T. thermophilus* ParAc is a Walker-type ATPase that shows conservative motifs also found in other chromosomal ParA proteins (Fig. 5D). Consistently, the sequence of the chromosomal *parSc* site is the proposed "universal" centromere-like sequence (Fig. 5C). It has been suggested that transcription of *par* operon is autoregulated by either *parA* or *parB* genes themselves (for reviews, see Gedes *et al.*, 2000, 2010). In the case that ParA proteins contain N-terminal DNA binding motifs, the ParAs tend to control the transcription of the *par* operons via binding to operator sequences in the promoter regions (Mori *et al.*, 1989; Davis *et al.*, 1992; Hayes *et al.*, 1994; Radnedge *et al.*, 1998). In *T. thermophilus*, ParAc does not possess an N-terminal DNA binding motif, indicating ParAc lacks an autoregulation function for the *parABc* operon. Thus, the transcription regulation of *parABc* may be exerted by ParBc, as is the case in other chromosomal Par systems, e.g. ParB proteins are suggested to be involved in the

autoregulation process by repressing promoters located in centromere regions (Gedes *et al.*, 2011). A recent study showed that ParAc can form dimmers in an ATP-dependent manner, and the ATP-bound dimmers associate with DNA non-specifically forming nucleoprotein filaments (Lenonard *et al.*, 2005). In the plasmid Par system (e.g. F plasmid), ParA filaments are suggested to afford force for active plasmid segregation, implying the ParAc filaments may also provide force for chromosome bulk nucleoid and/or origin regions segregations. Recently, the crystal structure of the *T. thermophilus* chromosomal ParB protein has been solved: it is a DNA-binding protein with its C-terminus mediating dimerization, and most properly dimerizes upon binding to *parS* sequences (Lenonard *et al.*, 2004).

#### 4.2.1.2 Functions of the chromosomal *par* loci

Using a standard allele exchange method, we succeeded in the deletion of the *parABc* genes in parallel ( $\Delta parABc$ ). Through analyzing the growth phenotype of the *parABc* mutant, it was found that it did not display apparent defects with respect to the cell growth in both nutrient and minimal media (Fig. 7A, B). Through microscopic analyses, it was observed that the cell shape, cell division, or DNA morphology of  $\Delta parABc$  were also not affected (Fig. 7C). The replicated DNA was also found to segregate normally into the daughter cells, and the frequencies of anucleate or DNA-less cells were not increased compared with those of wild type (Fig. 7C; Table 7). Moreover, the qPCR results measuring the copy numbers of the chromosome and megaplasmid at multiple sites (TT\_P0043 and TT\_P0195 on the megaplasmid, and loci near *oriCc* and *terc* on the chromosome, respectively) also showed that deletion of *parABc* did not impair chromosome or megaplasmid replications (Fig. 8C). Thus, it seems *parABc* is probably insignificant for either the chromosome or the megaplasmid bulk DNA replication and segregation.

However, *parABc* may have other roles. Indeed, the *in vitro* DNA-binding assays showed that ParBc could bind the *parSc* site specifically, indicating it is a functional ParB protein (Fig. 10A, C). ParBc can bind *parSc* means it can actually associate with the chromosomal origin region, as *parSc* is positioned right in this region (about 6 kbp from *oriCc*, Fig. 5C). *In vivo*, when ParBc-sGFP proteins were

expressed in wild-type *T. thermophilus* cells, they formed well-defined fluorescent foci. Since the *in vitro* binding assay has indicated that ParBc binds *parSc* specifically, these fluorescent foci must be ParBc-*parSc* nucleoprotein complexes. Further, the ParBc-*parSc* complexes were found to be localized to the poles in wild-type *T. thermophilus* cells (Fig. 11A, D), and this localization was dynamic. As the single *parSc* site in *T. thermophilus* is positioned right in the chromosome origin region, this result indicated the origin regions were bound by ParBc, and the nucleoprotein complexes were driven from "old" poles to "new" poles, probably through protein-protein interactions. It has been shown that, *in vitro*, ParAc can form dimmers and then associate with nonspecific DNA forming nucleoprotein filaments (similar to the ParA filaments in Fig. 1), suggesting ParAc has a potential capacity for mediating DNA movement (Leonard *et al.*, 2005). The ParBc-origin complexes would be probably anchored to the cell poles by the ParAc filaments. Thus, these observations raised a possibility that *parABC* is involved in the chromosome origin region localization and segregation. This suggestion was also proposed from the studies of some other Par systems. Fogel and Waldor (2006) recently provided *in vivo* evidence for mitotic-like pulling forces that mediate DNA movement in *V. cholerae*. In their studies, they found that ParB1 bound *parS1* sites near origin regions (*oriC1*) forming apparent complexes that asymmetrically localized and segregated with the origins. In this process, ParA1 was required to mediate polar localizations of the nucleoprotein complexes. Thus it seems the Par1 system in *V. cholerae* is required for the polar localizations and asymmetric segregations of the origin regions of chrI. A similar situation was also found in *C. glutamicum*, in which ParB is also polar-localized, and the positions are faithfully reflecting those of the origins, further, deletion of *parA* seems to affect the polar localization of ParB (Donovan *et al.*, 2010).

The *par* loci are well-known to ensure accurate DNA segregation in low-copy-number plasmids, disruption of any of the three components results in severe segregation defect. Interestingly, their chromosomal orthologs seem to possess various properties in different bacterial species, and their role in chromosome segregation is suggested to be less pivotal compared with that of their

counterparts in plasmids. In some bacteria, chromosome-encoded *par* loci play a direct role in chromosome segregation. *Caulobacter* has an active *par* system that is required for cell growth and ensuring its chromosome only replicate once each cell cycle (Marczynski, 1999; Mohl *et al.*, 2001). In *C. crescentus*, deletion mutants of *parAB* are lethal, suggesting that both proteins might equally be involved in some essential step of the developmental progressions in the cell cycle; the expression levels of ParA and ParB remain constant through most of the cell cycle, and overexpression of the *parAB* operon results in generation of anucleate cells (Mohl and Gober, 1997), indicating its role in chromosome partitioning. In some other bacteria, the role of *par* loci in chromosome segregation is obscure. Although deletion of *spoOj* (*parB*) of *B. subtilis* leads to a considerable increase of anucleate cells during vegetative growth, the remaining cells still exhibit a normal chromosome segregation pattern (Ireton *et al.*, 1994); moreover, deletion of *soj* (*parA*) has no significant effect on the chromosome segregation (Marston and Errington, 1999). In *Streptomyces coelicolor* and *P. putida*, *parAB* system is only needed for chromosome partitioning under certain conditions. In *S. coelicolor*, deletion of part of *parB* had no effect on the growth or appearance of colonies but caused a deficiency in DNA partitioning during the multiple septation events involved in converting aerial hyphae into long chains of spores (Kim *et al.*, 2000). In *P. putida*, the *parAB* genes are not essential, and *parA* and *parB* mutations do not influence cell growth or chromosome segregation in rich medium; however, in minimal medium different *parA* and *parB* mutations gave between 5 and 10% anucleate cells during the transition from exponential phase to stationary phase (Lewis *et al.*, 2002). In *V. cholerae*, cell growth is not altered upon deletion of *parA1*, and the chromosome I (chrI) is still faithfully partitioned to daughter cells; however, the polar localization pattern of the origin region is abrogated, indicating that the ParABS1 system functions to mediate the localization and segregation of the chrI origin region but not the bulk nucleoid (Fogel and Walder, 2006). The observation of *parABc* shows some similarity with that of the ParABS1 system from *V. cholerae*. Likely, the *T. thermophilus* chromosomal bulk nucleoid segregation is conducted by other mechanisms, such as the proposed DNA-, RNA- polymerase based system, or

even it proceeds in a species-specific manner (e.g., random partitioning). This idea is actually supporting the view that multiple and redundant facilities may be involved to regulate the bacterial chromosome replication and segregation (Errington *et al.*, 2005).

#### 4.2.2 Characteristics and functions of the megaplasmid *par* system

##### 4.2.2.1 Genetic structures and components of the megaplasmid *par* loci

The megaplasmid-encoded *par* loci have a different gene structure compared with those of the chromosome. The *T. thermophilus parABm* operon is located in the megaplasmid origin-proximal region (~ 10 kbp from *oriCm*, Fig. 5C), and has a genetic set-up similar to that of low-copy-number plasmids, in which the *parABm* operon is adjacent to the *repA* gene encoding a plasmid-like replication initiator, and also has a number of direct repeats resembling iterons clustered around. Like the case found in ParAc, the *parAm* gene also encodes a Walker-type ATPase containing conserved P-loop ATP binding motifs (Fig. 5D). The difference is in ParAm there is a Helix-Turn-Helix motif (HTH) at its N-terminus, a feature that normally appears in plasmid ParAs but not in chromosomal ones (Gerdes *et al.*, 2000) (Fig. 5D). Phylogenetically, ParAm is more near to the plasmid and phage ParA proteins (Fig. 5D). This indicates that *parABm* may display functions similar to other plasmid *par* systems. It has been suggested that the plasmid ParA proteins have dual functions: on one hand, they interact with promoter regions and repress transcription, and their interaction with ParB will enhance the repression; on the other hand, they contact ParB-*parS* complexes, and are involved in DNA partitioning (Gerdes *et al.*, 2000). Some *in vitro* DNA binding assays showed that, the ADP-bound form of ParA interacts with the promoter regions, while ATP-ParA form contacts ParB-*parS* complexes (Bouet and Funnell, 1999; Yates *et al.*, 1999). The *T. thermophilus* megaplasmid *parS* sequences are not known, however, several inverted repeats were found in the upstream and downstream of *parABm*; based on the properties (positions and sequences) of the *parS* sites from other plasmid Par systems, it would be highly possible that they serve as the megaplasmid ParBm binding sites.

#### 4.2.2.2 Functions of the megaplasmid *par* loci

To investigate the functions of the megaplasmid *par* loci, initially, the *parABm* operon was attempted to be exchanged by the *blm* cassette. However, it was impossible to obtain a homozygous *parABm* deletion mutant (Fig. 6B), suggesting essential roles for *parABm*. The essentiality of certain *par* genes was also observed in other bacterial species. The null mutant of *parB* in *C. crescentus* is lethal (Mohl *et al.*, 2001), and deletion of *parAB2* genes in *V. cholerae* chromosome II (a megaplasmid-derived genome, Heidelberg *et al.*, 2000) is also not feasible unless a wild-type version of these genes is provided from a plasmid *in trans* (Yamaichi *et al.*, 2007). Since it was impossible to delete the entire *parABm* operon, we later tried to replace the N-terminus-encoding region of *parAm* with a bleomycin cassette opposing the transcription direction of the *parABm* operon ( $\Delta parAmN-1$ , Fig. 6C), and delete *parBm* individually, on one hand aiming to knockdown the *parABm* genes, and also to understand which gene is essential. Further, to illustrate whether the resulting effect of the  $\Delta parAmN-1$  mutant is caused by deletion of the N-terminus-encoding region of *parAm* or down-regulated levels of ParABm, the same encoding region (amino acids 1-40) was also replaced by *blm* in a direction co-linear with the *parABm* transcription ( $\Delta parAmN-2$ , Fig. 6C). The results showed the *parAmN* mutants could be obtained ( $\Delta parAmN-1$  and  $\Delta parAmN-2$ ) (Fig. 6D), whereas the *parBm* mutant remained in a heterozygous state (Fig. 6E), indicating this gene is essential, thus it seems there are in addition other essential genes on the megaplasmid which needed to be maintained. Further, the transcription levels of the truncated *parAm* and *parBm* genes in  $\Delta parAmN-1$  and  $\Delta parAmN-2$  were determined by RT-qPCR. As expected, in  $\Delta parAmN-1$ , the transcription levels of the truncated *parAm*, *parBm* genes were decreased; by contrast, in  $\Delta parAmN-2$ , increased levels of the *parABm* expressions were detected (Fig. 6F).

The phenotypical consequences of the  $\Delta parAmN-1$  and  $\Delta parAmN-2$  strains were then analyzed from several aspects. Through observing the growth phenotypes of these two mutants, it was found that pronounced growth defect occurred in  $\Delta parAmN-1$  but not in  $\Delta parAmN-2$ , especially when the cells were grown in minimal medium (Fig. 7A, B). Through microscopic analyses, we found that cell



shapes, cell divisions, and frequencies of occurrence of anucleate cells were not changed in either  $\Delta parAmN-1$  or  $\Delta parAmN-2$  (Fig.7C; data not shown). However, in the case of  $\Delta parAmN-1$ , a considerable proportion of cells (33.02 %) were found containing less DNA when grown in TB medium, indicating defects of genome replication and segregation (Table 7). When grown in minimal medium, the frequency of DNA-less cells of  $\Delta parAmN-1$  was decreased (data not shown), suggesting the defect was more tolerated when the growth rate was reduced, probably due to the fact that less amount of ParABm protein was required. In addition to its severe growth defect and the increase of DNA-less cells, we further found this strain was deficient in the syntheses of carotenoids,  $\beta$ -glucosidase and  $\beta$ -galactosidase enzymes that are expressed from the megaplasmid, suggesting loss of the respective encoding genes (Fig. 8A, B). By comparison,  $\Delta parAmN-2$  which had considerably higher levels of ParABm expressions displayed wild-type comparable or slightly higher expression levels of these enzymes (Fig. 8A, B). Thus, it was conceivable that there might be megaplasmid sequence loss in the  $\Delta parAmN-1$  but not in  $\Delta parAmN-2$ . To confirm this hypothesis, we tried to determine the genome copy numbers of  $\Delta parAmN-1$  and  $\Delta parAmN-2$  via qPCR method. Two megaplasmid and chromosomal loci were respectively chosen as the target regions (TT\_P0043, and TT\_P0195, i.e. locus near *term*; loci near *oriCc* and *terc*, respectively). The qPCR results demonstrated that the copy numbers of the chromosomal loci in either  $\Delta parAmN-1$  or  $\Delta parAmN-2$  were not altered (Fig. 8C; Table 7), suggesting disruption of the megaplasmid *par* loci has no influence for the replication of the chromosome. For  $\Delta parAmN-2$ , the relative copy numbers of the two megaplasmid loci were mildly higher (Fig. 8C; Table 7), which is probably due to the relatively abundant expressions of ParABm. Interestingly, in  $\Delta parAmN-1$ , the locus TT\_P0043 was completely lost, while the copy numbers of the locus near the *term* region were even slightly higher than those of the wild type (Fig. 8C; Table 7), indicating only portions of the megaplasmid sequences had been lost. This hypothesis was further confirmed by PFGE analysis, which showed the megaplasmid of  $\Delta parAmN-1$  had been truncated to an extent of approximately 100 kbp, and the smaller megaplasmid somehow could not be partitioned efficiently as untangled megaplasmid after

replication could be observed (Fig. 8D). Moreover, the result of PCR amplifications of 10 loci distributed over the whole megaplasmid in combination with the above data suggested that the regions between approximately 11 kbp and 102 kbp from the megaplasmid *oriC* were completely lost, however, the regions located on the opposite site of *oriC* were still present (Fig. 8). These results suggested that the *parABm* system is required for the megaplasmid maintenance. The observation that only portions of the megaplasmid were missing is supportive of the fact that *parBm* is essential, and in addition there may be other important regions needed to be maintained. Indeed, despite various attempts undertaken in our group (unpublished results), to date it has not been possible to eliminate the whole megaplasmid from *T. thermophilus*. The missing portions are probably non-essential regions, which may be excised by recombinations between homologous sequences (considerably long direct and inverted repeats were found surrounding these regions, (data not shown)). When we tried to select for strains devoid of the megaplasmid from a library of *T. thermophilus* transposon insertion mutants (our group, unpublished data), we also found that some mutants carrying truncated megaplasmid variants. In this case, the locations of the lost regions were highly similar to those in  $\Delta parAmN-1$  (data not shown).

The localization patterns of the megaplasmid ParB proteins in *T. thermophilus* were also elucidated. As shown in Fig. 11E, ParBm-sGFP formed discrete foci when expressed in wild-type *T. thermophilus* cells, suggesting there were indeed ParBm binding sites (*parSm*). Moreover, as the case found in the ParBc-sGFP localizations, the ParBm-sGFP proteins were also found to be polar localized (Fig. 11E, H). In marked contrast, when ParBm-sGFP was expressed in the  $\Delta parAmN-1$  background, the average foci numbers were decreased, and the foci were drastically mislocalized (Fig. 11 F, I). The foci were mostly dissociated from the cell poles. Instead, they were inclined to be positioned near the cell center or cell quarter (Fig. 11 F, I). The ParBm locations are actually reflecting those of the megaplasmid *parS* sites (i.e., the megaplasmid origin regions). Thus, the above findings suggested that by lack of ParABm, the megaplasmid origin regions will not be segregated efficiently (decreased foci numbers) and positioned appropriately (dissociated from the cell

poles) in the daughter cells, which is highly supportive of the proposal that *parABm* is required for the megaplasmid segregation (Fig. 17).

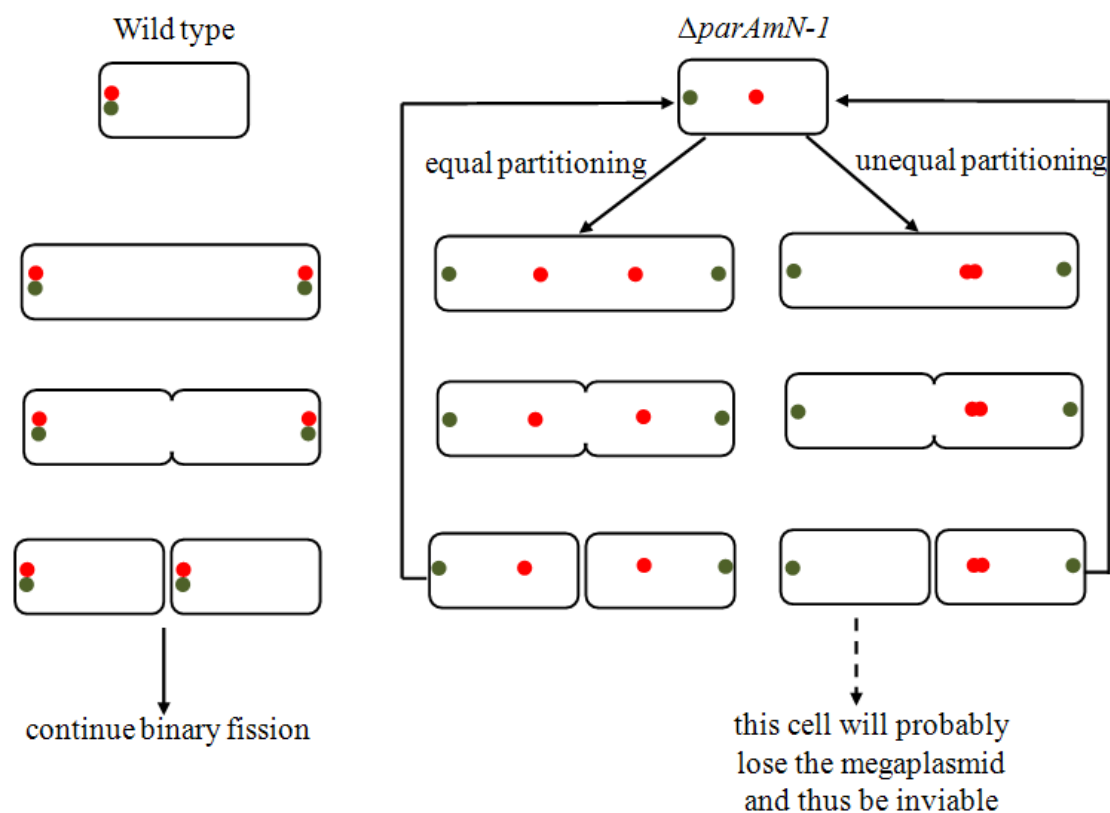


Fig. 17. A hypothesized model of chromosome and megaplasmid origin region segregations and the generation of DNA-less cells in *T. thermophilus*  $\Delta parAmN-1$ . (Left) Schematic representation showing the pattern of segregations of the origin regions of chromosome (green) and megaplasmid (red) in wild-type cells. (Right) The megaplasmid origin region is randomly localized in the  $\Delta parAmN-1$  mutant. Cell division can therefore probably result in daughter cells that either contain or lack megaplasmid.

It seems that the ParABm proteins can activate the factors (e.g., factors for megaplasmid DNA synthesis) that are involved in the megaplasmid replication. Thus, the activation was weakened in the  $\Delta parAmN-1$  mutant expressing insufficient amount of ParABm, which would probably render lack of the replication factors. Thereby, the non-essential regions (or redundant regions) should be excised to ensure there were enough factors for the replication of the essential regions. Supporting this idea, when ParAm or ParBm were overexpressed in wild-type *T. thermophilus* cells (TMP01 and TMP02), megaplasmid copy numbers were increased in the both cases (Fig. 8A, B, C, D; Table 7), indicating the role of

*parABm* in the megaplasmid replication process. This is somehow not surprising, studies of bacteria have shown that processes aiming to maintain genome content, such as replication, repair, and segregation, although able to function independently of each other, they also influence each other (Venkova-Canova *et al.*, 2013). The plasmid-borne Par system is initially considered to function only in DNA segregation, however, recent evidence showed that both ParA and ParB proteins can also influence replication. In *B. subtilis*, SpoOj (ParB) was found to recruit a SMC condensin protein to replication origin regions, and thereby promoting chromosome segregation (Sullivan *et al.*, 2009; Gruber and Errington, 2009). Sullivan *et al.* (2009) demonstrated that in *B. subtilis*, the subcellular localization of the SMC complex is disrupted in the absence of Spo0J or the *parS* sites; furthermore, the SMC complex co-localizes with Spo0J at the origin and insertion of *parS* sites near the terminus targets SMC to this position leading to defects in chromosome organization and segregation. The same phenomenon was also observed in *Streptococcus pneumoniae* (Minnen *et al.*, 2011). ParB2 encoded by *V. cholerae* chromosome II (chrII) was also found to influence the replication of chrII, in which ParB2 appeared to promote the replication (Yamaichi *et al.*, 2011), thus disruption of *parAB2* could lead to loss of the chromosome II (Yamaichi *et al.*, 2007). It has been shown that in *B. subtilis*, Soj (ParA) can directly interact with the chromosome replication initiator DnaA; Murray and Errington (2008) proved that the classical effect of Soj inhibiting sporulation is an indirect consequence of its action on DnaA through activation of the Sda DNA replication checkpoint, thus it seemed that the pleiotropy manifested by chromosomal *parABS* mutations could be the indirect effects of a primary activity regulating DNA replication initiation. The situation that ParA can interact with DnaA and thereby regulating chromosome replications was also found in the chromosome I of *V. cholera* (Kadoya *et al.*, 2011; Scholefield *et al.*, 2012). Together, it is conceivable that the ParABm system in *T. thermophilus* is important for maintaining the megaplasmid, probably through regulating its replication and segregation. Our results and conclusions for the *T. thermophilus* megaplasmid *par* system in some respect resemble that has been found for the *V. cholerae* chromosome II (chrII) which is also a megaplasmid-derived genome (Heidelberg *et*

*al.*, 2000). In both cases, it appears that there is no redundancy in the mechanisms that mediate the megaplasmid or chromosome II segregation in addition to the Par-based systems (Yamaichi *et al.*, 2007).

#### 4.2.3 Chromosomal and megaplasmid Par are two independent systems

As demonstrated, the chromosomal and megaplasmid *par* loci seem to function differently. Thereby, we speculated the two ParB proteins also act on different *parS* sequences. The chromosomal *parS* sequence was first identified in *B. subtilis*, and later it was found to be highly conserved in bacterial species. In *T. thermophilus*, the *parSc* site is located upstream of *parAc*, suggesting it is a potential chromosomal ParB binding site. Indeed, the *in vitro* DNA binding assays showed that ParBc bound this *parS* site in a specific manner, which could not be outcompeted by mutated sequences. By contrast, ParBm bound the *parSc* site in a unspecific manner (i.e., ParBm does not bind *parSc*), suggesting it has its own binding sequences. Although it was unable to perform the experiments of ParBm binding to its own *parS* sites, these findings are sufficient to pinpoint that the two ParB proteins act with different sequences. This conclusion was also supported by the *in vivo* ParB localization investigations in the *E. coli* cells, as the two ParBs seem to localize differently in this system. In *E. coli* cells, it was also found that ParBm-sGFP could form foci, implying the existence of ParBm binding site in the *E. coli* genome or the *parBm* coding sequences. The megaplasmid *par* system and that of the low-copy-number plasmids from *E. coli* share some structural similarity, indicating they may also contain similar *parS* sequences. On the other hand, inverted repeats can be identified in the *parBm* coding sequences (data not shown), which may serve as ParBm's binding sites. Nevertheless, the above data in combination with the fact that disruption or overexpression of *parABm* only affected the megaplasmid but not the chromosome, suggest that the two Pars are independent systems. This genome-specific ParB binding phenomenon was also observed in other Par systems. It has been shown that ParB1 and ParB2 proteins in *V. cholerae* also act on different *parS* sites: three *parS1* sites are found for ParB1, and 10 *parS2* sites are identified for ParB2, which differ in sequence from *parS1* (Yamaichi *et al.*, 2007). The genome

of *B. cenocepacia* is comprised of three chromosomes (c1, c2, c3) and one low-copy-number plasmid (p1), each replicon contains an *parAB* locus and a set of ParB binding *parS* sites (Dubarry *et al.*, 2006). The ParAB from the longest chromosome (c1) are phylogenetically clustered with the other chromosomal analogues, while the others located on the c2, c3, and p1 are more likely plasmid-evolved. Correspondingly, the *parS* of the main chromosome is the “universal” chromosomal *parS*, and the *parS* sites on the other three genomes are sequences specific to their replicons. Through an *E. coli* plasmid stabilization assay, Dubarry *et al.* (2006) showed that each *parAB* exhibits partition activity only with the *parS* of its own replicon. The above two examples accompanied with our data suggest that in bacteria containing multiple replicons, the *parABS* system is more likely behaving in a replicon-specific manner, rather than forming a communal system or network of interacting systems. This is probably evolved by selective pressure to avoid genome partitioning incompatibility (Dubarry *et al.*, 2006; Yamaichi *et al.*, 2007).

### 4.3 MreB does not play a role in the chromosome segregation of *T. thermophilus*

The investigation of the chromosomal *par* loci has shown that they properly function to position and segregate the chromosomal origin regions, but not the bulk DNA. This suggestion supports the rising view that bacterial chromosome partitioning is mediated by multiple, likely overlapping or redundant mechanisms (Errington *et al.*, 2005). To date, except for the plasmid-evolved partitioning system, many other bacterial mitotic-like apparatuses have been proposed to provide active chromosome segregations. One of the relatively well-studied systems is the MreB-mediated chromosome segregation machinery. MreB is a chromosome-encoded actin-homolog. The structure of monomeric MreB is very similar to yeast actin (van den Ent *et al.*, 2001), thus placing the evolutionary root of actin in the prokaryotic domain (van den Ent *et al.*, 2001). *In vitro*, MreB forms filaments, in an ATP-dependent manner, that closely resembles an actin protomer half-filament (van den Ent *et al.*, 2001). *In vivo*, MreB forms helical cables that traverse the length of the cell in all bacterial organisms examined (Kruse *et al.*, 2003; Shih *et al.*, 2003; Figge *et al.*, 2004). Interestingly, the MreB cables are dynamic structures that are continuously remodeled throughout the cell cycle (Figge *et al.*, 2004; Defeu Soufo and Graumann, 2004; Gitai *et al.*, 2004). In some classic rod-shaped bacteria, it has been shown that MreB not only determines the cell shapes, but also provides force for chromosome segregations (Kruse *et al.*, 2003; Defeu Soufo and Graumann, 2004; Gitai *et al.*, 2004). In *E. coli*, expression of mutant MreB inhibits cell division, and has a severe nucleoid segregation defect, moreover, the *oriC* and *terC* regions become drastically mislocalized, suggesting that MreB is required for origin and bulk DNA segregation in *E. coli* (Kruse *et al.*, 2003). In *B. subtilis*, depletion of MreB leads to a rapid chromosome segregation defect before defect in the cell shapes becomes visible (Soufo and Graumann, 2003).

In this study, the role of the MreB homolog regarding chromosome segregation in *T. thermophilus* was also analyzed. Although in certain bacteria, the *mreB* gene seems to be essential, *mreB* in *T. thermophilus* could be successfully inactivated (Fig. 12). The *mreB* mutant displayed more spherical-shapes compared with wild type, indicating MreB is also involved in cell shape maintenance in *T. thermophilus*. The

cells were not completely round (Fig. 13A), indicating that in addition to MreB other rod-shaped cell morphology determinants were present. Nevertheless, the *mreB* depletion strain had a similar chromosome partitioning pattern and growth rate as the wild type (Fig. 13). Thus, no apparent impairments of the chromosome segregation process had occurred in the *mreB* mutant. It seems that although MreB plays important roles in chromosome segregation in some bacteria like *B. subtilis* and *E. coli*, examples from other bacterial species showed that MreB does not function to mediate bulk chromosome segregation. A recent excellent work has shown that in *C. crescentus*, MreB was required for proper positioning of origin regions but not for other regions of the chromosome (Gitai *et al.*, 2005). In their study, they showed MreB was a direct target of A22 (S-3,4-dichlorobenzyl isothiourea, which is a new antibacterial compound that induces a round cell morphology and anucleate cells in *E. coli* and *C. crescentus* (Iwai *et al.*, 2002; Gitai *et al.*, 2005); and A22 completely blocks the movement of newly replicated loci near the origin region but has no qualitative or quantitative effect of other loci if A22 was added after origin segregation (Gitai *et al.*, 2005). In *Anabaena* sp. PCC 7120, MreB is also not required for chromosome segregation (Hu *et al.*, 2007), the same conclusion is obtained in *Stryptomyces coelicolor* (Mazza *et al.*, 2006). The results in this study also indicated that MreB is not required for bulk chromosome segregation in *T. thermophilus*. However, as the function of the chromosomal Par system, MreB may be participating in the localizations and segregations of the replication origins. To test this, further experiments should be performed, such as to visualize the subcellular localization pattern of the MreB protein.



## 4.4 Random partitioning of the chromosome copies

### 4.4.1 Separation of two alleles at one chromosomal locus is caused by random partitioning of chromosome copies into the daughter cells

Through the investigations of the roles of the Par and MreB systems, the conclusions that both of the systems are not active in the bulk chromosome segregation of *T. thermophilus* were drawn. Likely, in *T. thermophilus*, other active machineries are governing the chromosome partitioning, or even it is lacking those machineries and vulnerable to random partitioning. Random chromosome partitioning would be possible, on account of that *T. thermophilus* contains multiple chromosomes per cell. As introduced, the separation of two different alleles in one chromosomal locus can be observed in *T. thermophilus*, and it was hypothesized that this effect was caused by gene conversion or random chromosome partitioning. To test this, a heterozygous strain (HL01) containing both kanamycin and bleomycin markers at the chromosomal *pyrE* gene locus was constructed in *T. thermophilus* (Fig. 14), and this strain was continuously grown with agitation in antibiotic-free medium for 120 h, from which the gradual separation of these two markers was found (Fig. 15A). A similar allele separation mode was observed in the HB8 strain by Ohtani *et al.* (2010). The fact that the relative abundance of each allele kept constant while the fraction of apparent phenotypes changed in the whole population (Fig. 15) implied that the separation was probably caused by random partitioning of chromosomes in the daughter cells but not gene conversion (Fig.18). The random chromosome partitioning pattern has also been observed in certain polyploid cyanobacteria (Hu *et al.*, 2007; Schneider *et al.*, 2007). Thus, it seems random partitioning of chromosomes would require multiple copies of chromosomes per cell so that no cell death would occur because of random partitioning.

An interesting point demonstrated by Fig. 15A is that the fraction of the homozygous cells increased more rapidly in stationary phase than that in exponential phase, and although less obvious, this was also observed in the allele separation kinetics in HB8 (Ohtani *et al.*, 2010). This may be due to the fact that *T. thermophilus* HB27 is impressively natural competent in exponential phase.

Although cell divisions proceed faster, DNA exchange among the cells or uptake of free DNA released by dead cells may also occur (César *et al.*, 2011; Alvarez *et al.*, 2011), which may affect the frequency of the apparent genotypes of the two alleles. Indeed, when EDTA that would probably impede DNA uptake to the cells was supplemented in the allele separation reactions, more rapid separation of the two alleles was observed (data not shown). Further, probably due to reductive cell divisions in the late stationary phase (Kolter *et al.*, 1993; Navarro *et al.*, 2010), the genome copy number in one cell may also decrease, and this would favour the daughter cells to receive the same type of parental genome copies by random partitioning.

The proposal that the chromosome copies tend to partition randomly into the daughter cells was further tested by investigating the relative DNA contents (determined by DAPI signal intensities) in the daughter cells. It displayed that, in comparison to *B. subtilis*, the relative contents of the two daughter cells scattered more far away from 1.0 (Fig. 16), indicating the random partitioning was probably manifested as separation of different amount of replicated DNA into the daughter cells, which is reminiscent of the situations in cyanobacterial species (Schneider *et al.*, 2006; Hu *et al.*, 2007). It seems this is not surprising, since the two proposed mitotic-like chromosome partitioning machineries in *T. thermophilus* are not active, thus, lacking of redundant mechanisms to ensure each daughter cell obtain a same set of the replicated parental chromosomes. Taken together, unlike haploid bacteria, such as *B. subtilis* and *E. coli*, in which the genome partitioning is strictly controlled by active machineries to ensure one daughter cell receive at least one copy of chromosome, in *T. thermophilus*, multiple chromosome copies exist in one cell and this may make stringent controlling machineries unnecessary, thus random partitioning may occur.

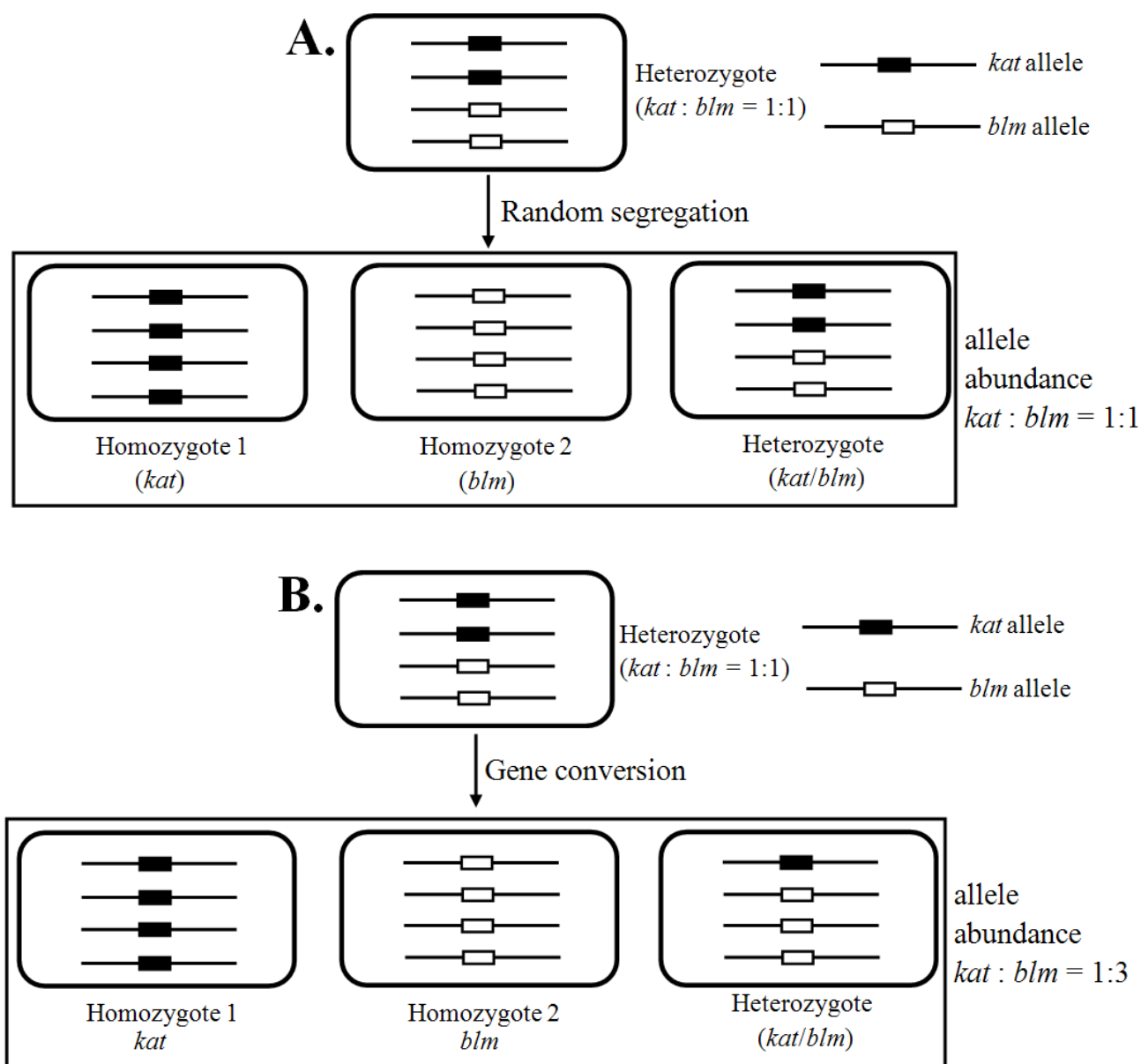


Fig. 18. Schematic drawings showing the differences between the processes of allele random segregation and gene conversion which are both expected to lead to homozygosity in a *T. thermophilus* heterozygous cells carrying *kat* and *blm* at the same chromosomal locus (the relative abundance of *kat* and *blm* was set as 1 in the original heterozygous cell). (A) If random chromosome partitioning occurred, the fraction of apparent phenotypes changed in the whole cell population, while the relative abundance of each allele kept constant (in this case,  $kat : blm = 1 : 1$ ). (B) On the contrary, if gene conversion occurred, the fraction of apparent phenotypes, and the relative abundance of each allele in the whole cell population would both be altered (in this case,  $kat : blm = 1 : 3$ ).

#### 4.4.2 Random partitioning of the chromosome copies favors generation of homozygous gene deletion mutants in *T. thermophilus*

*T. thermophilus* carries multiple chromosome copies. There seems to be a contradiction between polyploidy and the ease of generating chromosomal gene deletion mutants. For example by the use of the antibiotic resistant markers. In a *T. thermophilus* cell, integration of the selection marker in one of the chromosomal copies would lead to marker-caused resistance of the whole cell. Thus, it is conceivable that during the generation of gene deletion mutants, heterozygous state carrying both wild-type and mutant alleles would occur. However, in this study, it was found that marker-free chromosomal gene deletion mutants could be easily generated in *T. thermophilus* (Fig. 3B), and the frequency of obtaining the homozygous mutant was also considerably high (Fig. 3B). Therefore, there must be mechanism that would lead to the ease of obtaining of the marker-free gene deletion mutants in *T. thermophilus*. As illustrated in Fig. 15 and Fig. 16, partitioning of the *T. thermophilus* chromosome copies into the daughter cells may experience random event. Thus, it is highly possible that the ease of obtaining homozygous chromosomal gene deletion mutants at relatively high frequencies was assisted by the chromosome random partitioning process. The results from the allele segregation experiment (Fig. 15) suggested that during the process of generating gene deletion mutants (non-essential genes), after transformation of the desired allele on a non-replicating plasmid in *T. thermophilus*, it would be sufficient to screen for the presence of this allele in the genome in order to obtain a homozygous mutant strain. As in case the allele is found in a heterozygous state, the homozygous state of this allele would be obtained by simply growing the heterozygous strain in the absence of selection which would allow allele segregation (Fig. 18).

## 5. Summary

The plasmid partitioning system (Par) usually consists of three components: a DNA-binding protein (ParB), an ATPase (ParA), and a centromere-like site (*parS*). ParB binds *parS* and spreads along the DNA, forming a large nucleoprotein complex. Formation of this complex and its interaction with ParA are suggested to exert efficient plasmid segregation. Most bacterial chromosomes encode orthologs of the plasmid partitioning proteins (ParA and ParB), however, their role in chromosome segregation is less understood. MreB is a chromosomally encoded actin-like protein, which is important for cell morphology maintenance in rod-shaped bacteria. In some bacterial species (e.g., *E. coli*, *B. subtilis*, *C. crescentus*), it has been suggested that MreB can also provide force for chromosome segregation.

There are multiple copies of chromosome and megaplasmid in *T. thermophilus*, whether their segregations are stringently regulated is not known. Like many other bacterial genomes, both the chromosome and megaplasmid of *T. thermophilus* encode the *par* gene homologues (termed as *parABc* and *parABm*, respectively) and their corresponding *parS* sites (termed as *parSc* and *parSm*, respectively). *parABSc* and *parABSm* are respectively located in the vicinity of the origin regions of the chromosome and megaplasmid. The chromosome also contains a MreB homologue. In this study, the characteristics and functions of these potential genome partitioning machineries were investigated.

The main results with respect to the chromosome segregation were:

(i) Both the ParABc and MreB systems in *T. thermophilus* are not required for the chromosome bulk nucleoid segregation.

In the *parABc* deletion mutant, the cell growth and the frequency of DNA-less cells were not altered, indicating that the chromosomal bulk DNA segregation was not affected. Further, chromosome replication was also not impaired in the *parABc* null mutant. ParBc could bind *parSc* specifically, implying it is actually a functional ParB protein. In wild-type cells, the ParBc-*parSc* (i.e., ParBc-origin) complexes were found to be polar localized, indicating that *parABc* helps localization and segregation of the

chromosomal origin region but not of the bulk DNA.

The *mreB* null mutant displayed a change in cell shape, indicating the role of MreB in cell morphology determination in *T. thermophilus*. In the *mreB* mutant, the cell growth rate or the relative nucleoid contents in the daughter cells were not altered, suggesting the chromosomal bulk nucleoid segregation was not affected.

(ii) The megaplasmid Par system also does not contribute to the chromosome bulk nucleoid segregation. The ParBc and ParBm proteins bound to different *parS* sites, indicating that the chromosomal and megaplasmid Par systems act in a replicon-specific manner. Indeed, in the *parABm* mutant expressing insufficient amounts of ParABm, the replication and segregation of the chromosomal bulk DNA still progressed normally.

(iii) In a heterozygous *T. thermophilus* strain containing two different alleles at one chromosomal locus, gradual separation of the two alleles could be observed. The relative abundance of each allele remained largely constant, whereas the fraction of apparent phenotypes changed in the whole population, indicating the separation was probably caused by random partitioning of the chromosome copies in the daughter cells.

(iv) Using a new counterselection principle, which is based on the toxic effect exerted by cleavage of 5-bromo-4-chloro-3-indolyl- $\beta$ -D-glucopyranoside (BCI- $\beta$ -glu) by  $\beta$ -glucosidase (Bgl), chromosomal marker-free gene deletion mutants can easily be obtained. It seems that the ease of obtaining such marker-free chromosomal gene deletion mutants of *T. thermophilus* that contains multiple chromosome copies is probably aided by the chromosome random partitioning event which leads to homozygosity of the mutants.

Taken together, these experiments suggested that probably due to the lack of active chromosome partitioning machineries, the multiple chromosome copies in *T. thermophilus* undergo random partitioning.

The main results concerning the megaplasmid segregation in *T. thermophilus* were:

(i) The ParABm system of *T. thermophilus* functions to mediate the megaplasmid segregation. The *parABm* mutant expressing insufficient amounts of ParABm proteins

displayed severe growth defect, high frequency of DNA-less cells, and loss of approximately 100 kbp megaplasmid sequences. Further, the smaller megaplasmid could not be partitioned appropriately, as untangled megaplasmid after replication could be observed, and the megaplasmid *parSm* sites (their subcellular locations reflected those of the megaplasmid origin regions) were drastically mislocalized which was in marked contrast with the polar-localized pattern in wild-type cells. These findings indicated the role of ParABm in the megaplasmid subcellular localization and segregation.

(ii) It seems that ParABm can also activate the factors that are involved in megaplasmid replication. In the strains overexpressing either ParAm or ParBm, the megaplasmid copy numbers were increased, indicating the megaplasmid replication was enhanced. Therefore, it is possible that in the *parABm* mutant expressing insufficient amounts of ParABm proteins, this activation tended to be weakened, thereby the non-essential regions of the megaplasmid should be eliminated to ensure enough activated replication factors existed for the replication of the essential regions.

Taken together, these experiments suggested that compared with that of the chromosome, the megaplasmid partitioning is more stringently regulated in *T. thermophilus*. The megaplasmid ParABm system probably functions to regulate the megaplasmid replication and segregation, thereby maintaining the megaplasmid.

## Summary (German version)

Während der Zellteilung ist es wichtig die genetischen Informationen an die Tochterzellen weiter zugeben. Es wird vermutet, dass in Bakterien das Plasmid Trennungssystem (engl. plasmid partitioning) *parABS* und das Aktin-ähnliche Protein MreB die Genomsegregation unterstützen. In *Thermus thermophilus* sind mehrere Kopien des Chromosoms und des Megaplasmid in einer Zelle vorhanden, jedoch ist die Regulation ihrer Segregation noch nicht ausreichend erforscht. Auf dem Chromosom und dem Megaplasmid liegt jeweils eine *parAB* ähnliche Gensequenz (*parABc* und *parABm*) und die dazugehörige *parS* Bindestelle (*parSc* und *parSm*). Zusätzlich besitzt das Chromosom noch ein zu *mreB* homologes Gen. In dieser Arbeit wurden die Funktionen dieser potenziellen Trennungsmechanismen untersucht und neue Erkenntnisse über die Genomsegregation in *T. thermophilus* gewonnen.

In dieser Dissertation wurden folgende Erkenntnisse im Hinblick auf die Chromosomensegregation in *T. thermophilus* gewonnen:

(i) In Bezug auf die Chromosomensegregation konnte durch Mutationsexperimente gezeigt werden, dass die *parABSc* und MreB Systeme für die Segregation des Chromosoms und des Nucleoids nicht essentiell sind. Die *parABc* Deletionsmutante zeigte keine Veränderung in Zellwachstum, Chromosomenreplikation oder-segregation. Beim Wildtyp kann man jedoch beobachten, dass das Protein ParBc spezifisch an *parSc* bindet und sich der Komplex ParBc-*parSc* (z. B. ParBc-origin) polar in der Zelle verteilt. Deshalb könnte ParABc dabei helfen, die Origin Region des Replikationsursprungs (origin) auf dem Chromosom zu lokalisieren und zu segregieren. Obwohl die *mreB* Mutante eine modifizierte Zellform aufwies, blieben das Wachstum und die Segregation des Chromosoms und des Nucleoids unverändert.

(ii) Das Par System auf dem Megaplasmid scheint ebenso keine Funktion an der Chromosomen Bulk Nucleotid Segregation zu haben. Die unterschiedlichen Bindestellen für ParBc und ParBm weisen darauf hin, dass die Par Systeme spezifisch auf die Replikons des Chromosoms oder des Megaplasmid reagieren. Tatsächlich wurde in der *parABm* Mutante eine insuffiziente Menge an ParABm exprimiert.



Dennoch konnte sich der Replikations- und Segregationsapparat der Chromosomen normal entwickeln.

(iii) In einem heterologen *T. thermophilus* Stamm, der zwei verschiedene Allele an einem chromosomalen Locus trägt, konnte eine sukzessive Trennung der beiden Allele beobachtet werden. Die relative Häufigkeit der einzelnen Allele blieb größtenteils konstant, während sich der Anteil der modifizierten Phänotypen im Verhältnis zu der ganzen Population veränderte. Diese Beobachtung könnte auf eine ungerichtete Aufteilung der Chromosomenkopien auf die Tochterzellen hinweisen.

(iv) Mit einer neuen Gegenselektions Methode können schnell und einfach Mutanten mit einer chromosomal Marker-freien Gendeletion generiert werden. Das Prinzip basiert auf dem toxischen Effekt von 5-bromo-4-chloro-3-indolyl- $\beta$ -D-Glukopyranoside (BCI- $\beta$ -glu), welches bei der Spaltung durch die  $\beta$ -Glukosidase (Bgl) freigesetzt wird. Die unkomplizierte Erstellung solcher Marker-freien Gendeletionsmutanten bekräftigt die These, dass in *T. thermophilus* die Chromosomenverteilung zufällig stattfindet und zur Homozygotie der Mutanten führt.

Auf Basis dieser neuen Erkenntnisse ist zu vermuten, dass aufgrund des Fehlens einer aktiven Chromosomensegregationsmaschinerie, die vielen Kopien einem willkürlichen Aufteilungsprozess unterliegen.

Die wichtigsten Ergebnisse in Bezug auf die Segregation des Megaplasmid werden im Folgenden zusammengefasst:

(i) Das ParABm System in *T. thermophilus* spielt eine wichtige Rolle bei der Megaplasmid Segregation. So konnte man bei einer parABm Mutante, die eine unzureichende Menge an ParABm Proteinen exprimiert, folgende veränderte Phänotypen erkennen: erhebliche Wachstumsstörungen, erhöhte Häufigkeit an DNA-freien Zellen und den Verlust eines 100 kbp langen Fragments im Megaplasmid. Darüber hinaus wurde das verkleinerte Megaplasmid nicht mehr richtig auf die Tochterzellen verteilt, da die Megaplasmid nach der Replikation nicht mehr entwirrt werden konnten. Außerdem entsprach die subzelluläre Lokalisation der *parSm* Bindestellen der Lokalisation der Origin Region des Megaplasmid und war daher falsch lokalisiert. In Wildtypzellen befindet sich die Origin Region des Megaplasmid

an den Zellpolen. Beide Beobachtungen verdeutlichen die Rolle des ParABm an der subzellulären Lokalisierung und der Segregation.

(ii) Es scheint, dass ParABm außerdem in der Lage ist, die in die Replikation des Megaplasמידs involvierten Faktoren zu aktivieren. In den Mutationstämmen, die eine Überexpression an ParAm oder ParBm aufweisen, war die Kopienzahl des Megaplasמידs ebenfalls erhöht. Dies spricht für eine verstärkte Megaplasמידreplikation.

Zusammenfassend zeigen die Ergebnisse, dass die Aufteilung der Megaplasמידe, im Vergleich zu den Chromosomen, stringenter reguliert wird. Es ist anzunehmen, dass das ParABm System die Replikation und Segregation des eigenen Megaplasמידs reguliert und es somit erhält.

## 6. Publication list

1. Angelov, Angel\*; **Li, Haijuan\***; Geissler, Andreas; Leis, Benedikt; Liebl, Wolfgang (2013): Toxicity of indoxyl derivative accumulation in bacteria and its use as a new counterselection principle. *Systematic and Applied Microbiology* 36 (8), S. 585-592. (\* authors contributed equally).
2. Leis, Benedikt; Angelov, Angel; **Li, Haijuan**; Liebl, Wolfgang: Genetic analysis of lipolytic activities in *T. thermophilus* HB27. Accepted by *Journal of Biotechnology*.
3. **Li, Haijuan**; Angelov, Angel; Pham Vu Thuy, Trang; Leis, Benedikt; Liebl, Wolfgang: Characterization of chromosomal and megaplasmid partitioning systems in *Thermus thermophilus* HB27. (draft manuscript).
4. Leis, Benedikt; Angelov, Angel; Mientus, Markus; **Li, Haijuan**; Pham Vu Thuy, Trang; Liebl, Wolfgang: Identification of novel esterase-active enzymes from hot environments by use of the host bacterium *Thermus thermophilus*. (draft manuscript).

## 7. References

- Adachi S, Hori K, Hiraga S. 2006. Subcellular positioning of F plasmid mediated by dynamic localization of SopA and SopB. *J Mol Biol.* 356:850-863.
- Agari Y, Kashihara A, Yokoyama S, Kuramitsu S, Shinkai A. 2008. Global gene expression mediated by *Thermus thermophilus* SdrP, a CRP/FNR family transcriptional regulator. *Mol Microbiol.* 70:60-75.
- Alvarez L, Bricio C, Gómez MJ, Berenguer J. 2011. Lateral transfer of the denitrification pathway genes among *Thermus thermophilus* strains. *Appl Environ Microbiol.* 77:1352-1358.
- Angelov A, Mientus M, Liebl S, Liebl W. 2009. A two-host fosmid system for functional screening of (meta)genomic libraries from extreme thermophiles. *Syst Appl Microbiol.* 32:177-185.
- Arnold C, Hodgson IJ. 1991. Vectorette PCR: a novel approach to genomic walking. *PCR Methods Appl.* 1:39-42.
- Austin S, Abeles A. 1983. Partition of unit-copy miniplasmids to daughter cells. II. The partition region of miniplasmid P1 encodes an essential protein and a centromere-like site at which it acts. *J Mol Biol.* 169:373-387.
- Averhoff B. 2004. DNA transport and natural transformation in mesophilic and thermophilic bacteria. *J Bioenerg Biomembr.* 36:25-33.
- Barilla D, Rosenberg MF, Nobbmann U, Hayes F. 2005. Bacterial DNA segregation dynamics mediated by the polymerizing protein ParF. *EMBO J.* 24:1453-1464.
- Baron, G.S., Nano, F.E. 1998. MglA and MglB are required for the intramacrophage growth of *Francisella novicida*. *Mol Microbiol.* 29:247-259.
- Bartosik AA, Lasocki K, Mierzejewska J, Thomas CM, Jagura-Burdzy G. 2004. ParB of *Pseudomonas aeruginosa*: interactions with its partner ParA and its target *parS* and specific effects on bacterial growth. *J Bacteriol.* 186:6983-6998.
- Bignell C, Thomas CM. 2001. The bacterial ParA-ParB partitioning proteins. *J Biotechnol.* 91:1-34.
- Bitan-Banin G, Ortenberg R, Mevarech M. 2003. Development of a gene knockout

- system for the halophilic archaeon *Haloferax volcanii* by use of the *pyrE* gene. J Bacteriol. 185:772-778.
- Blas-Galindo E, Cava F, Lopez-Vinas E, Mendieta J, Berenguer J. 2007. Use of a dominant *rpsL* allele conferring streptomycin dependence for positive and negative selection in *Thermus thermophilus*. Appl Environ Microbiol. 73:5138-5145.
- Bork P, Sander C, Valencia A. 1992. An ATPase domain common to prokaryotic cell cycle proteins, sugar kinases, actin, and hsp70 heat shock proteins. Proc Natl Acad Sci U S A. 89: 7290-7294.
- Bouet JY, Funnell BE. 1999. P1 ParA interacts with the P1 partition complex at *parS* and an ATP-ADP switch controls ParA activities. EMBO J. 18:1415-1424.
- Brabetz W, Liebl W, Schleifer KH. 1991. Studies on the utilization of lactose by *Corynebacterium glutamicum*, bearing the lactose operon of *Escherichia coli*. Arch. Microbiol. 155:607-612.
- Bradford, M. 1976. A rapid and sensitive method for quantification of microgram quantities of protein utilizing the principle of protein-dye binding. Anal Biochem.72: 248-254.
- Breier AM, Grossman AD. 2007. Whole-genome analysis of the chromosome partitioning and sporulation protein Spo0J (ParB) reveals spreading and origin-distal sites on the *Bacillus subtilis* chromosome. Mol Microbiol. 64:703-718.
- Bremer H, Dennis PP. 1996. Modulation of chemical composition and other parameters of the cell growth rate. In: *Escherichia coli* and *Salmonella*: cellular and molecular biology, 2nd ed. Neidhardt FC et al. (ed.). Washington, DC: ASM Press. pp. 1553-1569.
- Breuert S, Allers T, Spohn G, Soppa J. 2006. Regulated Polyploidy in Halophilic Archaea. PLoS ONE. 1:e92.
- Brouns SJ, Wu H, Akerboom J, Turnbull AP, de Vos WM, van der Oost J. 2005. Engineering a selectable marker for hyperthermophiles. J Biol Chem. 280:11422-11431.
- Bullock WO, Fernandez JM, Short JM. 1987. XL1-Blue: a high efficiency plasmid DNA transforming *recA* *Escherichia coli* strain with beta-galactosidase selection. Bio Techniques. 5:376-379.
- Castán P, de Pedro MA, Risco C, Vallés C, Fernández LA, Schwarz H, Berenguer J.

2001. Multiple regulatory mechanisms act on the 5' untranslated region of the S-layer gene from *Thermus thermophilus* HB8. *J Bacteriol.* 183:1491-1494.

Cava F, de Pedro MA, Blas-Galindo E, Waldo GS, Westblade LF, Berenguer J. 2008. Expression and use of superfolder green fluorescent protein at high temperatures in vivo: a tool to study extreme thermophile biology. *Environ Microbiol.* 10:605-613.

Cava F, Laptenko O, Borukhov S, Chahlaifi Z, Blas-Galindo E, Gomez-Puertas P, Berenguer J. 2007. Control of the respiratory metabolism of *Thermus thermophilus* by the nitrate respiration conjugative element NCE. *Mol Microbiol.* 64:630-646.

César CE, Álvarez L, Bricio C, van Heerden E, Littauer D, Berenguer J. 2011. Unconventional lateral gene transfer in extreme thermophilic bacteria. *Int Microbiol.* 14:187-199.

Comai L. 2005. The advantages and disadvantages of being polyploid. *Nat Rev Genet.* 6:836-846.

Davis MA, Martin KA, Austin SJ. 1992. Biochemical activities of the ParA partition protein of the P1 plasmid. *Mol Microbiology.* 6:1141-1147.

de Grado M, Castan P, Berenguer J. 1999. A high-transformation-efficiency cloning vector for *Thermus thermophilus*. *Plasmid.* 42:241-245.

de Grado M, Lasa I, Berenguer J. 1998. Characterization of a plasmid replicative origin from an extreme thermophile. *FEMS Microbiol Lett.* 165:51-57.

Defeu Soufo HJ, Graumann PL. 2003. Actin-like proteins MreB and Mbl from *Bacillus subtilis* are required for bipolar positioning of replication origins. *Curr Biol.* 13:1916-1920.

Donovan C, Schwaiger A, Krämer R, Bramkamp M. 2010. Subcellular localization and characterization of the ParAB system from *Corynebacterium glutamicum*. *J Bacteriol.* 192:3441-3451.

Dubarry N, Pasta F, Lane D. 2006. ParABS systems of the four replicons of *Burkholderia cenocepacia*: new chromosome centromeres confer partition specificity. *J Bacteriol.* 188:1489-1496.

Dworkin J, Losick R. 2002. Does RNA polymerase help drive chromosome segregation in bacteria? *Proc Natl Acad Sci U S A.* 99:14089-14094.

Dye NA, Pincus Z, Theriot JA, Shapiro L, Gitai Z. 2005. Two independent spiral

- structures control cell shape in *Caulobacter*. Proc Natl Acad Sci USA. 102: 18608-18613.
- Ebersbach G, Gerdes K. 2001. The double *par* locus of virulence factor pB171: DNA segregation is correlated with oscillation of ParA. Proc Natl Acad Sci U S A. 98: 15078-15083.
- Ebersbach G, Gerdes K. 2005. Plasmid segregation mechanisms. Annu Rev Genet. 39: 453-479.
- Errington J, Murray H, Wu LJ. 2005. Diversity and redundancy in bacterial chromosome segregation mechanisms. Philos Trans R Soc Lond B Biol Sci. 360: 497-505.
- Fabret C, Ehrlich SD, Noirot P. 2002. A new mutation delivery system for genome-scale approaches in *Bacillus subtilis*. Mol Microbiol. 46:25-36.
- Fernández-Herrero LA, Olabarrá G, Castón JR, Lasa I, Berenguer J. 1995. Horizontal transference of S-layer genes within *Thermus thermophilus*. J Bacteriol. 177:5460-5466.
- Fiebig A, Keren K, Theriot JA. 2006. Fine-scale time-lapse analysis of the biphasic, dynamic behaviour of the two *Vibrio cholerae* chromosomes. Mol Microbiol. 60:1164-1178.
- Figge RM, Divakaruni AV, Gober JW. 2004. MreB, the cell shape-determining bacterial actin homologue, co-ordinates cell wall morphogenesis in *Caulobacter crescentus*. Mol Microbiol. 51:1321-1332.
- Fogel MA, Waldor MK. 2005. Distinct segregation dynamics of the two *Vibrio cholerae* chromosomes. Mol Microbiol. 55:125-136.
- Fogel MA, Waldor MK. 2006. A dynamic, mitotic-like mechanism for bacterial chromosome segregation. Genes Dev. 20:3269-3282.
- Formstone A, Errington J. 2005. A magnesium-dependent mreB null mutant: implications for the role of mreB in *Bacillus subtilis*. Mol Microbiol. 55:1646-1657.
- Fried MG, Daugherty MA. 1998. Electrophoretic analysis of multiple protein-DNA. Electrophoresis. 19:1247-1253.
- Friedman SA, Austin SJ. 1988. The P1 plasmid partition system synthesizes two essential proteins from an autoregulated operon. Plasmid. 19:103-112.

- Friedrich A, Hartsch T, Averhoff B. 2001. Natural transformation in mesophilic and thermophilic bacteria: identification and characterization of novel, closely related competence genes in *Acinetobacter* sp. strain BD413 and *Thermus thermophilus* HB27. *Appl Environ Microbiol.* 67:3140-3148.
- Friedrich A, Prust C, Hartsch T, Henne A, Averhoff B. 2002. Molecular analyzes of the natural transformation machinery and identification of pilus structures in the extremely thermophilic bacterium *Thermus thermophilus* strain HB27. *Appl Environ. Microbiol.* 68:745-755.
- Garner EC, Campbell CS, Mullins RD. 2004. Dynamic instability in a DNA-segregating prokaryotic actin homolog. *Science.* 306:1021-1025.
- Gay P, Le Coq D, Steinmetz M, Berkelman T, Kado C I. 1985. Positive selection procedure for entrapment of insertion sequence elements in gram-negative bacteria. *J. Bacteriol.* 164:918-921.
- Gerdes K, Howard M, Szardenings F. 2010. Pushing and pulling in prokaryotic DNA segregation. *Cell.* 141:927-942.
- Gerdes K, Møller-Jensen J, Bugge Jensen R. 2000. Plasmid and chromosome partitioning: Surprises from phylogeny. *Mol Microbiol.* 37:455-466.
- Gerdes K, Møller-Jensen J, Ebersbach G, Kruse T, Nordström K. 2004. Bacterial mitotic machineries. *Cell.* 116:359-366.
- Gibson DG, Young L, Chuang RY, Venter JC, Hutchison CA 3rd, Smith HO. 2009. Enzymatic assembly of DNA molecules up to several hundred kilobases. *Nat Methods.* 6:343-345.
- Gitai Z, Dye NA, Reisenauer A, Wachi M, Shapiro L. 2005. MreB actin-mediated segregation of a specific region of a bacterial chromosome. *Cell.* 120: 329-341.
- Glaser P, Sharpe ME, Raether B, Perego M, Ohlsen K, Errington J. 1997. Dynamic, mitotic-like behavior of a bacterial protein required for accurate chromosome partitioning. *Genes Dev.* 11:1160-1168.
- Glover BP, Pritchard AE, McHenry CS. 2001. tau binds and organizes *Escherichia coli* replication proteins through distinct domains: domain III, shared by gamma and tau, oligomerizes DnaX. *J Biol Chem.* 276:35842-35846.
- Godfrin-Estevenon AM, Pasta F, Lane D. 2002. The parAB gene products of *Pseudomonas putida* exhibit partition activity in both *P. putida* and *Escherichia coli*.



Mol Microbiol. 43:39-49.

Gordon GS, Sitnikov D, Webb CD, Teleman A, Straight A, Losick R, Murray AW, Wright A. 1997. Chromosome and low copy plasmid segregation in *E. coli*: visual evidence for distinct mechanisms. *Cell*. 90:1113-1121.

Gruber S, Errington J. 2009. Recruitment of condensin to replication origin regions by ParB/SpoOJ promotes chromosome segregation in *B. subtilis*. *Cell*. 137: 685-696.

Hansen MT. 1978. Multiplicity of genome equivalents in the radiation-resistant bacterium *Micrococcus radiodurans*. *J Bacteriol*. 134:71-75.

Hayes F, Barilla D. 2006. The bacterial segrosome: a dynamic nucleoprotein machine for DNA trafficking and segregation. *Nat Rev Microbiol*. 4:133-143.

Hayes F, Radnedge L, Davis MA, Austin SJ. 1994. The homologous operons for P1 and P7 plasmid partition are autoregulated from dissimilar operator sites. *Mol Microbiol*. 11:249-260.

Hegarty MJ, Hiscock SJ. 2008. Genomic clues to the evolutionary success of polyploid plants. *Curr Biol*. 18:R435-R444.

Heidelberg JF, Eisen JA, Nelson WC, Clayton RA, Gwinn ML, Dodson RJ, Haft DH, Hickey EK, Peterson JD, Umayam L, Gill SR, Nelson KE, Read TD, Tettelin H, Richardson D, Ermolaeva MD, Vamathevan J, Bass S, Qin H, Dragoi I, Sellers P, McDonald L, Utterback T, Fleishmann RD, Nierman WC, White O, Salzberg SL, Smith HO, Colwell RR, Mekalanos JJ, Venter JC, Fraser CM. DNA sequence of both chromosomes of the cholera pathogen *Vibrio cholerae*. 2000. *Nature*. 406:477-483.

Hellman LM, Fried MG. Electrophoretic mobility shift assay (EMSA) for detecting protein-nucleic acid interactions. *Nat Protoc*. 2007:1849-1861.

Henne A, Brüggemann H, Raasch C, Wiezer A, Hartsch T, Liesegang H, Johann A, Lienard T, Gohl O, Martinez-Arias R, Jacobi C, Starkuviene V, Schlenczek S, Dencker S, Huber R, Klenk HP, Kramer W, Merkl R, Gottschalk G, Fritz HJ. 2004. The genome sequence of the extreme thermophile *Thermus thermophilus*. *Nat Biotechnol*. 22:547-553.

Herdman M, Janvier M, Rippka R, Stanier RY. 1979. Genome size of cyanobacteria. *J Gen Microbiol*. 111:73-85.

Herschleb J, Ananiev G, Schwartz DC. 2007. Pulsed-field gel electrophoresis. *Nat Protoc*. 2:677-684.

- Hidaka Y, Hasegawa M, Nakahara T, Hoshino T. 1994. The entire population of *Thermus thermophilus* cells is always competent at any growth phase. *Biosci Biotechnol Biochem.* 58:1338-1339.
- Hu B, Yang G, Zhao W, Zhang Y, Zhao J. 2007. MreB is important for cell shape but not for chromosome segregation of the filamentous cyanobacterium *Anabaena* sp. PCC 7120. *Mol Microbiol.* 63:1640-1652.
- Inoue H, Nojima H, Okayama H. 1990. High efficiency transformation of *Escherichia coli* with plasmids. *Gene.* 96:23-28.
- Ireton K, Gunther NW 4th, Grossman AD. 1994. *spo0J* is required for normal chromosome segregation as well as the initiation of sporulation in *Bacillus subtilis*. *J Bacteriol.* 176:5320-5329.
- Jensen RB, Wang SC, Shapiro L. 2001. A moving DNA replication factory in *Caulobacter crescentus*. *EMBO J.* 20:4952-4963.
- Jacob F, Brenner S, Cuzin F. 1963. On the regulation of DNA replication in bacteria. *Cold Spring Harbor Symp. Quant Biol.* 23:329-348.
- Jakimowicz D, Brzostek A, Rumijowska-Galewicz A, Zydek P, Dołzbłasz A, Smulczyk-Krawczyszyn A, Zimniak T, Wojtasz L, Zawilak-Pawlik A, Kois A, Dziadek J, Zakrzewska-Czerwińska J. 2007a. Characterization of the mycobacterial chromosome segregation protein ParB and identification of its target in *Mycobacterium smegmatis*. *Microbiology.* 153:4050-4060.
- Jensen RB, Wang SC, Shapiro L. 2001. A moving DNA replication factory in *Caulobacter crescentus*. *EMBO J.* 20:4952-4963.
- Jones LJ, Carballido-López R, Errington J. 2001. Control of cell shape in bacteria: helical, actin-like filaments in *Bacillus subtilis*. *Cell.* 104:913-922.
- Kadoya R, Baek JH, Sarker A, Chattoraj DK. 2011. Participation of Chromosome Segregation Protein ParAI of *Vibrio cholerae* in Chromosome Replication. *J Bacteriol.* 193:1504-1514.
- Kang J, Lee MS, Gorenstein DG. 2005. Quantitative analysis of chemiluminescence signals using a cooled charge-coupled device camera. *Anal Biochem.* 345:66-71.
- Kato J, Suzuki H, Ikeda H. 1992. Purification and characterization of DNA topoisomerase IV in *Escherichia coli*. *J Biol Chem.* 267:25676-25684.

- Kiernan JA. 2007. Indigogenic substrates for detection and localization of enzymes. *Biotech Histochem.* 82:73-103.
- Kim HJ, Calcutt MJ, Schmidt FJ, Chater KF. 2000. Partitioning of the linear chromosome during sporulation of *Streptomyces coelicolor* A3(2) involves an *oriC*-linked *parAB* locus. *J Bacteriol.* 182:1313-1320.
- Kolter R, Siegele DA, Tormo A. 1993. The stationary phase of the bacterial life cycle. *Annu Rev Microbiol.* 47:855-874.
- Koonin EV. 1993. A superfamily of ATPases with diverse functions containing either classical or deviant ATP-binding motif. *J Mol Biol.* 229:1165-1174.
- Koyama Y, Arikawa Y, Furukawa K. 1990a. A plasmid vector for an extreme thermophile, *Thermus thermophilus*. *FEMS Microbiol Lett.* 72:97-102.
- Koyama Y, Hoshino T, Tomizuka N, Furukawa K. 1986. Genetic transformation of the extreme thermophile *Thermus thermophilus* and of other *Thermus* spp. *J Bacteriol.* 166:338-340.
- Koyama Y, Okamoto S, Furukawa K. 1990. Cloning of alpha- and beta-galactosidase genes from an extreme thermophile, *Thermus* strain T2, and their expression in *Thermus thermophilus* HB27. *Appl Environ Microbiol.* 56:2251-2254.
- Kruse T, Blagoev B, Lønner-Olesen A, Wachi M, Sasaki K, Iwai N, Mann M, Gerdes K. 2006. Actin homolog MreB and RNA polymerase interact and are both required for chromosome segregation in *Escherichia coli*. *Genes Dev.* 20:113-124.
- Kruse T, Bork-Jensen J, Gerdes K. 2005. The morphogenetic MreBCD proteins of *Escherichia coli* form an essential membrane-bound complex. *Mol Microbiol.* 55:78-89.
- Kruse T, Møller-Jensen J, Lønner-Olesen A, Gerdes K. 2003. Dysfunctional MreB inhibits chromosome segregation in *Escherichia coli*. *EMBO J.* 22:5283-5292.
- Labarre J, Chauvat F, Thuriaux P. 1989. Insertional mutagenesis by random cloning of antibiotic resistance genes into the genome of the cyanobacterium *Synechocystis* strain PCC 6803. *J Bacteriol.* 171:3449-3457.
- Lange C, Zerulla K, Breuert S, Soppa J. 2011. Gene conversion results in the equalization of genome copies in the polyploid haloarchaeon *Haloferax volcanii*. *Mol Microbiol.* 80:666-677.

Lasa I, Casto ñ JR, Fernandez-Herrero LA, de Pedro MA, Berenguer J. 1992a. Insertional mutagenesis in the extreme thermophilic eubacteria *Thermus thermophilus* HB8. *Mol Microbiol.* 6:1555-1564.

Lasa I, de Grado M, de Pedro MA, Berenguer J. 1992. Development of *Thermus-Escherichia* shuttle vectors and their use for expression of the *Clostridium thermocellum* *celA* gene in *Thermus thermophilus*. *J Bacteriol.* 174:6424-6431.

Lasocki K, Bartosik AA, Mierzejewska J, Thomas CM, Jagura-Burdzy G. 2007 . Deletion of the *parA* (*soj*) homologue in *Pseudomonas aeruginosa* causes ParB instability and affects growth rate, chromosome segregation, and motility. *J Bacteriol.* 189:5762-5772.

Lau IF, Filipe SR, Søballe B, Økstad OA, Barre FX, Sherratt DJ. 2003. Spatial and temporal organization of replicating *Escherichia coli* chromosomes. *Mol Microbiol.* 49:731-743.

Lee PS, Grossman AD. 2006. The chromosome partitioning proteins Soj (ParA) and Spo0J (ParB) contribute to accurate chromosome partitioning, separation of replicated sister origins, and regulation of replication initiation in *Bacillus subtilis*. *Mol Microbiol.* 60:853-869.

Lee PS, Lin DC, Moriya S, Grossman AD. 2003. Effects of the chromosome partitioning protein Spo0J (ParB) on *oriC* positioning and replication initiation in *Bacillus subtilis*. *J Bacteriol.* 185:1326-1337.

Lemon KP, Grossman AD. 1998. Localization of bacterial DNA polymerase: Evidence for a factory model of replication. *Science.* 282:1516-1519.

Lemon KP, Grossman AD. 2000. Movement of replicating DNA through a stationary replisome. *Mol Cell.* 6:1321-1330.

Leonard TA, Butler PJ, Löwe J. 2004. Structural analysis of the chromosome segregation protein Spo0J from *Thermus thermophilus*. *Mol Microbiol.* 53:419-432.

Leonard TA, Butler PJ, Löwe J. 2005. Bacterial chromosome segregation: structure and DNA binding of the Soj dimer--a conserved biological switch. *EMBO J.* 24: 270-282.

Leonard TA, Møller-Jensen J, Löwe J. 2005. Towards understanding the molecular basis of bacterial DNA segregation. *Philos Trans R Soc Lond B Biol Sci.* 360: 523-535.

- Levin PA, Margolis PS, Setlow P, Losick R, Sun D. 1992. Identification of *Bacillus subtilis* genes for septum placement and shape determination. *J Bacteriol.* 21:6717-6728.
- Lewis RA, Bignell CR, Zeng W, Jones AC, Thomas CM. 2002. Chromosome loss from *par* mutants of *Pseudomonas putida* depends on growth medium and phase of growth. *Microbiology.* 148:537-548.
- Li Y, Austin S. 2002. The P1 plasmid in action: Time-lapse photomicroscopy reveals some unexpected aspects of plasmid partition. *Plasmid.* 48: 174-178.
- Li Y, Dabrazhynetskaya A, Youngren B, Austin S. 2004. The role of Par proteins in the active segregation of the P1 plasmid. *Mol Microbiol.* 53:93-102.
- Liebl W. 2004. Genomics taken to the extreme. *Nat Biotechnol.* 22:524-525.
- Lim GE, Derman AI, Pogliano J. 2005. Bacterial DNA segregation by dynamic SopA polymers. *Proc Natl Acad Sci U S A.* 102:17658-17663.
- Lin DC, Grossman AD. 1998. Identification and characterization of a bacterial chromosome partitioning site. *Cell.* 92:675-685.
- Lin DC, Levin PA, Grossman AD. 1997. Bipolar localization of a chromosome partition protein in *Bacillus subtilis*. *Proc Natl Acad Sci U S A.* 94:4721-4726.
- Lioliou EE, Pantazaki AA, Kyriakidis DA. 2004. *Thermus thermophilus* genome analysis: benefits and implications. *Microb Cell Fact.* 3:5-7.
- Livak KJ, Schmittgen TD. 2001. Analysis of relative gene expression data using real-time quantitative PCR and the 2<sup>-</sup>(-Delta Delta C(T)). *Method.* 25:402-408.
- Livny J, Yamaichi Y, Waldor MK. 2007. Distribution of centromere-like *parS* sites in bacteria: insights from comparative genomics. *J Bacteriol.* 189: 8693-8703.
- Malawski GA, Hillig RC, Monteclaro F, Eberspaecher U, Schmitz AA, Crusius K, Huber M, Egner U, Donner P, Müller-Tiemann B. 2006. Identifying protein construct variants with increased crystallization propensity-a case study. *Protein Sci.* 15: 2718-2728.
- Maldonado R, Jiménez J, Casades J. 1994. Changes of ploidy during the *Azotobacter vinelandii* growth cycle. *J Bacteriol.* 176:3911-3919.
- Maloy S R, Nunn W D. 1981. Selection for loss of tetracycline resistance by *Escherichia coli*. *J Bacteriol.* 145:1110-1111.

- Marczynski GT. 1999. Chromosome methylation and measurement of faithful, once and only once per cell cycle chromosome replication in *Caulobacter crescentus*. J Bacteriol. 181:1984-1993.
- Marston AL, Errington J. 1999. Dynamic movement of the ParA-like Soj protein of *B. subtilis* and its dual role in nucleoid organization and developmental regulation. Mol Cell. 4:673-682.
- Mather MW, Fee JA. 1992. Development of plasmid cloning vectors for *Thermus thermophilus* HB8: expression of a heterologous, plasmid-borne kanamycin nucleotidyltransferase gene. Appl Environ Microbiol. 58:421-425.
- Maxam A, Gilbert WS. 1977. A new method for sequencing DNA. Proc Natl Acad Sci U S A. 74:560-565.
- Mazza P, Noens EE, Schirner K, Grantcharova N, Mommaas AM, Koerten HK, Muth G, Flärdh K, van Wezel GP, Wohlleben W. 2006. MreB of *Streptomyces coelicolor* is not essential for vegetative growth but is required for the integrity of aerial hyphae and spores. Mol Microbiol. 60:838-852.
- Minnen A, Attaiech L, Thon M, Gruber S, Veening JW. 2011. SMC is recruited to oriC by ParB and promotes chromosome segregation in *Streptococcus pneumoniae*. Mol Microbiol. 81: 676-688.
- Mohl DA, Easter J Jr, Guber JW. 2001. The chromosome partitioning protein, ParB, is required for cytokinesis in *Caulobacter crescentus*. Mol Microbiol. 42:741-755.
- Mohl DA, Guber JW. 1997. Cell cycle-dependent polar localization of chromosome partitioning proteins in *Caulobacter crescentus*. Cell. 88:675-684.
- Møller-Jensen J, Borch J, Dam M, Jensen RB, Roepstorff P, Gerdes K. 2003. Bacterial mitosis: ParM of plasmid R1 moves plasmid DNA by an actin-like insertional polymerization mechanism. Mol Cell. 12:1477-1487.
- Møller-Jensen J, Jensen RB, Löwe J, Gerdes K. 2002. Prokaryotic DNA segregation by an actin-like filament. EMBO J. 21:3119-3127.
- Moreno R, Zafra O, Cava F, Berenguer J. 2003. Development of a gene expression vector for *Thermus thermophilus* based on the promoter of the respiratory nitrate reductase. Plasmid. 49:2-8.
- Mori H, Mori Y, Ichinose C, Niki H, Ogura T, Kato A, Hiraga S. 1989. Purification and characterization of SopA and SopB proteins essential for F plasmid partitioning. J

- Biol Chem. 264:15535-15541.
- Murray H, Errington J. 2008. Dynamic control of the DNA replication initiation protein DnaA by Soj/ParA. *Cell*. 135:74-84.
- Musso M, Bianchi-Scarrà G, Van Dyke MW. 2000. The yeast CDP1 gene encodes a triple-helical DNA-binding protein. *Nucleic Acids Res*. 28:4090-4096.
- Nakamura A, Takakura Y, Kobayashi H, Hoshino T. 2005. *In vivo* directed evolution for thermostabilization of *Escherichia coli* hygromycin B phosphotransferase and the use of the gene as a selection marker in the host-vector system of *Thermus thermophilus*. *J Biosci Bioeng*. 100:158-163.
- Nardmann J, Messer W. 2000. Identification and characterization of the dnaA upstream region of *Thermus thermophilus*. *Gene*. 261:299-303.
- Navarro Llorens JM, Tormo A, Martínez-García E. 2010. Stationary phase in gram-negative bacteria. *FEMS Microbiol Rev*. 34:476-495.
- Niki H, Hiraga S. 1997. Subcellular distribution of actively partitioning F plasmid during the cell division cycle in *E. coli*. *Cell*. 90:951-957.
- Niki, H, Hiraga, S. 1998. Polar localization of the replication origin and terminus in *Escherichia coli* nucleoids during chromosome partitioning. *Genes Dev*. 12:1036-1045.
- Ogura T, Hiraga S. 1983. Partition mechanism of F plasmid: two plasmid gene-encoded products and a cis-acting region are involved in partition. *Cell*. 32:351-360.
- Ogura Y, Ogasawara N, Harry EJ, Moriya S. 2003. Increasing the ratio of Soj to Spo0J promotes replication initiation in *Bacillus subtilis*. *J Bacteriol*. 185:6316-6324.
- Ohta T, Tokishita S, Imazuka R, Mori I, Okamura J, Yamagata H. 2006. Glucosidase as a reporter for the gene expression studies in *Thermus thermophilus* and constitutive expression of DNA repair genes. *Mutagenesis*. 21:255-260.
- Ohtani N, Tomita M, Itaya M. 2010. An extreme thermophile, *Thermus thermophilus*, is a polyploid bacterium. *J Bacteriol*. 192:5499-5505.
- Oshima T, Imahori K. 1971. Isolation of an extreme thermophile and thermostability of its transfer ribonucleic acid and ribosomes. *J Gen Appl Microbiol*. 17:513-517.
- Oshima T, Imahori K. 1974. Description of *Thermus thermophilus* (Yoshida and

- Oshima) comb. nov., a nonsporulating thermophilic bacterium from a Japanese thermal spa. *Int J Syst Bacteriol.* 24:102-112.
- Peck RF, DasSarma S, Krebs M.P. 2000. Homologous gene knockout in the archaeon *Halobacterium salinarum* with Ura3 as a counterselectable marker. *Mol Microbiol.* 35: 667-676.
- Pedelacq JD, Cabantous S, Tran T, Terwilliger TC, Waldo GS. 2006. Engineering and characterization of a superfolder green fluorescent protein. *Nat Biotechnol.* 24:79-88
- Prescott M, Battad JM, Wilmann PG, Rossjohn J, Devenish RJ. 2006. Recent advances in all-protein chromophore technology. *Biotechnol Annu Rev.* 12:31-66.
- Pritchett MA, Zhang JK, Metcalf WW. 2004. Development of a markerless genetic exchange method for *Methanosarcina acetivorans* c2a and its use in construction of new genetic tools for methanogenic archaea. *Appl Environ Microbiol.* 70:1425-1433.
- Radnedge L, Youngren B, Davis M, Austin S. 1998. Probing the structure of complex macromolecular interactions by homolog specificity scanning: the P1 and P7 plasmid partition systems. *EMBO J.* 17:6076-6085.
- Rasimas JJ, Kar SR, Pegg AE, Fried MG 2007. Interactions of human O6-alkylguanine-DNA alkyltransferase (AGT) with short single-stranded DNAs. *J Biol Chem.* 282:3357-3366.
- Ringgaard S, van Zon J, Howard M, Gerdes K. 2009. Movement and equi-positioning of plasmids by ParA filament disassembly. *Proc Natl Acad Sci U S A.* 106: 19369-19374.
- Russell CB, Dahlquist FW. 1989. Exchange of chromosomal and plasmid alleles in *Escherichia coli* by selection for loss of a dominant antibiotic sensitivity marker. *J Bacteriol.* 171:2614-2618.
- Rye HS, Drees BL, Nelson HC, Glazer AN. 1993. Stable fluorescent dye-DNA complexes in high sensitivity detection of protein-DNA interactions. Application to heat shock transcription factor. *J Biol Chem.* 268:25229-25238.
- Saint-Dic D, Frushour BP, Kehrl JH, Kahng LS. 2006. A *parA* homolog selectively influences positioning of the large chromosome origin in *Vibrio cholerae*. *J Bacteriol.* 188:5626-5631.
- Sambrook J, Russel D. 2001. *Molecular Cloning: A Laboratory Manual*, 3rd edn. Cold Spring Harbor, NY: Cold Spring Harbor Laboratory.



- Sambrook, J, Fritsch EF, Maniatis T. 1989. Molecular Cloning: a Laboratory Manual, 2nd edn. Cold Spring Harbor, NY: Cold Spring Harbor Laboratory.
- Schneider D, Fuhrmann E, Scholz I, Hess WR, Graumann PL. 2007. Fluorescence staining of live cyanobacterial cells suggest non-stringent chromosome segregation and absence of a connection between cytoplasmic and thylakoid membranes. BMC Cell Biol. 8:39.
- Scholefield G, Errington J, Murray H. 2012. Soj/ParA stalls DNA replication by inhibiting helix formation of the initiator protein DnaA. EMBO J. 31:1542-1555.
- Schwarzenlander C, Averhoff B. 2006. Characterization of DNA transport in the thermophilic bacterium *Thermus thermophilus* HB27. FEBS J. 273:4210-4218.
- Selmer M, Dunham CM, Murphy FV 4th, Weixlbaumer A, Petry S, Kelley AC, Weir JR, Ramakrishnan V. 2006. Structure of the 70S ribosome complexed with mRNA and tRNA. Science. 313:1935-1942.
- Semon M, Wolfe KH. 2007. Consequences of genome duplication. Curr Opin Genet Dev. 17:505-512.
- Sharpe ME, Errington J. 1996. The *Bacillus subtilis* soj-spo0J locus is required for a centromere-like function involved in prespore chromosome partitioning. Mol Microbiol. 21:501-509.
- Sharpe ME, Errington J. 1999. Upheaval in the bacterial nucleoid. An active chromosome segregation mechanism. Trends Genet. 15:70-74.
- Shih YL, Kawagishi I, Rothfield L. 2005. The MreB and Min cytoskeletal-like systems play independent roles in prokaryotic polar differentiation. Mol Microbiol. 58: 917-928.
- Shih YL, Le T, Rothfield L. 2003. Division site selection in *Escherichia coli* involves dynamic redistribution of Min proteins within coiled structures that extend between the two cell poles. Proc Natl Acad Sci U S A. 100:7865-7870.
- Skarstad K, Boye E, Steen HB. 1986. Timing of initiation of chromosome replication in individual *Escherichia coli* cells. EMBO J. 5:1711-1717.
- Soufo HJ, Graumann, PL. 2003. Actin-like proteins MreB and Mbl from *Bacillus subtilis* are required for bipolar positioning of replication origins. Curr Biol. 13: 1916-1920.

- Spizizen, J. 1958. Transformation of biochemically deficient strains of *Bacillus subtilis* by deoxyribonucleate. Proc Natl Acad Sci U S A. 44:1072-1078.
- Sullivan NL, Marquis KA, Rudner DZ. 2009. Recruitment of SMC by ParB-*parS* organizes the origin region and promotes efficient chromosome segregation. Cell. 137: 697-707.
- Tamakoshi M, Yaoi T, Oshima T, Yamagishi A. 1999. An efficient gene replacement and deletion system for an extreme thermophile, *Thermus thermophilus*. FEMS Microbiol Lett. 173:431-437.
- Tamakoshi M, Yaoi T, Oshima T, Yamagishi A. 1999. An efficient gene replacement and deletion system for an extreme thermophile, *Thermus thermophilus*. FEMS Microbiol. Lett. 173:431-437.
- Tandeau de Marsac N. 1994. Differentiation of hormogonia and relationships with other biological processes. In: The Molecular Biology of Cyanobacteria. Bryant DA. (ed.). Dordrecht: Kluwer Academic Publishers, pp. 825-842.
- Teleman AA, Graumann PL, Lin DC, Grossman AD, Losick R. 1998. Chromosome arrangement within a bacterium. Curr Biol. 8:1102-1109.
- Tolstonog GV, Li G, Shoeman RL, Traub P. 2005. Interaction in vitro of type III intermediate filament proteins with higher order structures of single-stranded DNA, particularly with G-quadruplex DNA. DNA Cell Biol. 24:85-110.
- Toro E, Hong SH, McAdams HH, Shapiro L. 2008. *Caulobacter* requires a dedicated mechanism to initiate chromosome segregation. Proc Natl Acad Sci U S A. 105: 15435-15440.
- van den Ent F1, Møller-Jensen J, Amos LA, Gerdes K, Löwe J. 2002. F-actin-like filaments formed by plasmid segregation protein ParM. EMBO J. 21:6935-6943.
- Vassylyev DG, Sekine S, Laptenko O, Lee J, Vassylyeva MN, Borukhov S, Yokoyama S. 2002. Crystal structure of a bacterial RNA polymerase holoenzyme at 2.6 Å resolution. Nature. 417:712-719.
- Venkova-Canova T1, Baek JH, Fitzgerald PC, Blokesch M, Chattoraj DK. 2013. Evidence for two different regulatory mechanisms linking replication and segregation of *vibrio cholerae* chromosome II. PLoS Genet. 9(6):e1003579.
- Vieille C, Zeikus GJ. 2001. Hyperthermophilic enzymes: sources, uses, and molecular mechanisms for thermostability. Microbiol Mol Biol Rev. 65:1-43.

- Viollier PH, Thanbichler M, McGrath PT, West L, Meewan M, McAdams HH, Shapiro L. 2004. Rapid and sequential movement of individual chromosomal loci to specific subcellular locations during bacterial DNA replication. *Proc Natl Acad Sci U S A*. 101:9257-9262.
- Webb CD, Graumann PL, Kahana JA, Teleman AA, Silver PA, Losick R. 1998. Use of time-lapse microscopy to visualize rapid movement of the replication origin region of the chromosome during the cell cycle in *Bacillus subtilis*. *Mol Microbiol*. 28:883-892.
- Webb CD, Teleman A, Gordon S, Straight A, Belmont A, Lin DC, Grossman AD, Wright A, Losick R. 1997. Bipolar localization of the replication origin regions of chromosomes in vegetative and sporulating cells of *B. subtilis*. *Cell*. 88:667-674.
- Wu LJ, Errington J. 2003. RacA and the Soj-Spo0J system combine to effect polar chromosome segregation in sporulating *Bacillus subtilis*. *Mol Microbiol*. 49:1463-1475.
- Yamaichi Y, Fogel MA, McLeod SM, Hui MP, Waldor MK. 2007. Distinct centromere-like *parS* sites on the two chromosomes of *Vibrio* spp. *J Bacteriol*. 189:5314-5324.
- Yamaichi Y, Fogel MA, Waldor MK. 2007. *par* genes and the pathology of chromosome loss in *Vibrio cholerae*. *Proc Natl Acad Sci U S A*. 104:630-635.
- Yamaichi Y, Gerding MA, Davis BM, Waldor MK. 2011. Regulatory cross-talk links *Vibrio cholerae* chromosome II replication and segregation. *PLoS Genet*. 7:e1002189.
- Yamaichi Y, Niki H. 2000. Active segregation by the *Bacillus subtilis* partitioning system in *Escherichia coli*. *Proc Natl Acad Sci U S A*. 97:14656-11461.
- Yanisch-Perron C, Vieira J, Messing J. 1985. Improved M13 phage cloning vectors and host strains: nucleotide sequences of the M13mp18 and pUC19 vectors. *Gene*. 33:103-119.
- Yates P, Lane D, Biek DP. 1999. The F plasmid centromere, *sopC*, is required for full repression of the *sopAB* operon. *J Mol Biol*. 290:627-638.
- Yokoyama S, Matsuo Y, Hirota H, Kigawa T, Shirouzu M, Kuroda Y, Kurumizaka H, Kawaguchi S, Ito Y, Shibata T, Kainosho M, Nishimura Y, Inoue Y, Kuramitsu S. 2000. Structural genomics projects in Japan. *Nat Struct Biol*. 7:943-945.

## Appendix: primers used in the study

Name	Sequence (5' - 3')*	Usage
42.F	CTTCGGCCTGTGGAACTTCG	cloning of the <i>bgl</i>
42.R	TGGGCGCAGGCCACATAAAC	region
42m-Bgl.F	CCCAAAGGAATTTTTTCGGAGATCTCGGTCATAGGCGTTTCTC	site-direct mutagenesis of <i>bgl</i>
42m-Bgl.R	GGA GCGGATCGC GCGGGCCCA GATCTAA GTGCCCCGCCA GAG	
TKO4-1	cggtttgcgtattggcgctctTCCCCGGGA GTATAACA GAAACC	amplify <i>kat</i> for pTKO-4
TKO4-2	ggcgtttctctccaagAATTCGGTTCAAAATGGTATG	
TKO4-3	cataccatttgaacgaaTTCTTGGAGGA GAAACGCCTATG	amplify <i>bgl</i> for pTKO-4
TKO4-4	gagcgagcgagtcagtgagcgaggaTGGCGGGGCACTTAGGTCTG	
340.F	GAGGATGGCCACCTTCTTCG	cloning of the 340 region
341.R	AACGCGGTCCAGACCGCATTCTC	
340m-Bgl.F	TCCTCAAGGAGGTAGATCTATGAGGTTCCGCGT	site-direct mutagenesis of 340
341m-Bgl.R	CCCTCGAGGAGATCTCTAAGCCTGGCCA	
mreB-1-F	catgcctgcaggtcgactAAACGGGACCGATTCCTC	amplify <i>mreB</i> downstream
mreB-1-R	agagcgccaatacgcgaaaccGAGCTCGCCTCGGACATCTAC	flanking region for pUC- $\Delta$ <i>mreB</i> :: <i>kat</i>
mreB-2-F	cttgaggagaaacgccTGCCGATGTCTTCGCCTTTAAGC	amplify <i>mreB</i> upstream
mreB-2-R	cggtagccggggtatcctGGGTGGACCTCATCATTGAC	flanking region for pUC- $\Delta$ <i>mreB</i> :: <i>kat</i> , and Southern blot probe template generation for <i>mreB</i> mutant detection
kat-2-F	cggtttgcgtattggcgctctTCCCCGGGA GTATAACA GAAACC	amplify “ <i>kat</i> ” for
kat-2-R	ggcgtttctctccaagAATTCGGTTCAAAATGGTATG	pUC- $\Delta$ <i>mreB</i> :: <i>kat</i>
parABc-1-F	catgcctgcaggtcgactCCTCGGCTTCCTCAA GCTCTTC	amplify <i>parABc</i>
parABc-1-R	agagcgccaatacgcgaaaccGAAGGGCAA GGTGGTATCCA G	downstream flanking region for pUC- $\Delta$ <i>parABc</i> :: <i>kat</i>
parABc-2-F	cttgaggagaaacgccGGCCCTTAGCATAACGGATACC	amplify <i>parABc</i> upstream
parABc-1-R	cggtagccggggtatcctCAAGTACGCGGGCTACATTG	flanking region for pUC- $\Delta$ <i>parABc</i> :: <i>kat</i>
kat-1-F	cggtttgcgtattggcgctctTCCCCGGGA GTATAACAGAAACC	amplify “ <i>kat</i> ” for
kat-1-R	ggcgtttctctccaagAATTCGGTTCAAAATGGTATG	pUC- $\Delta$ <i>parABc</i> :: <i>kat</i>

*Appendix: primers used in the study*

parc-R	gcataccatttgaacggaaCCGAA GA GGA CGCGCA CCGC	combining with parABc-1-F, amplify the template for the probe of Southern blot detection of <i>ΔparABc</i> in <i>Tth</i>
parABm-1-F	tgcatgcctgcaggtcgactGAACATCCACGGTGCCGTA G	amplify <i>parABm</i>
parABm-1-R	gttatactcccgggatcccGTCTTGCGGAA GGA GAA GGC	downstream flanking region for pUC- <i>ΔparABm::blm</i>
parABm-2-F	gactgatctagaggatccCCATCTCGCTCA CGGGAA CCA G	amplify <i>parABm</i> upstream flanking region for pUC- <i>ΔparABm::blm</i>
parABm-2-R	gctcggtagccgggatcctACGA GA CCGGGAA GTACGA G	
blm-1-F	gccttctcctccgcaagacGGGATCCCCGGGA GTATAAC	amplify “ <i>blm</i> ” for pUC- <i>ΔparABm::blm</i>
blm-1-R	ctgggtcccgtgagcgagatGGGGATCCTCTA GATCA GTC	
parBm-1-R	gttatactcccgggatcccTAGA GGGGCCGA GGTAACG	combining with parABm-1-F, amplify <i>parBm</i> downstream flanking region for pUC- <i>ΔparBm::blm</i>
parBm-2-F	gactgatctagaggatccccGTGCCCA GAA CCTCGTCCA G	amplify <i>parBm</i> upstream flanking region for pUC- <i>ΔparBm::blm</i>
parBm-2-R	ggtacccgggatcctctagCTACTGGTACGTGCGGGAA C	
blm-4-F	GGGATCCCCGGGA GTATAAC	amplify <i>blm</i> for pUC- <i>ΔparBm::blm</i>
blm-4-R	GGGGATCCTCTA GATCA GTC	
parm-F	AGTCAA GGCCA CGGGTGTCTTC	primers for PCR detection of <i>ΔparABm</i> mutants
parm-R	CCA GA CCATCGTCTA CGTCTTC	
parm-R-2	CCA GGTTTTCGCCCTCCA CA	combining with parm-F for PCR detection of <i>ΔparBm</i>
parAmN-1-F	tgcatgcctgcaggtcgactCTTCTTGCCCTTGA GGATCG	amplify <i>parAmN</i>
parAmN-1-R	gttatactcccgggatcccTACGTGCGGGAAACGGGAGGG	downstream flanking region for pUC- <i>ΔparAmN-1</i> , pUC- <i>ΔparAmN-2</i>
parAmN-2-F	gactgatctagaggatccccATGGGCCTA GA CTATCCCAA	combining with parABm-2-R, amplify <i>parAmN</i> upstream flanking region for

Appendix: primers used in the study

		pUC- $\Delta parAmN-1$ , pUC- $\Delta parAmN-2$ ; combining with parBm-2-R, amplify the template for Southern blot detection of the <i>parAmN</i> mutants
blm-2-F	ccctcccgtcccgcacgtaGGGATCCCCGGGA GTATAAC	amplify “ <i>blm</i> ” for
blm-2-R	ttggatagtagtagcccatGGGGATCCTCTA GATCA GTC	pUC- $\Delta parAmN-1$
blm-3-F	gggatccccgggagtataacGGGGATCCTCTA GATCA GTC	amplify “ <i>blm</i> ” for
blm-3-R	ggggatccttagatcagtcGGGATCCCCGGGA GTATAAC	pUC- $\Delta parAmN-2$
parAmRT-F	TGCA GGAA CTCTCCGTCA G	primers for RT-qPCR
parAmRT-R	ACAACCGGGTGCTGGA GAAG	measuring <i>parAm</i> expression level in $\Delta parAmN-1$ and $\Delta parAmN-2$
parBmRT-F	CACCTCTTCCACCGA CTTC	primers for RT-qPCR
parBmRT-R	TCCTGGA CCTCTCCGA GAAG	measuring <i>parBm</i> expression level in $\Delta parAmN-1$ and $\Delta parAmN-2$
pMK-1-F	GGATGTGCTGCAA GGC GATTAA GTTGG	amplify PMK18 backbone
pMK-1-R	TCAAAATGGTATGCGTTTTG	for PMK- <i>parAm</i> and pMK- <i>parBm</i>
parAm-F	caaaacgcataccatttgaTGGGGGATA CTTGGCAAACG	amplify <i>parAm</i> for
parAm-R	aatgccttgagcacatCCTCGTCCA GCCGGCTCATTC	PMK- <i>parAm</i>
parBm-1-F	caaaacgcataccatttgaCTGGA GGA GGTGGC GGAATG	amplify <i>parBm</i> for
parBm-1-R	aatgccttgagcacatccAACGA GA GGGC GTTA CCTCG	PMK- <i>parBm</i>
P43-F	ACCTGCGCCTTGTCCATGTC	primers for generating
P43-R	TGGGCGCA GGCCA CATAAAC	TT_P0043 standard fragment for qPCR
P43-R-1	GAGGCCATCTCCGA GGGAAA G	accompanying with P43-F, use for qPCR reactions of detecting TT_P0043 copy numbers
terCm-F	TCCTGGTCCA GTGAAG ACAA G	primers for generating the
terCm-R	GGCA GTACTCCGTGTTTTGAAG	megaplas mid terminus region TT_P0195 ( <i>term</i> )

*Appendix: primers used in the study*

		standard fragment for qPCR
terCm-F-1	TTGCATAAGGTGGCCTTCG	primers for qPCR reactions of detecting TT_P0195 copy numbers
terCm-R-1	GTCTTGGC GGTGTA CTTCTTG	
oriCc-F	TCAA GGA GAA GGGCTA CA G	generating <i>oriCc</i> standard fragment for qPCR
oriCc-R	CCTTGTA GCTCA CGGAA A C	
oriCc-F-1	ACGCCATCCTGGTCAAGGTG	primers for qPCR reactions of detecting <i>oriCc</i> copy numbers
oriCc-R-1	AGGTCGGC GATGAA GCTGTC	
terCc-F	CCGGCA GGTA GA CGTCAAAG	primers for generating chromosomal terminus region ( <i>terc</i> ) standard fragment for qPCR
terCc-R	TGA GCCGGA GGGA GTTTGAG	
tercC-F-1	GTGA CCACCA CGCTTTCGGG	primers for qPCR reactions of detecting <i>terc</i> copy numbers
tercC-R-1	TTAGGCCGCCA GGATCA GTACG	
1-F	CGCCTGGAGAACGTCTTGTG	the 1 to 10 primer pairs for detecting megaplas mid loss in the <i>parAmN-1</i> mutant
1-R	GCTCTTTCGCCGACAACGTG	
2-F	CGTAGAGGAGGAGCATCAC	
2-R	TCCGGGAGAA GGTCTACTG	
3-F	CTTCGGCCTCTACTACGTG	
3-R	GCCTCTTCCA GAA GGTCTC	
4-F	AGGCTTAGGCA CCA CAAC	
4-R	TTGCCCA GGTGGCTATTCA G	
5-F	GCTCCTCTACCA CCTGTCTG	
5-R	CTCTTCA CCTCCGCCTA CTC	
6-F	CCTCCTGTGGCTTTCTATC	
6-R	GCTCTGGAGAGGAGTTTG	
7-F	CACCATCCA GCGCAGAAA GC	
7-R	ACGACTTCCGGCCCGATTAC	
8-F	CAGGACGCCCAA GACTTAG	
8-R	CGGACTGGAA GCTGAA CTC	
9-F	CCGCA CA GTATCTCGGTCTC	
9-R	CAGGAA GCGCCCTCTTAA GC	
10-F	TGGACACCGATCAGGTAAC	
10-R	GGTGGGTATGCGATTCAAG	

*Appendix: primers used in the study*

parBc-F	ttaaagaaggagatatacataTGTCCA GGAA GCCTA GCGGT	amplify <i>parBc</i> for
parBc-R	gtggtggtggtggtggtgctcgagCGCCTGGTA GCCGA GGCGCC	pET21a- <i>parBc</i>
parBm-F	ttaaagaaggagatatacatATGA GCCGGCTGGA CGA GGT	amplify <i>parBm</i> for
parBm-R	tcagtgggtggtggtggtgctcgagCCTCGGCCCTCTA GGA CCC	pET21a- <i>parBm</i>
pMK-F	GGATGTGCTGCAA GGC GATTAA GTTGG	amplify pMK18 backbone
pMK-R	ttgcgcatatgcctcacacctcTTCAAAATGGTATGCGTTTTG	for pMK <i>sgfp</i>
sgfp-F	gtgtcaaacgcataccattttGAA GGA GGTGTGA GGCATATGC	amplify <i>sgfp</i> for pMK <i>sgfp</i>
sgfp-R	aatgccttcgagcacatccTCTTACTTGTA GA GCTCGTC	
pMK- <i>sgfp</i> -F	ggaggaggaggaCGCAA GGCGGA GGA GCTCTT	amplify pMK <i>sgfp</i>
pMK- <i>sgfp</i> -R	TCAAAAATGGTATGCGTTTTG	backbone for pMK <i>parBc-sgfp</i> , pMK <i>parBm-sgfp</i>
parBc- <i>sgfp</i> -F	caaaacgcataccattttGA GA GGA GGTGATGGCCCGTGT	amplify <i>parBc</i> for
parBc- <i>sgfp</i> -R	cccttgctcctcctcctccCGCCTGGTA GCCGA GGCGC	pMK <i>parBc-sgfp</i>
parBm- <i>sgfp</i> -F	caaaacgcataccattttgaCTGGA GGA GGTGGC GGAATG	amplify <i>parBm</i> for
parBm- <i>sgfp</i> -R	cccttgctcctcctcctccCCTCGGCCCTCTA GGA CCC	pMK <i>parBm-sgfp</i>
pyr-F	CCGA GCCCTTGGCCCATATC	amplify <i>pyrFE</i> region for
pyr-R	CAGGA CCGCCA CCCTCATA	pJ- <i>pyrFE</i>
pyrEm-Nde.F	GAGGAA GCG <b>CATATGA</b> GA CCTCCTCC	site-directed mutagenesis
pyrEm-Nde.R	CAGGA CGT <b>CATATG</b> CCCCTACTCTAC	of <i>pyrE</i>
pyrF-F	CCGA GCCCTTGGCCCATATC	probe template generation
pyrF-R	GGACCCTCCCGGTACCTTTC	for Southern blot of <i>Tth</i> <i>ΔpyrE::kat</i> , <i>ΔpyrE::blm</i> , and HL01 mutants
pyr-R-2	GCTTTCAGGTTGACGGTAA GC	combining with pyr-F for PCR detecting of <i>Tth</i> <i>ΔpyrE::kat</i> , <i>ΔpyrE::blm</i> , and HL01 mutants

\* Enzyme restriction sites are in bold and sequences that create the overlaps for the Gibson assembly reactions are in lowercase.



## **Acknowledgement**

First of all, I would like to thank China Scholarship Council (CSC) for financial support, and Prof. Dr. Liebl for giving me the opportunity to work in his group and for his willingness to share with me his knowledge. Also, I greatly appreciate his help during the preparation, and accomplishment of this thesis.

I am very grateful for Dr. Angelov for supporting me during the whole time of my work, for the plenty of constructive discussions, for the patient and devoting guidance, for the altruistic sharing of knowledge and expertise, and for the thorough review of this thesis.

I want to thank all my current and former colleagues from the working group of Prof. Liebl: Dr. Wolfgang Schwarz, Dr. Wolfgang Ludwig, Dr. Armin Ehrenreich, Dr. Vladimir Zverlov; Trang Pham, Benedikt Leis, Maria Übelacker, Beate Schumacher, Xu Zheng, Liu Ziyong, Lena Bruder, Markus Mientus, Claudia Held, Sibylle Schadhauser, Helga Gaenge, Kornelia Garus, Daniel Hönicke, Justyna Lesiak, Huang Ching-ning, David Kostner etc. for creating a pleasant atmosphere in the lab and helping me throughout my work.

Special thanks to Trang Pham and Benedikt Leis for the plenty of vital discussions of the work, reviewing of this thesis, and their hospitality to help me out from living difficulties.

Finally, I want to thank my family for their patience, understanding and support during the time of this work.



## **Lebenslauf**

### **Persönliche Angaben**

---

Name	Haijuan Li
Geburtstag und Ort	02. April 1984 in Fujian, China
Nationalität	Chinesin

---

### **Ausbildung**

---

09/2003-07/2007	Studium Phytopathologie, College of Plant Protection, Northwest A&F University, Yangling, Shaanxi, China Abschluss: B.Sc
09/2007-07/2010	Studium Phytopathologie, College of Plant Protection, Northwest A&F University, Yangling, Shaanxi, China Abschluss: M.Sc
10/2010-09/2014	Doktorandin, Lehrstuhl für Mikrobiologie, Technische Universität München

---